ON THE ORTHO - PARA ENHANCEMENT OF MOLECULAR IODINE BY SELECTIVE LASER EXCITATION

by

JAMES L. BOOTH

B.Sc., McGill University, 1983

A THESIS SUBMITTED IN PARTIAL FULFILMENT OF

THE REQUIREMENTS FOR THE DEGREE OF

MASTER OF SCIENCE

in

THE FACULTY OF GRADUATE STUDIES

Deptartment of Physics

We accept this thesis as conforming

to the required standard

THE UNIVERSITY OF BRITISH COLUMBIA

October 15, 1985

In presenting this thesis in partial fulfilment of the requirements for an advanced degree at the The University of British Columbia, I agree that the Library shall make it freely available for reference and study. I further agree that permission for extensive copying of this thesis for scholarly purposes may be granted by the Head of my Department or by his or her representatives. It is understood that copying or publication of this thesis for financial gain shall not be allowed without my written permission.

Department of Physics

The University of British Columbia
2075 Wesbrook Place
Vancouver, Canada
V6T 1W5

Date: October, 1985

ABSTRACT

Based upon the results reported by Balykin, V. S., Letokhov, V. S., Mishen, V. I., and Semchishen, V. A., Chem. Phys., 17, 111 (1976), an attempt was made to shift the ortho-iodine to para-iodine ratio by (1) selectively predissociating the ortho-iodine molecules with the 5145 Å argon ion laser line and (2) by reacting the selectively excited ortho molecules with the scavengers, 2-hexene, acetylene, nitric oxide, nitrosyl chloride, and ethyl iodide. In both cases the ortho to para ratio was monitored via the fluorescence induced by a scanning dye laser beam. Neither tactic prooved effective, in contradiction with the aforementionned authors. In the case of systems containing low pressures of iodine vapour alone, time dependent differential quenching of the vibrational $B^3\Pi_{0^+u}$ $X^1\Sigma^+_g$ transitions was observed attributed to outgasing of the test cells over the course of the experiment and may be the cause of the apparant shift claimed by Letokhov et al. In mixtures of iodine and scavenger, the null result was probably due to the formation of radical chains during the photo-induced reactions capable of rapidly relaxing any shift that had occurred.

Table of Contents

List of Tables

List of Figures

Acknowledgements

I would like to thank my supervisor, Dr. F. W. Dalby, for his help and infusion of common sense when it was most needed. I would also like to thank him for the useful discussions and suggestions he provided throughout the course of this research. In addition I wish to extend my gratitude to Dr. S. Parmar who contributed greatly to the purification of the chemical species and the preparation of the test cells used in this research, and who, with K. Mah, offered many helpful comments and made the environment more pleasant. Further, I would like to express my appreciation to Dr. J. Vanderlinde for his enthusiasm and guidance during his brief stays at the University of British Columbia. Finally, I would like to thank Dr. N. Basco for the loan of some of his equipment and Mr. E. McWilliams for the glassblowing work he provided.

This thesis is dedicated to J. C.

I. THE BASIC IDEA

The idea for this project originated with my supervisor, Dr. F. W. Dalby, and was proposed to me when I first arrived at the University of British Columbia. As is the case with most interesting ideas, this one had a somewhat colorful history . In 1972 Dr. Dalby had taken a sabbatical at the École Normale in Paris. During this time, among other things, he attempted to selectively deplete the ortho-iodine population in a sample of ordinary molecular iodine and thereby create a shift in the usual ortho to para ratio. After some preliminary experiments which displayed no evidence for such a shift the attempt was abandonned .

Some years later, back at the University of British Columbia , he uncovered a paper written by V. S. Letokhov et al[1] concerning this very subject published in 1973. This paper claimed that, indeed, such a shift had been observed in molecular iodine. This revitalized Dr. Dalby's interest especially as the technique employed could easily be duplicated and even improved upon using the equipment available in his own research laboratory .

In order to describe the method proposed to produce the desired effect, it is first necessary to describe a few of the properties of molecular iodine . Iodine is a diatomic molecule composed of two identical atoms each of having nuclear spin $\frac{5}{2}$. Hence the net nuclear spin of any given molecule, I, may range from zero to five in integral steps. Further, molecular iodine has been observed to obey Fermi -

Dirac statistics and, to a good approximation, a consequence of this is that, in the ground electronic state, the even rotational levels are coupled to the even nuclear spin states and the odd rotational levels are coupled to the odd nuclear spin states . To the same approximation, the energy of a given rotational - vibrational state is independent of the nuclear spin, I, thereby leading to a degeneracy of each rotational state given by

$$g_I^{even} = \sum_{I=0,2,4} (2I+1) = 15 \qquad (1.1\,a)$$

$$g_I^{odd} = \sum_{I=1,3,5} (2I+1) = 21 \qquad (1.1\,b)$$

Those states with higher nuclear degeneracy are called ortho states (i.e. the odd rotational states) and those with lower statistical nuclear weight (the even rotational states) are called para states.

At a fixed temperature, T, the equilibrium ratio of the ortho -iodine to para-iodine is

$$\frac{N^o}{N^p} = \frac{\sum_{J,odd} 21\,(2J+1)\,e^{-\frac{E}{kT}}}{\sum_{J,even} 15\,(2J+1)\,e^{-\frac{E}{kT}}} \qquad (1.2)$$

which at room temperature reduces to $\frac{N^o}{N^p} \simeq 1.4$

the naturally occurring ratio. To change this ratio one may take advantage of the fact that the molecular iodine has a well-studied dense spectrum in the visible region with many spectral lines leading to a phenomenon known as predissociation. Predissociation occurs when two electronic states, one stable and the other dissociative, overlap. Upon making a transition from one stable state to a region near this overlap there is a finite probability that the molecule will follow the unstable electronic curve and break up rather than going into the stable state. This dissociation of the molecule is called predissociation. Hence, by selecting either an even or odd R or P transition in molecular iodine leading to predissociation one may, in theory, selectively destroy either the ortho or para molecules. Of course this is not the whole story as there are bound to be problems with this method, namely, collisions with paramagnetic contaminants and with iodine atoms will probably be able to cause transitions from ortho to para states (and vice-versa) in the remaining molecules. Whether a net shift of the ortho-para ratio is feasible will depend strongly upon the ability of the iodine atoms to scramble the remaining molecules . If one is not able to produce any shift in molecular iodine alone , or if one wishes to increase the shift achieved, then one needs only add a species to the system that will react preferentially with either the iodine atoms or the excited molecules .

V.S.Letokhov et al[1,2,3] have claimed to have produced a substantial change in the ortho to para ratio in systems containing molecular iodine alone and in mixtures of iodine and 2-hexene by employing precisely the aforementioned technique.

With these promising claims, my thesis project was launched with the aim of reproducing, and perhaps even improving upon the results of Letokhov et al and then studying the relaxation process of any shift produced catalysed by various paramagnetic species. The findings of these investigations are reported here, divided into four main chapters . Chapter two contains some general quantum mechanical details used to describe a homonuclear diatomic molecular system and then addresses the ortho and para symmetry properties of such a system. Specifically, the meaningfulness of these labels is addressed and some order of magnitude estimates of an ortho to para conversion (or vice-versa) mediated via collisions with paramagnetic particles or radiation are discussed .

The third chapter contains a brief history of some of the research that has been undertaken into the properties of ortho- and para-hydrogen and then presents and discusses the results of Letokhov et al .

Chapters four and five describe the investigations and results of this work in detail and then present some general conclusions drawn from the study, ending with a few suggestions for future experiments .

II. GENERAL THEORETICAL REMARKS

According to quantum mechanics, each of the possible states of a physical system are characterized by a wavefunction, $|\Psi\rangle$. It is postulated that the modulus squared of this wavefunction is the probability of finding the system in such a state $|\Psi\rangle$.

$$|\Psi|^2 = \langle\Psi|\Psi\rangle = \int \Psi^* \Psi \, d\tau \qquad (2.1)$$

Further, all observables are represented by linear Hermetian operators whose (real) eigenvalues are the possible values of their corresponding observable.

In analogy with classical mechanics, one is able to write down the Hamiltonian of the system and, in the absense of external forces, the Hamiltonian represents the total energy of the system.

$$H(\vec{p}_i, \vec{q}_i) = E(\vec{p}_i, \vec{q}_i) \qquad (2.2)$$

The Schrodinger equation is then used to solve the dynamical evolution of the system,

$$i\hbar \frac{\partial|\Psi\rangle}{\partial t} = H|\Psi\rangle = E|\Psi\rangle \qquad (2.3)$$

where the classical quantities such as position, $\bar{q}$, angular momentum, I, etc. are replaced by their corresponding quantum mechanical operators.

In the case of a diatomic molecule with Z_1+Z_2 electrons the Hamiltonian may be expressed, to first order, as

$$H = \sum_i \frac{P_i^2}{2M_i} + \sum_{j=1}^{Z_1+Z_2} \frac{p_j^2}{2m_j} - \sum_{j=1}^{Z_1+Z_2} \frac{Z_1 e^2}{r_{1j}} - \sum_{j=1}^{Z_1+Z_2} \frac{Z_2 e^2}{r_{2j}} + \frac{Z_1 Z_2 e^2}{R_{12}} + \sum_{i>j} \frac{e^2}{r_{ij}} \qquad (2.4)$$

where $\bar{P}_i$ is the linear momentum of nucleus i, $\bar{p}_j$ is the linear momentum of nucleus j, M_i is the mass of nucleus i, m_j is the mass of an electron, r_{Ij} is the distance between nucleus I and electron j, R_{12} is the internuclear distance, and r_{ij} is the distance between electrons i and j. [Note that the to this approximation, all the fine structure and hyperfine structure terms have been omitted]

Alternately, this may be generalized as,

$$H = \sum_{i=1}^{2} \frac{P_i^2}{2M_i} + \sum_{j=1}^{Z_1+Z_2} \frac{p_j^2}{2m_j} + V_e + V_n + V_{ne} \qquad (2.5)$$

An exact solution to equation (2.5) is not possible. However, owing to the fact that the electrons move much faster than the nuclei, one may approximate the wavefunction of the system as

$$|\Psi\rangle = |\psi_e\rangle|\psi_n\rangle \qquad (2.6)$$

This, the Born - Oppenheimer approximation, states that the electrons take up their equilibrium positions immediately for any given nuclear position. Mathematically, this means that first and second order derivatives of the electronic wavefunction with respect to internuclear distance may be neglected.

Following Herzberg[4], the Schrodinger equation is separated into

$$\sum_i \nabla_i^2 \psi_e + \frac{2m}{\hbar^2}(E_e - V_e - V_{ne})\psi_e = 0 \qquad (2.7a)$$

$$\sum_j \frac{\hbar^2}{2M_j} \nabla_j^2 \psi_n + (E - E_e - V_n)\psi_n = 0 \qquad (2.7b)$$

Equation (2.7a) is solved numerically for various internuclear distances to yield a plot of $E_e(R_{12})$. These results may be replaced in (2.7b) and this equation solved for the total energy of the system, E.

A. THE NUCLEAR WAVEFUNCTION

For practical purposes, $E_e + V_n$ is usually replaced by an effective potential, $U(r-r_e)$. Working in the nuclear center of mass coordinates, (2.7b) finally becomes

$$\left\{\left[\frac{1}{r^2}\frac{\partial}{\partial r}\left(r^2\frac{\partial}{\partial r}\right) + \frac{1}{r^2\sin\theta}\frac{\partial}{\partial\theta}\left(\sin\theta\frac{\partial}{\partial\theta}\right) + \frac{1}{r^2\sin^2\theta}\frac{\partial^2}{\partial\varphi^2}\right] + \frac{2\mu}{\hbar^2}(E - U(r-r_e))\right\}\psi_n = 0 \qquad (2.8)$$

where $r = R_{12}$ is the internuclear distance and μ is the reduced mass of the nuclei.

Whether or not the equation is analytically soluble depends upon the choice of effective potential. For example, if one models the nuclei as a simple harmonic oscillator, then one may separate the nuclear motion into a vibrational term and a rotational term[5]

$$\left\{\left[\frac{1}{r^2}\frac{\partial}{\partial r}\left(r^2\frac{\partial}{\partial r}\right) + \frac{\hat{R}^2(\theta,\phi)}{2r^2}\right] + \frac{2\mu}{\hbar^2}(E - V_{H.O.})\right\}\frac{1}{r}|\Psi_v\rangle|\Psi_R\rangle = 0 \qquad (2.9)$$

where

$$\hat{R}^2(\theta,\phi) = \frac{1}{\sin\theta}\frac{\partial}{\partial\theta}\left(\sin\theta\frac{\partial}{\partial\theta}\right) + \frac{1}{\sin^2\theta}\frac{\partial^2}{\partial\phi^2}$$

which yields the energy of a given rotational - vibrational state,

$$E(v,R) = BR(R+1) + \omega_e(v+0.5) - DR^2(R+1)^2 \qquad (2.10)$$

$$E_R = BR(R+1) - DR^2(R+1)^2 \qquad (2.10a)$$

$$E_v = \omega_e(v+0.5) \qquad (2.10b)$$

with the rotational eigenfunctions being spherical harmonics and the vibrational eigenfunctions are Hermite polynomials of the argument ξ where

$$\xi = r - r_e - \left(\frac{BR(R+1)r_e}{3BR(R+1) + \frac{1}{2}kr_e^2}\right) \qquad (2.11)$$

One observes that the energy of the system is dependent upon the quantum numbers v and R so that we may represent the state as

$$|v,R\rangle = \frac{1}{r}\psi_v(r-r_e)\psi_R \qquad (2.12)$$

The above approximation holds well for low vibrational and rotational states of the molecule but it breaks down for higher states. As the vibrational quantum number, v, increases so does the internuclear distance to such a point that eventually the molecule should fall apart which is obviously not the case for the simple harmonic oscillator model.

Also, for high rotational states, the nuclei are subject to centrifugal forces which tend to stretch them apart. Hence, separation of the nuclear wavefunction as a rotational part and a vibrational part is not rigorously possible.

To take these two difficulties into account anharmonicity and centrifugal distortion terms may be added to the effective potential, $U(r-r_e)$, to ultimately yield an energy of the state $|v,R\rangle$

$$E_{v,R} = \omega_e\nu - \omega_e x_e \nu^2 + \ldots \qquad (2.13)$$
$$+ [B_e - a_e\nu]R(R+1) + [D_e - \beta_e\nu]R^2(R+1)^2 + \ldots$$

(where $\nu = (v+0.5)$ here) and the total energy of the system

may be resolved as

$$E = E_e + G(v) + F(v,R) \tag{2.14}$$

where E_e is the electronic energy of the state, F(v,R) is the rotational energy, and G(v) is the vibrational energy.

B. THE ELECTRONIC CONTRIBUTION

In reality the electrons are also rotating about the nuclei and give a nonzero contribution to the net angular momentum of the system. A diatomic molecule may be treated a symmetric top in analogy with classical mechanics expressing the Hamiltonian in terms of the angular momenta, the moments of inertia of the system referred to the preferred coordinates attached to the molecule. i.e. $\bar{J}_3$ lies along the axis of symmetry of the molecule and $\bar{J}_1=\bar{J}_2$ complete the orthogonal coordinate system.

$$H_{ROT} = \frac{J_1^2}{2I_1} + \frac{J_2^2}{2I_2} + \frac{J_3^2}{2I_3} = I_1(\omega_1^2 + \omega_2^2) + I_3\omega_3^2 \tag{2.15}$$

As per usual, the body-fixed system may be related to a space-fixed one via the Euler angles[6] ϕ,χ,θ.

$$\omega_1 = \dot{\theta}\sin\chi - \dot{\phi}\sin\theta\cos\chi \tag{2.16a}$$

$$\omega_2 = \dot{\theta}\cos\chi + \dot{\phi}\sin\theta\sin\chi \tag{2.16b}$$

$$\omega_3 = \dot{\phi}\cos\theta + \dot{\chi} \qquad (2.16c)$$

Replacing these in the formula (2.15) one ultimately obtains [7]

$$H_{ROT} = \frac{p_\theta^2}{2I_1} + \frac{p_\chi^2}{2I_3} + \frac{\cos^2\theta}{2I_1\sin^2\theta}\,p_\chi^2 + \frac{p_\phi^2}{2I_1\sin^2\theta} - \frac{\cos\theta}{I_1\sin^2\theta}\,p_\phi p_\chi \qquad (2.17)$$

One replaces the p_ξ (where $\xi = \theta, \phi, \chi$) with their quantum mechanical operators,

$$p_\xi = \frac{\hbar}{i}\frac{\partial}{\partial\xi} \qquad (2.18)$$

to finally obtain an expression for the energy of a given state,

$$E = BJ(J+1) + (A-B)\Lambda^2 \qquad (2.19)$$

where J is the total angular momentum of the system excluding spin, Λ is the projection of the angular momentum along the internuclear axis, and A, B are constants proportional to the moments of inertia of the different axes of the body.

More intuitively, a diatomic molecule has an intrinsic cylindrical symmetry. Hence the total angular momentum of the system is not conserved but only the projection of the

internuclear axis, Λ. The electronic states are labelled by this quantity in analogy with atomic states, Σ (Λ=0), Π (Λ=1), Δ (Λ=2), etc.

Neglecting all fine structure and hyperfine interactions the energy of the system is independent of the net electronic spin $\bar{S}$. This results in spin degeneracy, 2S+1, for each state Λ. The total electronic angular momentum along the internuclear axis is

$$\Omega = |\Lambda+\Sigma| \qquad (2.20)$$

where Σ is the projection of the spin along the axis, and the state is labelled by

$$^{2S+1}\Lambda_{|\Lambda+\Sigma|} \qquad (2.21)$$

Several angular momenta have thus far been mentionned, $\bar{S}$, the total electronic spin, $\bar{L}$, the total electronic orbital angular momentum, and, $\bar{R}$, the rotational angular momentum of the nuclei. The problem arises that one must couple together these quantities to produce the constants of motion, if any exist. Various schemes were explored by Hund, of which the relevant case for iodine is Hund's case (a). This case is characterized by[8]

$$\Delta E_e >> \Delta E_{fs} >> \Delta E_{rot} \qquad (2.22)$$

where the first term is the difference between electronic energy states, the second is the fine structure splitting, and the third is the rotational state separation.

The coupling is accomplished as follows : the interaction of electronic and nuclear motion is very weak and the electronic motion is strongly coupled to the internuclear axis, making Λ,Σ,Ω good quantum numbers. The vector $\bar{L}+\bar{S}=\bar{K}$ is formed and added to $\bar{R}$ to form the resultant, $\bar{J}$.

This coupling leads to the rotational energy of the form,

$$E_R = B_v[J(J+1)-\Omega^2] \qquad (2.23)$$

and the eigenfunctions may be represented by the quantum numbers,

$$|\Psi\rangle = |\, S,\Sigma,\Lambda,\Omega,v,J\,\rangle \qquad (2.24)$$

Such a scheme is the case predominant for heavy molecules such as iodine. (One may further specialize this formula for cases in which $\Omega = 0$, the cases of interest for this thesis. Hence, $\bar{J} = \bar{R}$.)

C. SYMMETRY PROPERTIES OF ELECTRONIC WAVEFUNCTIONS

In addition to the above quantum numbers, electronic states are described by their symmetry properties. For

diatomic homonuclear molecules, the midpoint of the two nuclei is a center of symmetry for the molecule which shall be denoted "cs".

1. U AND G SYMMETRY

Consider $\hat{O}_e$, an operator which reflects the electronic coordinates at the cs. As $[\hat{O}_e, H_e] = 0$, then $\hat{O}_e$ is an eigenoperator of the electronic wavefunction. Further, by applying this operation twice to a given electronic state one must obtain the original state, hence the eigenvalues of this operator must be +1 or -1. Those states with eigenvalue +1 are known as g states while those with eigenvalue -1 are u states.

2. REFLECTION THROUGH THE INTERNUCLEAR AXIS

Let $\hat{O}_z$ be an operator which reflects the molecule in a plane passing through the internuclear axis. As above, this operation is an eigenoperator of the electronic wavefunction having eigenvalues +1 and -1. States having the eigenvalue +1 are labelled "+" and those having the value -1, "-". Thus a state $^1\Sigma_g^+$ is symmetric with respect to both of the above symmetry operations (eigenvalues=+1), has S=0, Λ=0, and Ω=0.

3. PARITY OF THE WAVEFUNCTION

Parity is the operator which takes all the coordinates of the particles of the system to their inverse, i.e. $\bar{r}_{ei}$ to $-\bar{r}_{ei}$ and $\bar{R}_{nj}$ to $-\bar{R}_{nj}$. As the Hamiltonian contains only even powers of the coordinates this operator commutes with the Hamiltonian and, by the same argument as before, one expects to have eigenvalues ±1.

This operator, $\hat{P}$, may be expressed as

$$\hat{P} = \hat{O}_z \hat{R} \tag{2.25}$$

where R is a rotation of the molecule by π about an axis a perpendicular to the internuclear axis through the cs and $\hat{O}_z$ is a reflection of the molecule in a plane passing through the internuclear axis and perpendicular to the axis a.

The electronic eigenfunction remains unchanged by the operation of $\hat{R}$ as it is defined as function of the electronic coordinates relative to the nuclear positions.

$$\begin{aligned} \hat{P}|\Psi\rangle &= \hat{O}_z \hat{R} |\psi_e\rangle|\psi_v\rangle|\psi_R\rangle \\ &= \hat{O}_z |\psi_e\rangle \hat{R}\{|\psi_v\rangle|\psi_R\rangle\} \end{aligned} \tag{2.26}$$

Further, the vibrational wavefunction depends only upon the relative distance between the nuclei and is therefore not affected by $\hat{R}$ either. The rotational eigenfunction for states with $\Omega=0$ (i.e. $\bar{J}=\bar{R}$) may be approximated as

$$|\psi_R\rangle = Y_{J,M}(\theta\phi) \qquad (2.27)$$

and

$$R|\psi_R\rangle = (-1)^J|\psi_R\rangle \qquad (2.28)$$

Finally the reflection, $\hat{O}_z$, acts only upon the electronic eigenfunction so that the net result becomes,

$$P|\Psi\rangle = \lambda_z(-1)^J|\Psi\rangle \qquad (2.29)$$

where λ_z is +1 for + electronic states and -1 for - states.

4. INTERCHANGE OF THE NUCLEI

The final symmetry operation to be considered for homonuclear diatomic molecules is the interchange of the nuclei, $\hat{N}$. This operation may be performed by first applying a parity operation followed by a reflection of the electronic coordinates through the cs (the u-g symmetry operation) : $\hat{N} = \hat{O}_e\hat{P}$.

$$\hat{N}|\Psi\rangle = \lambda_z\lambda_{u-g}(-1)^J|\Psi\rangle \qquad (2.30)$$

To this point all the terms coupling nuclear and electronic motion have been neglected thereby allowing one to affect a separation of the two. In reality some of these terms play an important role in the experiments which were

performed, and thus, require closer inspection.

5. FINE STRUCTURE

The fine structure Hamiltonian may be expressed as a sum of terms coupling the electronic motion and the nuclear rotation. M. Broyer[8] has studied this in detail and he expresses it as

$$H_{fs} = H_{so}+H_{ss}+H_{ro}+H_{rs} \qquad (2.31)$$

where H_{so} is the electronic spin-orbital coupling, H_{ss} is the electronic spin-spin coupling, H_{ro} is the coupling between the electronic orbital motion and the nuclear rotation, and H_{rs} is the nuclear rotation and electronic spin coupling.

M.Broyer and J.Vigué have both looked at this Hamiltonian in some detail[8,9]. Table 2.1 below, taken from reference 8, page 21, summarizes the selection rules for the fine structure Hamiltonian and compares the order of magnitude of each of the terms in the case of iodine.

Table 2.1 Estimate of the energy of the off-diagonal terms of the for molecular iodine.

TERM	$\|\Delta J\|$	$\|\Delta\Lambda\|$	$\|\Delta S\|$	$\|\Delta\Sigma\|$	$\|\Delta\Omega\|$	STRENGTH (cm^{-1})
H_v	0	0	0	0	0	200
H_{SO}	0	0,1	0,1	0,1	0	5000
H_{SS}	0	0,1,2	0,1,2	0,1,2	0	<1
H_{SR}	0	0,1	0,1	0,1	0,1	10^{-4}J
H_{RO}	0	0,1	0	0	0,1	10^{-4}J
$\hbar^2L^2/2\mu r^2$	0	0	0	0	0	0.03
$\hbar^2(\bar{L}\cdot\bar{S})/\mu r^2$	0	0	0,1	0,1	0	0.03
$-\hbar^2(\bar{J}\cdot\bar{S})/\mu r^2$	0	0	0	0,1	0,1	0.06
$-\hbar^2(\bar{J}\cdot\bar{L})/\mu r^2$	0	0,1	0	0	0,1	0.06

and $u \not\leftrightarrow g$, $0^+ \not\leftrightarrow 0^-$.

Clearly the fine structure components which are the most important are H_{so} and H_{ss}. However they can couple only states with the same value of Ω. As such, they are not of much interest for the purposes of this thesis as this means that they can couple to states several thousand cm^{-1} higher in energy than either the $B^3\Pi_{0^+u}$ or the $X^1\Sigma_g^+$ of molecular iodine, the principal states of interest in this study.

Terms like $\bar{J}\cdot(\bar{L}+\bar{S})$ from the rotational part of the Hamiltonian, however, may couple states with $\Delta\Omega=0,\pm1$. Hence the

$^1\Pi_u$ a dissociative state, may couple to the $B^3\Pi_{0^+u}$ state this way and lead to a natural predissociation.

The rotational and vibrational dependence of the predissociation of the $B^3\Pi_{0^+u}$ state was studied in detail by J.Vigué[9]. His results are summarized in Table 2.2 and in the equations for the predissociation rate below.

$$\Gamma_p^{ortho} = C_v^2 J(J+1) + 6.8a_v^2 \qquad (2.32)$$

$$\Gamma_p^{para} = C_v^2 J(J+1) + 4.7a_v^2 \qquad (2.33)$$

(taken from reference 9 page 222.)

TABLE 2.2 The Value of the Predissociation Constants $C_{v'}^2$ and $a_{v'}^2$ for the Vibrational States $9 \leq v' \leq 22$. (This table originally appeared in reference 9 page 264)

v'	$\Gamma_{rad}(v')$	$a_{v'}^2$	$C_{v'}^2$
	$10^6 s^{-1}$	$10^3 s^{-1}$	s^{-1}
9	0.9±0.15	138±35	...
10	0.82±0.12	103±35	86±35
11	0.79±0.10	52±25	59±20
12	0.72±0.07	24±10	40±18
13	0.74±0.05	8± 6	22±16
14	0.74±0.05	4± 3	3± 3
14	0.70±0.06	6± 4	3± 3
16	0.71±0.07	18±11	9± 8
17	0.70±0.08	30±14	15± 9
18	0.81±0.10	39±16	20±10
19	0.76±0.10	57±25	34±15
20	0.77±0.10	62±28	40±17
21	0.73±0.15	73±35	51±20
22	0.72±0.15	79±45	60±30

D. HYPERFINE STRUCTURE

1. ORTHO AND PARA CHARACTER

If one neglects the coupling between nuclear spin, I, and any other quantities in the molecule one may represent the nuclear wavefunction as

$$|\Psi_n\rangle = |\psi_v\rangle|\psi_R\rangle|\chi(I_1,I_2)\rangle \qquad (2.34)$$

where $|\chi(I_1,I_2)\rangle$ is the nuclear spin wavefunction.

Defining the operator $\hat{X}_I$, which interchanges the nuclear spin coordinates, one expects that the wavefunction of the molecule will be either symmetric or antisymmetric with respect to this interchange as this operator will commute with the Hamiltonian if one neglects the hyperfine terms. Indeed, using the same arguments as before, one expects that its eigenvalues will be ±1. In fact, from reference 8 page 27,

$$\hat{X}_I|I_1,I_2\rangle = (-1)^{I_1+I_2-I}|I_1,I_2\rangle \qquad (2.35)$$

The consequences of whether the nuclei behave like fermions or bosons under interchange is profound. Suppose one interchanges the nuclei as well as their nuclear spins. This is accomplished by applying the operator $\hat{N}$ which, as previously defined, interchanges the nuclear coordinates followed by $\hat{X}_I$. This results in

$$\hat{\Xi}|\Psi\rangle = \hat{X}_I\hat{N}|\Psi\rangle = \lambda_z\lambda_{u-g}(-1)^J(-1)^{I_1+I_2-I}|\Psi\rangle \qquad (2.36)$$

where I is the total nuclear spin of the system and I_1 and I_2 are the nuclear spins of atoms 1 and 2 in the molecule.

Hence if the nuclei behave like bosons then the eigenvalue on the right hand side of equation (2.37) will be +1, and if they behave like fermions then the eigenvalue will be -1. In the case of iodine in which the atoms have nuclear spin $\frac{5}{2}$ it has been observed that the nuclei behave as fermions. Thus one has

$$-1 = \lambda_z \lambda_{u-g} (-1)^{J-I+5} \qquad (2.37)$$

As these experiments dealt primarily with the $X^1\Sigma_g^+$ and $B^3\Pi_{0^+u}$ states, these will be considered explicitly. For the $X^1\Sigma_g^+$ state, after one places the appropriate eigenvalues in equation (2.37), one observes that I+J must be even. This implies that the even rotational states (J=R=even) are coupled to the even nuclear states (I=0,2,4) while the odd nuclear states (I=1,3,5) are coupled to the odd rotational states. One refers to each of these modifications as para and ortho levels respectively.

For the $B^3\Pi_{0^+u}$ state this coupling is reversed (i.e. the even rotational states are coupled to the odd nuclear states and vice-versa) owing to the change in the value of λ_{u-g}.

The expected weighting of ortho levels to para levels in the absence of any hyperfine interactions (i.e. the energy of a given state is independent of the nuclear spin

of that state) is readily determined by performing the sum $\Sigma(2I+1)$ over odd nuclear spin values, (1,3,5), for ortho and over the even possible nuclear spin values, (0,2,4), for para and dividing the two. The result is, obviously, 7:5.

E. THE EFFECTS OF HYPERFINE INTERACTIONS

A basic premise in this research is that the ortho and para character of the iodine molecule is well defined in the two electronic states of interest, at least for low rotational and vibrational states. This is not immediately apparant as the hyperfine interactions, which have thus far been neglected, do not all commute with the original Hamiltonian. Therefore the operator, $\hat{\Xi}$, is not rigorously an eigenoperator of the system and some mixing of the ortho and para levels is allowed.

The hyperfine interactions for the case of iodine have been studied in detail by M.Broyer et al[10] and is briefly outlined below.

$$H_{hf} = H_{MD} + H_{EQ} + H_{MO} + H_{EH} + \cdots \qquad (2.38)$$

where H_{MD} is a magnetic dipole term, H_{EQ} is an electric quadrupole term, H_{MO} is a magnetic octupole, H_{EH} is an electric hexadecapole, etc.

These interactions couple the nuclear spins to the nuclear rotation, electronic rotation and spin. One result of this is that the angular momentum of the molecule, $\bar{J}$, and

the total nuclear spin, $\bar{I}$, are no longer good quantum numbers but are coupled to form, $\bar{I}+\bar{J}=\bar{F}$. The wavefunctions used to describe the states now become,

$$|\Psi\rangle = | S,\Sigma,\Lambda,\Omega,v,J,I,F,M_F \rangle \qquad (2.39)$$

The hyperfine interactions are a relatively minor contribution to the total energy of the system so that one may treat H_{hf} as a perturbation on the system. The eigenstates of the total Hamiltonian, including hyperfine terms, can be constructed of states like those in equation (2.39).

$$|\Psi_{hf}\rangle = |\nu, I\rangle + \sum_{\substack{I' \neq I \\ \nu'}} \frac{\langle \nu' I' | H_{hf} | \nu I \rangle}{(E_{\nu I} - E_{\nu' I'})} |\nu' I'\rangle \qquad (2.40)$$

Furthermore, each of the terms in equation (2.38) may be subdivided as,

$$H_i = H_i(1) + H_i(2) + H_i(1,2) \qquad (2.41)$$

where i = MD,EQ,MO,EH,etc. and $H_i(j)$ is the interaction between nucleus j and the electrons, and $H_i(1,2)$ is the interaction between the two nuclei.

The order of magnitude of each term was estimated by Broyer et al for the case of molecular iodine and, according to these authors, the major contributions come from the magnetic dipole and electric quadrupole terms.

For the purpose of this thesis the terms which couple states with $\Delta I = \pm 1, \pm 3$, etc. are considered as these are the terms that will mix ortho and para levels. To determine exactly which terms will do this one needs consider the symmetry properties of each term of the hyperfine Hamiltonian, H_{hf}, explicitly.

(a) Magnetic Dipole Interaction

The magnetic dipole interaction may be expressed as (in gaussian units)

$$H_{MD}(i) = H_{LI}(i) + H_{SI}(i) + H_{FI}(i) \tag{2.42}$$

where

$$H_{LI}(i) = -\sum_e 2\mu_B \mu_N g_{I_i} \frac{\vec{I}_i \cdot \vec{l}_e}{r_{ie}^3} \tag{a}$$

$$H_{SI}(i) = -\sum_e g_s g_{I_i} \mu_B \mu_N \left\{ \frac{3(\vec{S}_e \cdot \vec{r}_{ie})(\vec{I}_i \cdot \vec{r}_{ie}) - (\vec{I}_i \cdot \vec{S}_e)(\vec{r}_{ie} \cdot \vec{r}_{ie})}{r_{ie}^5} \right\} \tag{b}$$

$$H_{FI}(i) = -\sum_e g_s g_{I_i} \mu_B \mu_N \left(\frac{8\pi}{3}\right) \vec{I}_i \cdot \vec{S}_e \, \delta(\vec{r}_{ie}) \tag{c}$$

and

$$H_{MD}(1,2) = H_{IR}(1,2) + H_{I_1 I_2}(1,2) \tag{2.43}$$

$$H_{IR}(1,2) = 2(2g_I - 1) \sum_{M_N} \mu_N^2 (\vec{I}_1 + \vec{I}_2) \cdot \vec{R} \tag{a}$$

$$H_{I_1 I_2}(1,2) = -g_I^2 \mu_N^2 \left\{ \frac{3(\vec{I}_1 \cdot \vec{r}_{12})(\vec{I}_2 \cdot \vec{r}_{12}) - (\vec{I}_1 \cdot \vec{I}_2)(\vec{r}_{12} \cdot \vec{r}_{12})}{r_{12}^5} \right\} \tag{b}$$

(b) Electric Quadrupole

Following Broyer again,

$$H_{EQ}(i) = \sum (-1)^m Q^2_m(p)\, V^2_{-m}(e) \qquad (2.44)$$

$$Q^2_m(p) = \sqrt{\frac{4\pi}{5}}\, e r_p^2\, Y_{2m}(\theta,\phi) \qquad (a)$$

$$V^2_m(e) = \sqrt{\frac{4\pi}{5}}\, \frac{e}{r_e^3}\, Y_{2m}(\theta,\phi) \qquad (b)$$

However, it is more instructive to rewrite the quadrupole interaction following Ramsey[11]

$$H_{EQ}(i) = -\frac{e\,Q}{I_i(2I_i-1)(2J-1)(2J+3)} \left(\frac{\partial^2 V_e}{\partial z^2_{inter}}\right)_{Av.} \left\{3(\vec{I}_i\cdot\vec{J})^2 + \tfrac{3}{2}(\vec{I}_i\cdot\vec{J}) - \vec{I}_i^2 J^2\right\}$$

where $Q = \langle I_z = I \mid \frac{3z_p^2 - r_p^2}{2} \mid I_z = I \rangle$ (2.45)

V_e is electric potential created by the electrons about the nucleus.

Finally,

$$H_{EQ}(1,2) = \sum_m (-1)^m \left\{ Q^2_m(1)\, V^2_{-m}(1,2) + Q^2_m(2) V^2_{-m}(2,1) \right\} \qquad (2.46)$$

where $Q^2_M(i)$ and $V^2_{-M}(1,2)$ are defined by equations (2.44a) and (2.44b) respectively.

(c) Symmetry Properties

The symmetry properties of each of the terms in the hyperfine Hamiltonian are discussed in detail in reference 8 pages 34-36. To summarize,

$$\langle \nu', u, I' | H_{hf}(2) | \nu, u, I \rangle = (-1)^{I+I'} \langle \nu', u, I' | H_{hf}(1) | \nu, u, I \rangle \tag{2.47}$$

$$\langle \nu', g, I' | H_{hf}(2) | \nu, u, I \rangle = (-1)^{I+I'+1} \langle \nu', g, I' | H_{hf}(1) | \nu, u, I \rangle \tag{2.48}$$

$$\langle \nu', u, I' | H_{hf}(1,2) | \nu, u, I \rangle = (-1)^{I+I'} \langle \nu', u, I' | H_{hf}(1,2) | \nu, u, I \rangle \tag{2.49}$$

$$\langle \nu', g, I' | H_{hf}(1,2) | \nu, u, I \rangle = 0 \tag{2.50}$$

From equations (2.47) to (2.50) one may observe that the part of the hyperfine Hamiltonian which acts between the nuclei, ($H_{hf}(1,2)$), can couple only u to u states or g to g states and not mix ortho and para levels. On the other hand, the hyperfine terms acting between the individual nuclei and the electrons can couple ortho and para states in separate u and g electronic states. (i.e. an ortho level in a "u" electronic state can mix with a para level in a "g" electronic state.)

The strength of this mixing due to the magnetic dipole and electric quadrupole terms is estimated in Appendix A yielding the result

$$\langle \nu', u, I' | H_{MD}^{o-p} + H_{EQ}^{o-p} | \nu, g, I \rangle \simeq 10^{-2} cm^{-1} \tag{2.51}$$

so that equation (2.40) becomes

$$|\Psi\rangle = |\nu, I\rangle + \left(\frac{10^{-2} cm^{-1}}{E_{\nu,I} - E_{\nu',I+1}} \right) |\nu', I+1\rangle + \left(\frac{10^{-2} cm^{-1}}{E_{\nu,I} - E_{\nu',I-1}} \right) |\nu', I-1\rangle$$

For the ground state of iodine, $X^1\Sigma_g^+$, the nearest state with which it may couple an ortho and para level is the $^3\Pi_{1u}$ or a $^3\Pi_{0u}$ which lie roughly ten thousand cm^{-1} above the ground state, making the strength of the coupling of the order of 10^{-6}.

$$|\Psi\rangle \simeq |\nu,g,I\rangle + 10^{-6}|\nu',u,I+1\rangle + 10^{-6}|\nu',u,I-1\rangle \quad (2.52)$$

Hence the ortho and para character of the molecular ground state is well preserved even when the hyperfine interactions are taken into account.

In the case of the $B^3\Pi_{0^+u}$ electronic state, however, this is not so obvious especially near the dissociation limit, v'=87. In this region many electronic states lie close together so that the energy difference in the denominator of equation (2.40) becomes much smaller and the Franck-Condon overlap integrals may be large enabling a significant u–g ortho and para level mixing. In fact, J.Pique et al[12] have recently reported such hyperfine induced symmetry breaking near the B state dissociation limit in iodine.

In this work only low lying vibrational levels were used ($v' \leq 43$). For these states the nearest g states that may couple are the $^3\Pi_{0g}$ or the $^1\Pi_{0g}$ which are roughly four thousand cm^{-1} above the states of interest. Hence the strength of the coupling here is of the order of 10^{-5}. Again this is negligible and the ortho and para character is well

maintained.

$$|\Psi\rangle \simeq |\nu,u,I\rangle + 10^{-5}|\nu',g,I+1\rangle + 10^{-5}|\nu',g,I-1\rangle \quad (2.53)$$

1. RADIATIVE DECAY

Another method of going from an ortho state to a para state is through the spontaneous emission of a photon resulting in such a decay. In the absense of hyperfine interactions this process is strictly forbidden inside a given electronic state via a dipole interaction. However, as has been seen, the hyperfine Hamiltonian weakly couples u and g ortho and para states and thereby allows these transitions. It is expected that the probability of such a transition is extremely low owing to the weakness of the ortho and para coupling and this is indeed the case as is outlined below.

Raich and Good[13] addressed this problem in detail for the case of molecular hydrogen. Their calculation is used as a guide to obtain an estimate of the transition probability in the case of a ground state iodine molecule. (Only the ground state is considered as during an experiment any given molecule is in the $B^3\Pi_{0^+u}$ state for a short period of time $\simeq 10^{-6}$ seconds per excitation.)

The transition probability is given by

$$W_{if} = \frac{4}{3}\frac{\omega^3}{\hbar c^3}\,\vec{\mu}^*\cdot\vec{\mu} \quad (2.54)$$

where $\vec{\mu}$ is the dipole transition moment between a ground state ortho level and para level, and $\hbar\omega$ is the energy of the emitted photon.

Thus one estimates μ as

$$\vec{\mu} = 10^{-6}\langle X^1\Sigma_g^+, J, I|\Sigma e\vec{r}_i|\nu', J', I'\rangle + 10^{-6}\langle\nu'', J'', I''|\Sigma e\vec{r}_i|X^1\Sigma_g^+, J, I\rangle \tag{2.55}$$

where $I', I'' = I \pm 1$. This leads to

$$\vec{\mu} \simeq 4\cdot 10^{-6}(\bar{R}^{dipole}) \tag{2.56}$$

Thus,

$$\vec{\mu}^*\cdot\vec{\mu} \simeq 16\cdot 10^{-12}|\bar{R}^{dipole}|^2 \tag{2.57}$$

The value of $|\bar{R}^{dipole}|^2$ may be estimated from the mean lifetime of transitions between the X to B states by

$$\bar{\tau} = \frac{3h}{64\pi^4 \nu_{nm} |R^{dipole}|^2} \tag{2.58}$$

where ν_{nm} is the transition from state n to m in cm^{-1}. With this equation (2.54) becomes

$$W_{if} \cong \frac{4}{3}\frac{\omega^3}{\hbar c^3}(16\times 10^{-12})\frac{3\hbar}{32\pi^3\nu_{nm}^3\bar{\tau}} \tag{2.59}$$

$$W_{if} \cong \frac{8B_v^2(1.6\times 10^{-11})}{\nu_{nm}^3\bar{\tau}} J^3$$

Using the values $\nu_{nm} \simeq 10^{4}cm^{-1}$, and $\tau \simeq 10^{-6}$ seconds from Vigué[9], and $B_v \simeq 0.0375cm^{-1}$ from Herzberg[4] one ultimately obtains for the transition probability,

$$W_{if} \simeq \left(\frac{J^3}{4.7\times10^{12}yr}\right) \qquad (2.60)$$

Thus the probability of a transition from an ortho-iodine state to a para-iodine state (or vice-versa) via dipole radiation in the $X^1\Sigma_g^+$ electronic state is completely negligible over the course of an experiment.

2. COLLISIONALLY INDUCED ORTHO-PARA TRANSITIONS

Finally, a homonuclear diatomic molecule possessing ortho and para modifications may transit between the two only if the nuclear spin of one of the nuclei can be reoriented with respect to the other. This is difficult to do but may be accomplished by bringing the molecule in contact with a magnetic or electric field gradient across the nuclei. Such a condition occurs when the molecule collides with a paramagnetic species. In fact, the para to ortho relaxation in molecular hydrogen has been studied by A.Farkas[14] in just such a manner. The theoretical basis for this effect was introduced by Wigner[15] and refined by Kalker and Teller[16] circa 1934. Following these authors, the effect may be viewed as follows:

Upon collision with a paramagnetic particle, the nuclei of the diatomic molecule feel an inhomogenous magnetic field set up by the magnetic moment, μ_c, of the colliding species. This, treated as a perturbation, may be written as

$$V' = \mu_p[\bar{I}_1 \cdot \bar{H}_c(\bar{r}_1) + \bar{I}_2 \cdot \bar{H}_c(\bar{r}_2)] \qquad (2.61)$$

where $\bar{H}_c(\bar{r}_i)$ is the magnetic field set up by the paramagnetic colliding species at nucleus "i".

The potential, V', may be symmetrized and antisymmetrized as

$$V_S' = \frac{\mu_p}{2}[(\bar{I}_1+\bar{I}_2)\cdot(\bar{H}(\bar{r}_1) + \bar{H}(\bar{r}_2))] \qquad (2.62a)$$

$$V_A' = \frac{\mu_p}{2}[(\bar{I}_1-\bar{I}_2)\cdot(\bar{H}(\bar{r}_1) - \bar{H}(\bar{r}_2))] \qquad (2.62b)$$

The antisymmetric part alone is capable of producing an ortho-para transition and, thus, this is the part which will be considered here. As $\bar{I}_1-\bar{I}_2 = 2\bar{I}-\bar{I}_1$, and knowing that only the $2\bar{I}_1$ part may couple states with $\Delta I=\pm 1$, i.e. ortho states to para states, then the effective potential, U, may be written as

$$U = \mu_p[\bar{I}_1 \cdot (\bar{H}(\bar{r}_1) - \bar{H}(\bar{r}_2))] \qquad (2.63)$$

Expanding the $(\bar{H}(\bar{r}_1) - \bar{H}(\bar{r}_2))$ term as

$$[\vec{H}(\vec{r}_1) - \vec{H}(\vec{r}_2)]_i \simeq \sum_j \frac{\partial \vec{H}_i}{\partial x_i}(x_{1j} - x_{2j}) \qquad (2.64)$$

and letting

$$\frac{\partial \vec{H}_i}{\partial x_j} = \frac{3\mu_c}{r^4}\delta_{ij} \qquad (2.65)$$

one finally obtains

$$U = \frac{3\mu_p\mu_c}{r^4}\left[\frac{I_{i+}(X_-) + I_{i-}(X_+)}{2} + I_{iz}X_z\right] \qquad (2.66)$$

where $X_i = (x_1 - x_2)_i$.

For the purposes of an order of magnitude calculation one may approximate the potential as

$$U \simeq \frac{9\mu_p\mu_c}{r^4} R_N I_{sz} \cos\theta \qquad (2.67)$$

where R_N is the internuclear distance, and θ is the angle between a space-fixed axis and the internuclear axis.

Using the potential in (2.67) as a time dependent perturbation and representing the wavefunction of the system as

$$|\Psi\rangle = \Sigma\, a_n(t)|\psi_n\rangle \mathrm{EXP}-(i\frac{E_n t}{\hbar}) \qquad (2.68)$$

where the $|\psi_n\rangle$ are the time independent solutions to the unperturbed Hamiltonian. Solving the Schrodinger equation lead to the well known solution for the $a_1(t)$

$$a_\ell(t) \simeq \frac{2i\langle \psi_\ell | U | \psi_k\rangle}{(E_k - E_\ell)} e^{-\frac{i\omega_{k\ell}t}{2}} \sin\left(\frac{\omega_{k\ell}t}{2}\right) \qquad (2.69)$$

and, thus, the probability of transition from a state $|\psi_k\rangle$ to a state $|\psi_1\rangle$ is

$$|a_l(t)|^2 \sim \frac{4|\langle \psi_l | U | \psi_k \rangle|^2}{(E_k - E_l)^2} \sin^2\left(\frac{\omega_{kl}}{2} t\right) \qquad (2.70)$$

In the case of iodine the unperturbed states have the form, $| S,\Sigma,\Lambda,\Omega,v,J,I,F,M_F >$ so that the matrix element, M, becomes

$$M = d\langle S',\Lambda',\Omega',v',J',I',F',M_F'| \; I_{1z}\cos\theta \; |S,\Sigma,\Lambda,\Omega,v,J,I,F,M_F\rangle \qquad (2.71)$$

where $d = (9\mu_p\mu_c R)/r^4$ Evaluating this with the help of Appendix A one obtains

$$M \simeq dI_1\xi_J\delta(J',J\pm1)\delta(I',I\pm1)\langle v'|v\rangle \qquad (2.72)$$

where ξ_J is the matrix element, $\langle J',\Omega'|\cos\theta|J,\Omega\rangle$.

Thus,

$$\left|a_{I\pm1}^{J\pm1}\right|^2 \sim \frac{4\cdot81\,\mu_p^2\mu_c^2}{r^8} R_N^2 I_1^2 \xi_{J\pm1}^2 |\langle v'|v\rangle|^2 \sin^2\left(\frac{\Delta E^{J,J\pm1}}{\hbar} t\right) \qquad (2.73)$$

The most probable transitions will occur in cases where the energy difference between the two levels is the least. This means a transition between different rotational levels alone so that

$$\left|a_{J\pm1}^{v'=v}\right|^2 \sim \frac{81\,\mu_p^2\mu_c^2 R_N^2 I_1^2 \xi_{J\pm1}^2}{r^8 B_v^2 J^2} \sin^2\left(\frac{2B_v J}{\hbar} t\right) \qquad (2.74)$$

From equation (2.74) it is immediately recognized that the probability of an ortho to para transition upon collision with a paramagnetic particle is very sensitive to the point of impact, r, and to the spacing of the rotational energy levels, B_v. For example, all other factors being equal, except for nuclear spin, the difference of the rotational spacing between hydrogen and iodine, and the rotational quantum numbers, one observes that the ratio of transition probabilities for each of these molecules is

$$R = \frac{W_{o\text{-}p}^{I_2}}{W_{o\text{-}p}^{H_2}} \simeq \frac{B_{v_{H_2}}^2 J_{H_2}^2 I^2 \sin^2\left(\frac{B_{v_{I_2}} J_{I_2} t}{\hbar}\right)}{B_{v_{I_2}}^2 J_{I_2}^2 I_{H_2}^2 \sin^2\left(\frac{B_{v_{H_2}} J_{H_2} t}{\hbar}\right)}$$

$$\left(\frac{I_{I_2}^2}{I_{H_2}^2}\right) \lesssim R \lesssim \left(\frac{B_{v_{H_2}}^2 J_{H_2}^2 I_{I_2}^2}{B_{v_{I_2}}^2 J_{I_2}^2 I_{H_2}^2}\right)$$

$$25 \lesssim R \lesssim 6 \times 10^5 \qquad (2.75)$$

As the spacing of the rotational levels of molecular iodine is quite small, one expects it to be quite sensitive to such collisionally induced transitions.

In effect, the hyperfine mixing of ortho and para levels in the $X^1\Sigma_g^+$ and $B^3\Pi_{0^+u}$ states (at least for low lying vibrational levels) and the radiative coupling of such states is completely negligible. Paramagnetic catalysed ortho to para transitions in iodine, however, may play a very important role in scrambling any ortho- and para-iodine separation attempted.

III. PREVIOUS RESULTS

This chapter is divided into two parts ; first , past experiments involving ortho- and para-hydrogen will be reviewed and their relevance as regards molecular iodine is presented . Second , some recent experiments carried out by V.S.Letokhov et al on ortho- and para-iodine will be summarized .

A. ORTHO - AND PARA - HYDROGEN

As has been discussed previously, homonuclear diatomic molecules possess ortho and para modifications . In the case of both hydrogen and iodine , whose ground electronic states are $^1\Sigma_g^+$ and whose nuclei both obey Fermi-Dirac statistics , the even rotational levels are coupled to the even nuclear spin states (para states) while the odd nuclear spin states (ortho states) are coupled to the odd rotational levels . By adding up the total number of states possible for ortho modifications and para modifications for a nucleus with spin I_1 , one obtains the fact that the intensities of an ortho rotational transition to a para transition should follow

$$R = \frac{\mathcal{I}^{ortho}}{\mathcal{I}^{para}} = \frac{I_1 + 1}{I_1}$$

$$I_1^{\mu_2} = \frac{1}{2}$$

$$I_1^{I_2} = \frac{5}{2} \qquad (3.1)$$

For hydrogen the existence of ortho and para forms was postulated by Heisenberg[18] and Hund[19] and such intensity alternation was observed.

In equilibrium, the ratio of ortho-hydrogen to para-hydrogen may be written using the partition function,

$$\frac{N^o}{N^p} = \frac{\sum_{J\,odd} g_J g^o e^{-\frac{E(v,J)}{kT}}}{\sum_{J\,even} g_J g^p e^{-\frac{E(v,J)}{kT}}} \qquad (3.2)$$

where E(v,J) is the energy of the rotational and vibrational state characterized by the quantum numbers v, and J, g^o or p is the nuclear spin degeneracy of the ortho or para states (3 and 1 respectively for hydrogen) and $g_J = 2J+1$ is the rotational degeneracy of the state. Table 3.1 shows some values of the ortho to para ratio at various temperatures. (taken from reference 14 page 14)

TABLE 3.1 Parahydrogen to Orthohydrogen Ratio at Various Temperatures.

Temperature (K)	Parahydrogen Orthohydrogen	Percent Parahydrogen
20	544.8	99.82
50	3.327	76.89
80	0.9377	48.39
100	0.6262	38.51
150	0.3994	25.72
210	0.3463	25.54
273	0.3357	25.13
∞	0.3333	25.00

From these results it would appear that a simple way to enhance the para to ortho ratio in hydrogen is to simply cool the molecules down from room temperature. This follows one's intuition that, as the hydrogen cools, the molecules are expected to fall into their lowest energy state, J=0, a parahydrogen state. Unfortunately, when this was first tried no such enhancement was obtained owing to the nonmixing of ortho and para states discussed in chapter 2. An alternate technique used by Harteck and Bonhoeffer[20,21,22,23] was to cool the hydrogen over charcoal. As the gas was adsorbed ortho and para character could be changed probably due to some paramagnetic surface effects. Hence, a sample containing a

specified fraction of parahydrogen could be prepared and, courtesy of the nonmixing of the two species, could be stored for long periods even at room temperature.

Much work was carried out on the conversion of orthohydrogen to parahydrogen and vice-versa circa 1930. Two methods of this conversion will be considered here, namely by exchange of a hydrogen atom,

$$H + o\text{-}H_2 \longleftrightarrow p\text{-}H_2 + H \qquad (3.3)$$

and via collisions with paramagnetic species

$$X + o\text{-}H_2 \longleftrightarrow p\text{-}H_2 + X \qquad (3.4)$$

1. HYRDROGEN ATOM EXCHANGE

Bonhoeffer and Harteck[21,22] investigated the possibility of ortho to para conversion in hydrogen due radiation by filling a container with 200 torr of normal hyrogen (ratio of 3:1) and placing it in liquid air. Absolutely no conversion was observed over the course of four weeks showing that the radiative conversion does not occur rapidly, if at all.

Next some hydrogen was placed in a brass container and kept at 150 atmospheres pressure at liquid air temperature. Conversion to parahydrogen was observed here and attributed to a catalytic wall reaction by Farkas. In fact several

different materials were tested by Bonhoeffer and Farkas[14] and it is notable that they found that even glass vessels catalysed the conversion. (at 2 atmospheres pressure and -185°C a sample went from 25 to 30 percent parahydrogen in 6 days)

A.Farkas studied the reaction of hydrogen atoms on parahydrogen molecules by preparing a cell with 47 percent parahydrogen and then placing the sample in an oven to elevate the temperature to between 700°C and 800°C. This results in spontaneous production of hydrogen atoms and their effect upon the ortho to para ratio was studied. The time dependence of the parahydrogen concentration, p_t, was observed to follow,

$$(p_t - p_\infty) = (p_0 - p_\infty)\mathrm{EXP}-(k[H]t) \qquad (3.5)$$

where p_0 is the original parahydrogen concentration, and p_∞ is the equilibrium concentration. This formula agrees with the mechanism described in equation (3.3). Indeed, it may be deduced that the value for k is four times the ortho to para conversion rate. From Farkas' results k may be written as

$$k \simeq 1.186 \cdot 10^9 \sqrt{T}\ \mathrm{EXP}-(5500/RT) \qquad (3.6)$$

measured in liters per mole per second.

Experiments performed by Geib and Harteck[25] in which hydrogen atoms were introduced into a system of enriched

parahydrogen yielded values for k of the same order of magnitude as that given above. Using these results (as the experiments of Geib and Harteck were performed in a temperature range of 10° to 100°C) one may estimate the half-life of the conversion as

$$\tau_{\frac{1}{2}} = \frac{\ln 2}{k[H]} \simeq \Big|_{273K} \frac{7.6\times10^{-6}}{[H]} \frac{mole\cdot s}{l} \qquad (3.7)$$

2. PARAMAGNETIC CONVERSION

Farkas and Sachsse[26] also investigated the homogeneous conversion of parahydrogen to normal hydrogen catalysed by various paramagnetic impurities such as oxygen and nitric oxide. The theoretical treatment of this effect has already been given in chapter 2 and the results of the experimental investigations are given below.

Starting with a given amount of orthohydrogen, o, and parahydrogen, p, the action of a paramagnetic species, X, on hydrogen is described by equation (3.4). Indeed, an identical time dependence for the parahydrogen is obtained as given in equation (3.5),

$$(p_t - p_\infty) = (p_o - p_\infty)\mathrm{EXP}-(k[X]t)$$

In the case of oxygen as the paramagnetic species, Farkas and Sachsse determined that the order of magnitude of this conversion, k, was about 9.2 liters per mole per minute to yield a halflife of $\tau_{\frac{1}{2}} = \frac{\ln 2}{k[O_2]} \simeq \frac{4.50}{[O_2]} \frac{mole\cdot s}{l}$ (3.8)

Nitric oxide yielded very similar results to these, however, in the case of nitric oxide only those molecules which are in the electronic state $^2\Pi_{\frac{3}{2}}$ are paramagnetic. Hence equation (3.5) should read,

$$(p_t - p_\infty) = (p_0 - p_\infty)\mathrm{EXP}-(k[NO^*]t) \qquad (3.9)$$

where $[NO^*]$ is the concentration of paramagnetic nitric oxide. Again, one may estimate the rapidity of the conversion through the halflife ,

$$\tau_{\frac{1}{2}} \simeq \frac{\ln 2}{k[NO^*]} \simeq \frac{1.10}{[NO^*]} \frac{\text{mole}\cdot\text{s}}{\text{l.}} \qquad (3.10)$$

By comparing the three values for 1 torr of each substance one has

$$\tau_{\frac{1}{2}}^{H} << \tau_{\frac{1}{2}}^{NO^*} < \tau_{\frac{1}{2}}^{O_2} \qquad (3.11)$$

Hence the ability of hydrogen atoms to scramble ortho and parahydrogen far outweighs the ability of the other two. Hence, if one assumes a similar behaviour in iodine it would seem useful to perform experiments in which as few free atoms are produced as possible and also to use test cells that are as free from contamination (by air) as possible.

B. ORTHO AND PARA ENHANCEMENT IN IODINE

Iodine, as hydrogen, displays ortho and para modifications. Unfortunately, unlike hydrogen, the fraction of para-iodine is not enhanced by simply cooling molecular iodine over charcoal. This becomes clear if one considers the ratio of para-iodine to ortho-iodine as a function of temperature as shown in Table 3.2.

TABLE 3.2 Para-Iodine to Ortho-Iodine versus Temperature

Temperature (K)	para-iodine ortho-iodine	percent para-iodine
0.2	51.800	98.1
0.4	3.517	77.9
0.6	1.464	59.4
0.8	0.9924	50.2
1.0	0.8282	45.3
10.0	0.7143	41.7
50.0	0.7143	41.7
100.0	0.7143	41.7
300.0	0.7143	41.7
∞	0.7143	41.7

(These values have been calculated using the rotational and vibrational constants supplied by Herzberg[4] and performing the summation over states J"=0 to 101 and v"=0 to 5.)

As the rotational level spacing is much closer in iodine as compared to hydrogen one must go to much lower temperatures to obtain a substantial para-iodine enhancement. However, at such low temperatures molecular iodine forms a solid and has no vapour pressure at all. (i.e. at -70°C the vapour pressure of iodine is roughly 10^{-6} torr.) Hence, if iodine forms a molecular solid then, because of the nonmixing of ortho and para states, the system will not spontaneously go over into the equilibrium

ratio for that temperature and if iodine forms an atomic solid, then upon heating up the sample enough to obtain substantial vapour pressure, the vapour will immediately take on the equilibrium ratio for that temperature which will be, for all intents and purposes, the usual 7:5.

Another method of separation is required, then. The first people to carry out an experiment which hinted at the possibility of a separation of ortho- and para-iodine were R. M. Badger and J. W. Urmston[27]. In 1930 these men carried out an experiment on molecular iodine in the presence of 2-hexene. Their idea was to preferentially excite the ortho-iodine molecules with the 5461 Å mercury line and have these molecules react with a suitable agent, 2-hexene.

The mercury 5461 Å line was shone into a cell containing 170 mtorr of iodine and 6 torr of 2-hexene for 24 hours. After this time the authors claimed that 50% of the iodine had reacted. The contents of the test cell were tested for any ortho to para enchacement by holding a second container filled with the same amount of 2-hexene beside the test cell and filling it with iodine vapour until an observer decided that the color in the two cells matched. Next, white light from a tungsten lamp was passed through the two cells and their fluorescence intensities compared. The white light fluorescence was judged to be the same in the two cells while the 5461 Å mercury line's fluorescence was judged to be weaker in the test cell. From these results, (albeit qualitative) it was concluded that some

enhancement had been obtained. However, no further work on the matter was forthcoming to the best of my knowledge.

1. THE EXPERIMENTS OF V. S. LETOKHOV ET AL

After a forty year interlude and the advent of the laser the subject was taken up once again by V. S. Letokhov et al. In a paper published in 1973[1] it was reported that a partial ortho- to para-iodine ratio enhancement had been achieved. The technique employed was the following : a cylindrical test cell of length 6 cm and volume 20 cm^3 was filled with 250 mtorr of iodine vapour. This cell was then irradiated with the 5145 Å line of an argon ion laser which excites the $B^3\Pi_{0^+u} \rightarrow X^1\Sigma_g^+$ (43'-0") P(13) and R(15) transitions of molecular iodine. Both of these transitions involve ortho states and lead to some predissociation. Hence, by selectively exciting and breaking up the ortho-iodine molecules Letokhov et al were able to obtain a shift ortho to para ratio.

Experimentally, the authors observed the argon ion induced fluorescence intensity decrease over a 10 to 20 minute period and then level off. It was claimed that the total number of iodine molecules remained constant as they were monitored with the 5461 Å line a mercury arc lamp with a 4 cm^{-1} linewidth and the fluorescence induced remained constant. Hence a shift in the ratio had occurred.

The dominant reactions were claimed to be

$$o\text{-}I_2 \longrightarrow 2I \qquad W$$

$$I + o\text{-}I_2 \longleftrightarrow p\text{-}I_2 + I \qquad X$$

$$2I \longrightarrow o\text{-}I_2 \text{ or } p\text{-}I_2 \qquad k$$

which leads to the equilibrium conditions,

$$o\text{-}I_2(\infty) = \frac{I}{24} C \left[1 + \frac{p^2}{2} - p\left(\frac{p^2}{4}+1\right)^{\frac{1}{2}} \right] \tag{3.12}$$

$$p\text{-}I_2(\infty) = \frac{C}{2} + \frac{W}{16k} - \frac{I}{24} C \left[-\frac{p}{2} + \sqrt{\frac{p^2}{4}+1} \right]^2 \tag{3.13}$$

$$I(\infty) = \sqrt{\frac{7CW}{24K}} \left[-\frac{p}{2} + \sqrt{\frac{p^2}{4}+1} \right] \tag{3.14}$$

where $p = \sqrt{\frac{kW}{7.24C}} \left(\frac{10}{X} + \frac{7}{k} \right)$

C is the total number of iodine atoms present in the system in any form.

and assuming that the exchange rate, X, is much less than the recombination rate, k, one has,

$$p = \frac{5}{2} \sqrt{\frac{kW}{2I}} \frac{1}{k_c} \tag{3.15}$$

with

$$K_c = X\left(\frac{C}{2}\right)$$

However, there are two main difficulties with this paper; first, the vapour pressure of the iodine reported in

this paper corresponds to a temperature of about 22°C, very close to room temperature. This is undesirable as some crystals of iodine may form if the temperature drops. Such crystals could act both as a source of iodine and as a site for scrambling of ortho and para iodine both of which are bad from the point of view of an enhancement. Second, if one uses the data provided by the authors and substitutes this into the formula for the fluorescence intensity of the ortho-iodine at t=0 to t=∞ one obtains,

$$\frac{I_{fl}(0)}{I_{fl}(\infty)} = 0.998 \qquad (3.16)$$

at a laser power of 0.4 W in contradiction with the observed value of 1.7.

Another paper by V. S. Letokhov and V. A. Semchishen[39] appeared in 1974 in which the work of Badger and Urmston was built upon. A test cell 4 centimeters in length and 3 cm^3 in volume was prepared with 0.2 torr of iodine vapour and 2.8 torr of 2-hexene. As before, the reaction was driven by the 5145 Å line of an argon ion laser. This time, periodically during the experiment, the argon ion 5017 Å line was sent through the test cell to monitor the para-iodine concentration as this frequency excites the $B^3\Pi_{0^+u} \leftarrow\!\!\rightarrow X^1\Sigma^+_g$ (62'-0") P(26) transition. The results of this experiment are shown in figure 3.1.(taken from reference 2)

Notice that the ortho-iodine fluorescence decreased over a period of an hour to roughly 5 to 6 % of the original

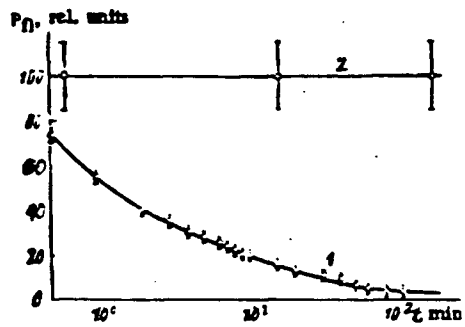

Figure 3.1 The above plot of the fluorescence induced by the 5145 Å, (1), and the 5017 Å, (2), argon ion laser lines in a mixture of 0.2 torr of iodine and 2.8 torr of 2-hexene is taken from reference 2. The 5145 Å line excites primarily ortho-iodine while the 5017 Å excites primarily para-iodine.

signal while the para-iodine fluorescence remained constant during this time.

The mechanism proposed for the reaction was a direct addition of an excited iodine molecule to the 2-hexene and no radical chain formation. If, indeed, a radical chain were the process by which the two species reacted then iodine atoms would be formed and by analogy with the case of hydrogen, these atoms would be expected to efficiently scramble the molecules. Hence, based on these results, an enrichment factor of almost 100% could be realized by this technique.

A final paper on this subject was produced by V. I. Balykin, V. S. Letokhov, V. I. Mishin, and, V. A. Semchishen[3] in 1976 which reviewed the previous results and in some instances contradicted previous findings. (For example, the claim that a shift in the ortho to para ratio is observable in a cell filled with 250 mtorr of iodine is refuted and, in the case of iodine plus 2-hexene, the observation that the para-iodine fluorescence remained constant was also contradicted.)

The technique involved in the experiments have previously been described and relied upon selective laser action to drive the process. In these experiments a molybdenum glass cell 12.5 cm long with 6 cm^3 volume, and 20 cm^2 surface area was evacuated to about 10^{-4} torr and then filled with the desired constituents.

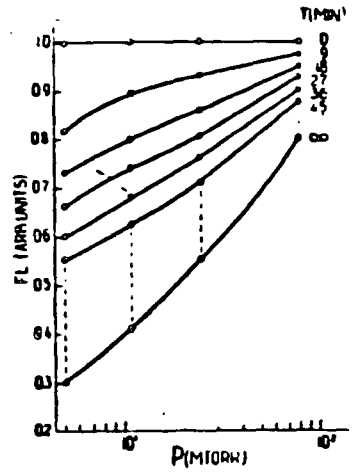

Figure 3.3 The fluorescence decay of iodine cells as a function of initial iodine pressure.(from reference 3)

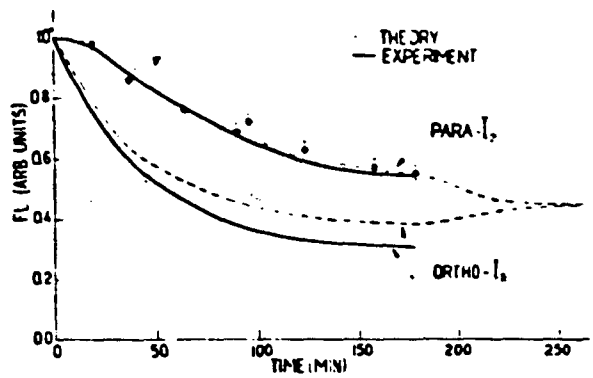

Figure 3.2 Fluorescence induced by the 5145 Å and 5017 Å argon laser lines reported by Letokhov et al in reference 3 observed in a cell containing 5 mtorr of iodine vapour.

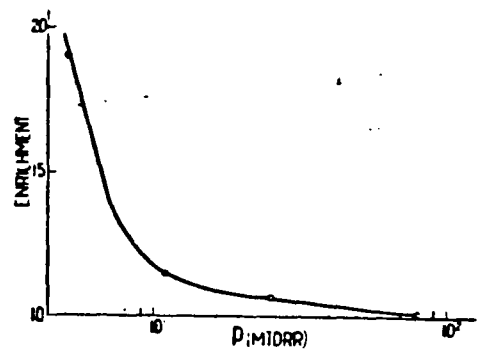

Figure 3.4 The Enrichment coefficient for ortho- to para-iodine as a function of initial iodine pressure. Notice that at low pressures enrichment coefficients of up to 2 are claimed by Letokhov et al while above about 80 mtorr no enrichment is observed. (from reference 3)

The results of the iodine vapour alone in the cell are summarized concisely on figures 3.2 to 3.5 taken from reference 3. The fluorescence of the ortho and para signals both decay but by different amounts.

An enrichment coefficient, E, defined by,

$$E = \frac{o\text{-}I_2(t) \; : \; p\text{-}I_2(t)}{o\text{-}I_2(o) \; : \; p\text{-}I_2(o)} \qquad (3.17)$$

where $o\text{-}I_2(t)$ and $p\text{-}I_2(t)$ are the ortho-iodine and para-iodine concentrations at time "t".

As can be seen, above 80 mtorr of initial iodine pressure no enrichment is observed and the enrichment increases as one decreases the initial iodine vapour pressure. However, as previously stated, this is in contradiction with the original paper on the subject as to the ability to obtain an enhancement at high iodine pressure and the mechanism involved.

The mechanism prescribed by Letokhov for the system involved having the atoms produced by selective predissociation adsorb onto the walls of the test cell. Hence, this mechanism effectively removes the atoms from the system to some extent. The process does not proceed 100 percent as the atoms are able to come off the walls again and scramble the iodine molecules that strike the adsorbed atoms according to the authors.

Following Letokhov's description of the system one has the paramters : N, the ortho iodine concentration, n, the para-iodine concentration, m, the vapour phase iodine atom concentration, m', the concentration of adsorbed iodine atoms, α, the predissociation rate constant, β, the ortho-para scrambling rate constant, δ, the iodine atom recombination rate, K, the adsorption rate constant, and, K', the desorption rate constant. With these so defined the reaction mechanism for the iodine vapour system is,

$$N \longrightarrow 2m$$

$$m \longleftrightarrow m'$$

$$m' + N \longleftrightarrow n + m'$$

$$m \longrightarrow \tfrac{1}{2}N, \tfrac{1}{2}n$$

The mathematical description presented by the authors require the assumptions that (1) the fluorescence signal decay is due solely to the disappearance of iodine molecules, (2) the scrambling of ortho- and para-iodine occurs primarily on the walls, (3) the number of iodine atoms is almost equal to the number adsorbed on the walls, and (4) the iodine atoms are effectively scavenged by the walls. These assumptions probably hold very well at low initial pressures of iodine vapour but may break down as the pressure is increased.

If one accepts the above description then a given cell will have N_S adsorption sites. At low initial pressures, 5

mtorr for example, most of the iodine atoms produced are able to stick to the walls. Thus the scrambling of ortho-iodine and para-iodine occurs only upon the collision of a molecule with an adsorbed atom. From this viewpoint the ortho-iodine fluorescence should decay rapidly at first while the para-iodine conversion should be slower and a net enrichment is expected.

As the pressure is increased, roughly the same percentage of iodine atoms are expected to be produced. However, the absolute number of available adsorption sites remain constant. The "extra" atoms formed remain in the vapour phase and collisionally relax any enrichment that had been obtained rather quickly.

Using the equations provided by Letokhov et al one may estimate the scrambling coefficient for the atoms on the molecules as follows. At a 5 mtorr initial pressure the concentration of adsorbed atoms is, $m'^5 \simeq 3.52 \cdot 10^{-10}$ moles/cm^3 while the original concentrations of the ortho and para molecules are, $N^5{}_0 \simeq 1.70 \cdot 10^{-10}$ moles/cm^3 , and, $n^5{}_0 \simeq 1.22 \cdot 10^{-10}$moles/cm^3. From the data supplied on figure 3.4 the final values of these species are, $N^5 \simeq 0.36 \cdot 10^{-10}$ moles/cm^3 $n^5 \simeq 0.73 \cdot 10^{-10}$ moles/cm^3 and this makes the free iodine atom concentration at equilibrium, $m^5 \simeq 3.52 \cdot 10^{-18}$ moles/cm^3. (Effectively zero)

At an 80 mtorr intial pressure similar calculations show, assuming that the number of adsorbed iodine atoms remains constant at the previous concentration, that the

equiibrium values of the ortho-iodine, para-iodine, and iodine atoms are $N^{80} \simeq 2.18 \cdot 10^{-9}$ moles/cm^3, $n^{80} \simeq 1.56 \cdot 10^{-9}$ moles/cm^3 and, $m^{80} \simeq 1.15 \cdot 10^{-9}$ moles/cm^3. Thus the scrambling rate of the atoms may be estimated from these facts and assuming that the scrambling obeys a formula of the type,

$$(n_t - n_\infty) = (n_t - n_\infty)\text{EXP-}(kmt)$$

where k is the scrambling rate, m is the atom concentration in the vapour phase, and t is the time. Hence, a halflife

$$\tau_{\frac{1}{2}} \simeq \frac{\ln 2}{k \cdot m}$$

may be defined.

In the case of the 80 mtorr cell the halflife must be less than 10 seconds as no ortho to para shift was observed at all. Thus, from equation (3.20) $k \simeq 6 \cdot 10^7$cm^3/(mole s) which is the same order of magnitude as the rate constant for the analogous reaction in hydrogen [$7.5 \cdot 10^7$cm^3/(mole s)].

As expected, the ability of iodine atoms to scramble any ortho-para enhancement is considerable.

Of course the obvious way to get around this problem is to add a scavenger à la Badger and Urmston. In the same paper, Letokhov et al reported on the para-iodine to ortho-iodine enhancement observed when 2-hexene was used as a scavenger for the selectively excited ortho molecules. The authors varied laser power, concentrations of iodine, and

2-hexene as summarized in figures 3.5 and 3.6.(taken from reference 3)

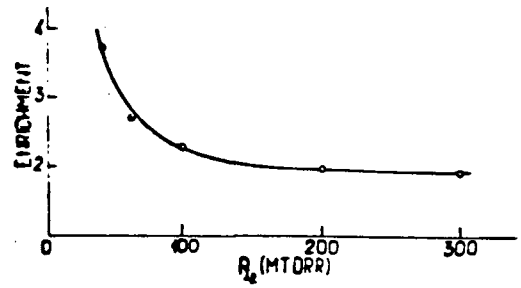

Figure 3.5 Enrichment coefficient dependence upon the initial iodine pressure in systems of mixtures of iodine and 2-hexene after 10 to 12 minutes of irradiation with an argon ion laser. Again, as the iodine pressure decreases, the enrichment increases. (from reference 3)

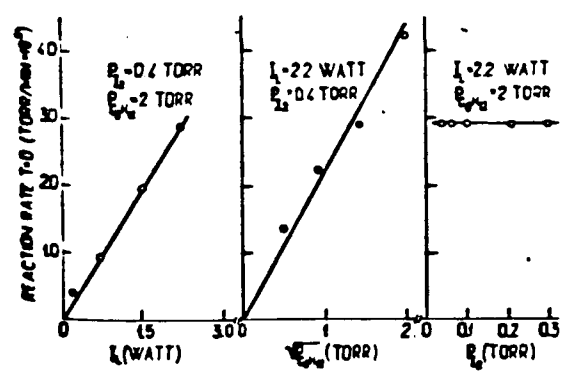

Figure 3.6 Dependence of the initial rate of change of the ortho-iodine concentration as a function of laser intensity, initial iodine concentration, and the square root of the 2-hexene pressure. (from reference 3)

The usual mechanism for such a reaction is via a radical chain as shown below.

$o\text{-}I_2 \longrightarrow 2I$	P_a
$I + X \rightleftharpoons XI$	k_2, k_{-2}
$XI + I_2 \rightleftharpoons XI_2 + I$	k_3, k_{-3}
$I \longrightarrow \frac{1}{2} I_2$	k_4
$2I + M \longrightarrow I_2 + M$	k_5

Under the assumptions that (1) the laser induced fluorescence is completely indicative of the amount of ortho or para iodine present; once the laser is turned on (2) the iodine atom concentration and the concentration of the species XI are constant (3) the reverse reaction 3 above is negligible, (4) chain rupture occurs via iodine formation at the walls, then one may express the rate equations for each species as

$$\frac{d(o\text{-}I_2)}{dt} \simeq -P_a + \frac{1}{24} k_4 I - \frac{1}{12} k_3 (XI)(o\text{-}I_2) \qquad (3.20)$$

$$\frac{d(I)}{dt} \simeq 2P_a - k_2(X)(I) + k_{-2}(XI) + k_3(XI)(I_2) - k_4(I) \qquad (3.21)$$

$$\frac{d(XI)}{dt} = k_2(X)(I) - k_{-2}(XI) - k_3(XI)(I_2) \qquad (3.22)$$

$$\frac{d(XI_2)}{dt} = k_3(XI)(I_2) \qquad (3.23)$$

Setting equations 3.21 and 3.22 to zero one has

$$(XI)\Big|_o \simeq \frac{k_2(X)(I)}{k_3(I_2) + k_{-2}} \qquad (3.24)$$

and,

$$(I)\Big|_o \simeq \frac{2P_a}{k_4} \qquad (3.25)$$

So that,

$$\frac{d(XI_2)}{dt}\Big|_o \simeq \frac{2P_a}{k_4} \cdot \frac{k_2(X)(I_2)}{[I_2 + k_{-2}/k_3]} \qquad (3.26)$$

which finally yields

$$\frac{d(o\text{-}I_2)}{dt}\Big|_o \simeq -P_a\left\{\frac{5}{12} + \frac{2k_2}{k_4}\frac{X(o\text{-}I_2)}{[I_2 + k_{-2}/k_3]}\right\} \qquad (3.27)$$

This is in disagreement with Letokhov's statement that

$$\frac{d(XI_2)}{dt}\Big|_o = -\frac{d(o\text{-}I_2)}{dt}\Big|_o \qquad (3.28)$$

It is important to make this distinction.

Based upon the data presented in figures 3.6 and 3.7 Letokhov et al state that the radical chain mechanism is not the correct interpretation as his data shows,

$$\frac{d(o\text{-}I_2)}{dt} \sim I_{laa}\sqrt{\lambda} \qquad (3.29)$$

which is not the same behaviour as equation (3.26). The reaction mechanism then remains uncertain.

It is notable that high enrichment was observed especially as the iodine pressure was decreased. This

increase in enrichment with decrease in pressure may in fact be due to a radical chain mechanism. As one decreases the amount of iodine present one also decreases the concentrations of the species such as XI and I which will scramble the enhancement. Therefore, it is possible that two or more mechanisms are at work simultaneously.

V. S. Letokhov et al have presented some promising, although somewhat contradictory, evidence that the ratio of para-iodine to ortho-iodine may be shifted away from the natural value of 5:7 both in a system of iodine vapour alone and, to a larger extent, in a system of iodine and 2-hexene via selective laser excitation.

IV. EXPERIMENTAL RESULTS

It is surprising that after having obtained some enhancement in the para-iodine to ortho-iodine ratio the reverse mechanism, i.e. the relaxation of this quantity to the natural value, was not studied by Letokhov et al. The purpose of this investigation was to reproduce and perhaps improve upon the Russians' results and to study the reconversion rate of ortho- and para-iodine by themselves and in the presence of some paramagnetic species à la Farkas.

The technique employed to produce an ortho to para ratio shift was very similar to that of Letokhov with the main difference being the method of monitoring the concentrations of these two species. A Coherent CR-15SG argon ion laser tuned to the 5145 Å line was used to selectively excite the ortho-iodine molecules.($B^3\Pi_{0^+u}$ $X^1\Sigma^+_g$ 43'- 0" P(13) and R(15) transitions) Periodically during the process the argon ion laser beam was redirected to power a Coherent CR-699-21 scanning dye laser. The dye laser beam was sent through the test cell and the frequency scanned across a given spectral region of iodine. With the aid of an iodine atlas[28], the rotational and vibrational constants of iodine supplied by Herzberg[4] and some predissociation data obtained by J. Vigué[9], a region which satisfied the following criteria could be found: the region chosen should (1) afford good dye laser output power (100 mW or better), (2) contain at least one ortho-iodine and one para-iodine

spectral line belonging to the same vibrational transition, (3) the spectral lines in the region should not be too cluttered and badly overlapped, and, (4) the transitions used to monitor the ortho and para concentrations should induce fairly low predissociation so as to disturb the system as little as possible.

Once chosen, the fluorescence of the iodine due the argon ion beam and the dye laser beam was monitored with an EMI 9558QB photomultiplier and recorded on a strip chart recorder. The time dependence of the ratio of an ortho-iodine to para-iodine peak height would (to first order) indicate whether or not any enhancement was occurring.

With the above technique in mind, the remainder of this chapter contains in depth descriptions of each of the investigations undertaken.

A. IODINE VAPOUR EXPERIMENTS

1. SINGLE LASER BEAM IRRADIATION TECHNIQUE

Based upon the results of Letokhov et al the greatest enrichment factors were obtained with low initial pressures of iodine vapour. Further, previous investigations of Farkas into molecular hydrogen indicated that paramagnetic impurities and excessive numbers of atoms could pose difficulties for this experiment. Hence, the first experiments involving iodine vapour alone were carried out

with low pressures of iodine vapour (about 3 mtorr) in a sealed cell.

A cylindrical test cell of length 30 cm and volume 79 cm^3 was evacuated on a greaseless gas manifold equipped with teflon stopcocks to a pressure of roughly $2x10^{-5}$ torr. The cell was then filled with the desired pressure of iodine vapour by placing a constant temperature bath around a container holding iodine crystals (BDH assured, analytical reagent grade, 99.99% pure) and allowing the vapour to diffuse into the test cell. Having thusly prepared a test sample, the cell was pinched off of the manifold and set in a constant temperature bath in the apparatus shown in figure 4.1.

A Coherent argon ion laser was used to drive a Coherent CR-699-21 dye laser which scanned across the $B^3\Pi_{0^+u} \longrightarrow X^1\Sigma^+_g$ 14'- 1" P(77) and R(82) spectral lines of molecular iodine. The sweep speed was set to 10 GHz in 25 seconds and the lines rescanned 5 to 10 times before initiating the experiment to give an initial ratio of the ortho-iodine to para-iodine concentration. Next, prism P1 (see figure 4.1) was inserted to deflect the argon ion laser beam through the test cell to begin the selective ortho-iodine predissociation. Notice that before entering the test cell the argon ion beam was expanded from about a 2 mm to an 8 mm diameter so as to irradiate as much of the test cell's volume as possible. The power of this beam, after expansion, entering the cell was typically between 3 and 4 watts.

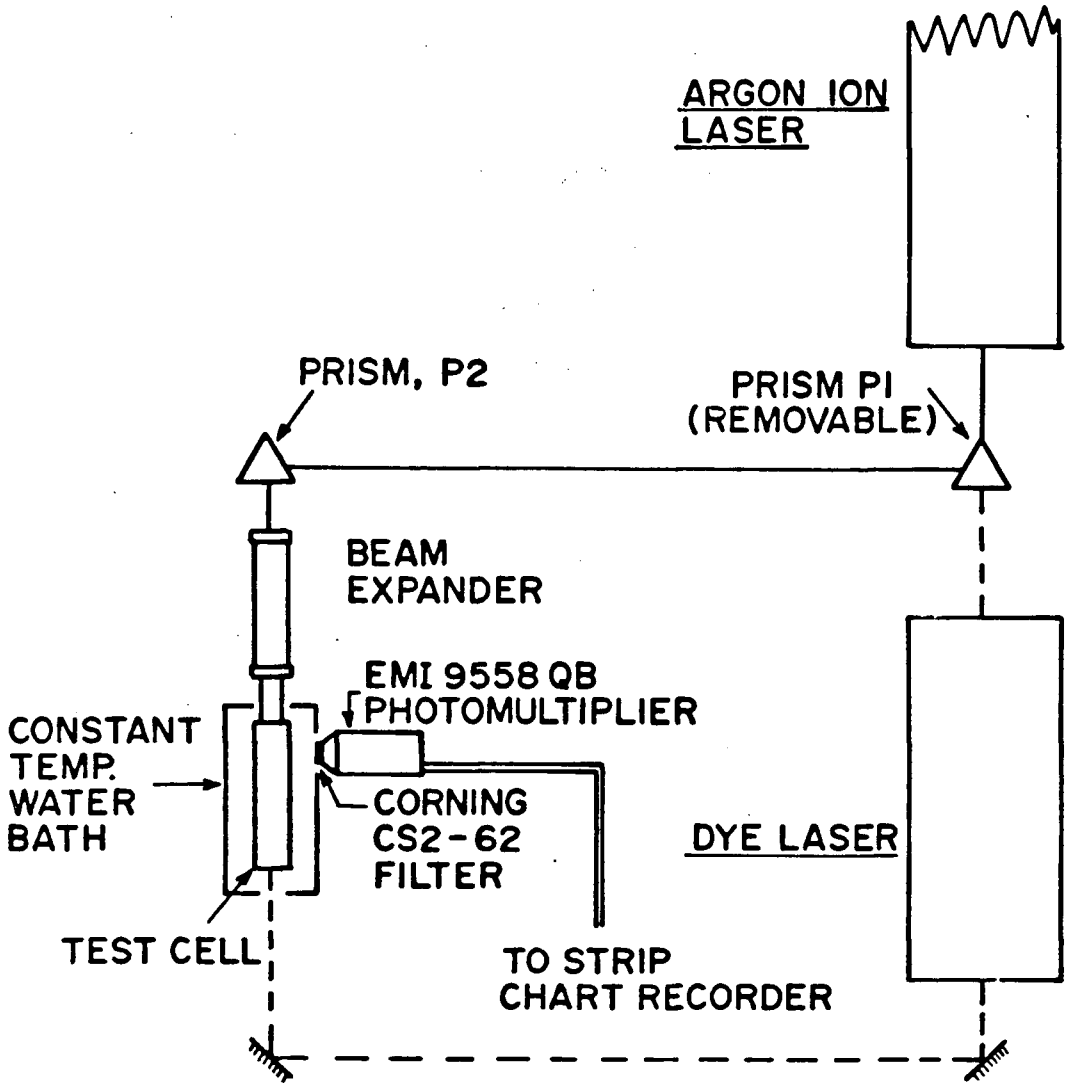

Figure 4.1. Single laser beam irradiation experimental arrangement for the selective exicitation of ortho-iodine. Test cells containing iodine vapour were placed in a constant temperature water bath and, with prism P1 in place, irradiated with the argon ion laser beam. By removing this prism, the dye laser was powered and a given spectral region of molecular iodine could be monitored. Note that both fluorescences were recorded using an EMI 9558QB photomultiplier shielded by a Corning CS2-62 red pass filter to eliminate the signal due to scattered laser light.

As the characteristic times of the ratio shift were claimed to be of the order of 150 to 200 minutes by Letokhov et al, the argon ion beam was sent to the dye laser at intervals of roughly one hour and the original spectral region was rerecorded. This rescanning period took between five and ten minutes after which time the argon ion laser beam was sent through the cell once more.

Some typical results obtained with a cell containing (3.75±0.15) mtorr of iodine vapour initially are summarized in Tables 4.1 to 4.3 and in figures 4.2 and 4.3.

TABLE 4.1 Experimental Conditions

BACKGROUND PRESSURE	3×10^{-5}torr
INITIAL IODINE PRESSURE	(3.75±0.15)mtorr
ARGON ION LASER POWER	(3.9±0.1)W
DYE LASER POWER	80mW
WATER BATH TEMPERATURE	(27±1)°C
DURATION OF EXPERIMENT	(125±5)minutes
DYE LASER MONITOR LINES	B X (14'- 0") P(77),R(82) $\nu\simeq17034$ cm^{-1}

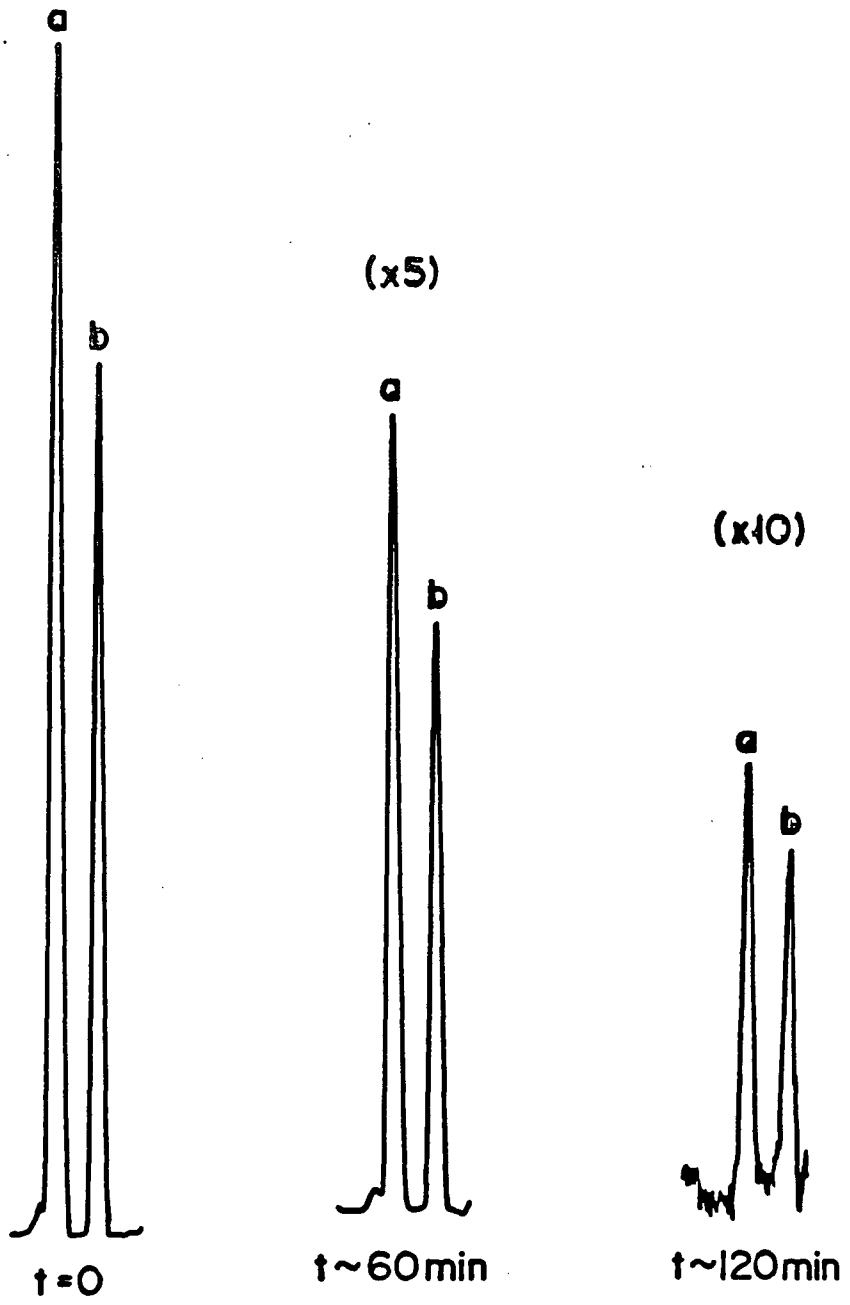

Figure 4.2. Typical appearance of the 14'-1" P(77) [peak (a)] and the 14'-1" R(82) [peak(b)] spectral lines after having irradiated the test cell with the 5145 Å argon ion laser beam for the amount of time indicated below each spectrum. (i.e. t=0 implies before any argon ion irradiation, t≃60 min. is after an hour of such irradiation, and, t≃120 min. is the same region after abour two hours of net argon ion laser irradiation.)

TABLE 4.2 Argon Ion and Dye Laser Induced Fluorescence versus Time

TIME (min.)	$\frac{Ar^+(t)}{Ar^+(0)}$	$\frac{[14'-1" P(77)]}{[14'-1" P(77)]}$	$\frac{[14'-1" R(82)]}{[14'-1" R(82)]}$
0	1.0	1.0	1.0
60±2	0.120±.008	0.136±0.003	0.137±0.003
125±5	0.032±.007	0.038±0.002	0.039±0.002

TABLE 4.3 Ortho and Para Peak Heights and Ratios versus Time

TIME (min.)	P(77) (arb.)	R(82) (arb.)	$\frac{P(77)}{R(82)}$
0	203.1±1.6	148.4±1.8	1.37±0.01
60±2	127.6±.4	20.3±0.2	1.37±0.01
125±5	7.8±0.3	5.8±0.2	1.34±0.04

From these results one immediately observes that although the argon ion induced fluorescence decreases to about 3 percent of the initial value as reported by Letokhov et al, the 14'-1" P(77) and R(82) peak heights both decrease by this amount also over the course of the experiment. Hence, no enrichment of para-iodine has been observed. This is in contradiction with Letokhov's claim that an enrichment factor of roughly 2 is to be expected at this initial pressure.

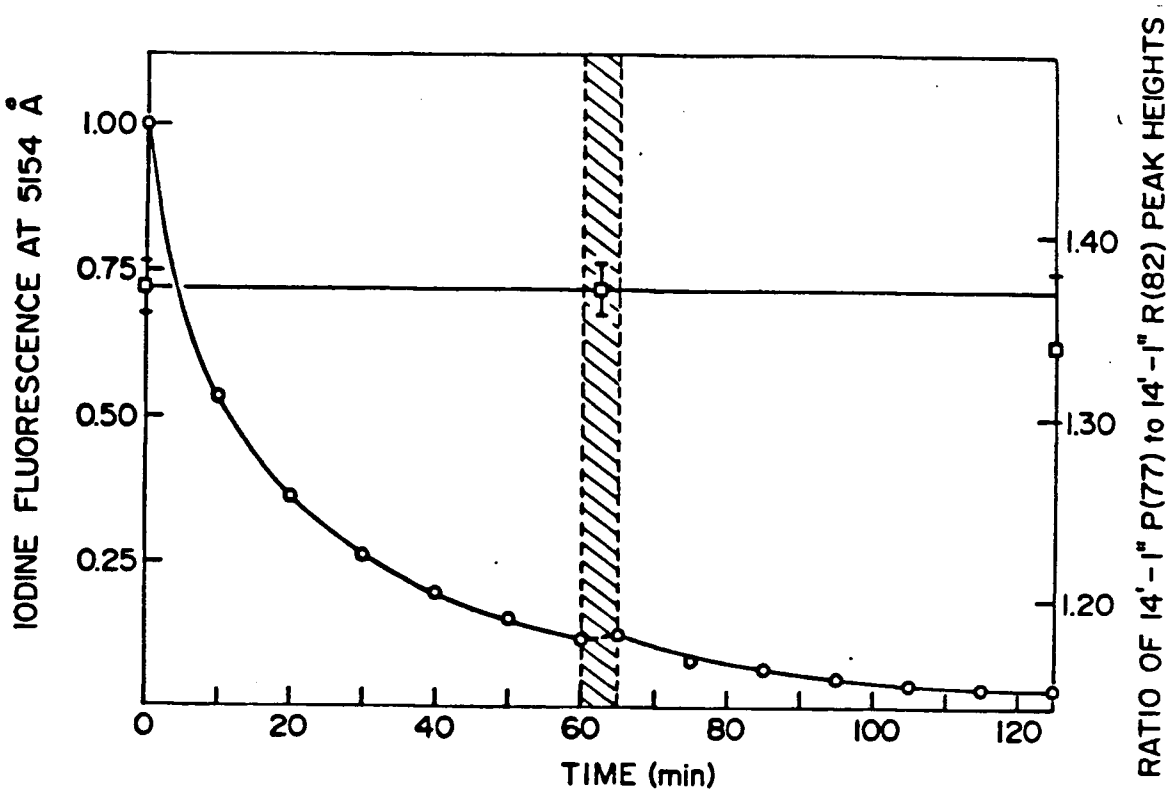

Figure 4.3. Plot of the fluorescence induced in a (3.75±0.15)mtorr iodine vapour cell (1.9 cm diameter, 30 cm length) by the 5145 Å line of the argon ion laser beam, (O), and the ratio of the 14'-2" P(77) to the 14'-1" R(82) peaks, (□), over the course of the experiment. As the experimental arrangement allowed only one laser beam enter the cell at a time, the periods when the iodine was exposed to the dye laser beam but not the argon ion beam are indicated by the shaded regions.

The immediate question arises, what are the differences between these experiments and those performed previously? Perhaps the difference was in the argon ion laser used. It is possible that the laser employed here to drive the reaction was sufficiently broad that appreciable amounts of para-iodine were being excited along with the ortho-iodine. To test this a fluorescence cell was was placed in front of a McPherson 0.75 meter grating monochrometer with a 30,000 line per inch grating used in second order. The cell was irradiated with the 5145 Å laser beam and, as the grating was rotated, the signal coming out of the monochrometer was recorded with a photomultiplier on a strip chart recorder. The results of this diagnostic check are shown in figure 4.4 which indicates that primarily the ortho-molecules are being excited by this laser radiation.

Another difference between the two experiments lies in the diameters of the test cells used. Letokhov et al employed cells of diameter roughly 0.64 cm while in the experiments performed by this author the cell's diameter was 1.9 cm. From some simple gas kinetic analysis at 3 mtorr initial pressure the mean free path of an iodine atom is roughly,

$$d = (N\sigma)^{-1}$$

where N is the number of particles per cm^3, and σ is the collisional cross-section between iodine atoms and

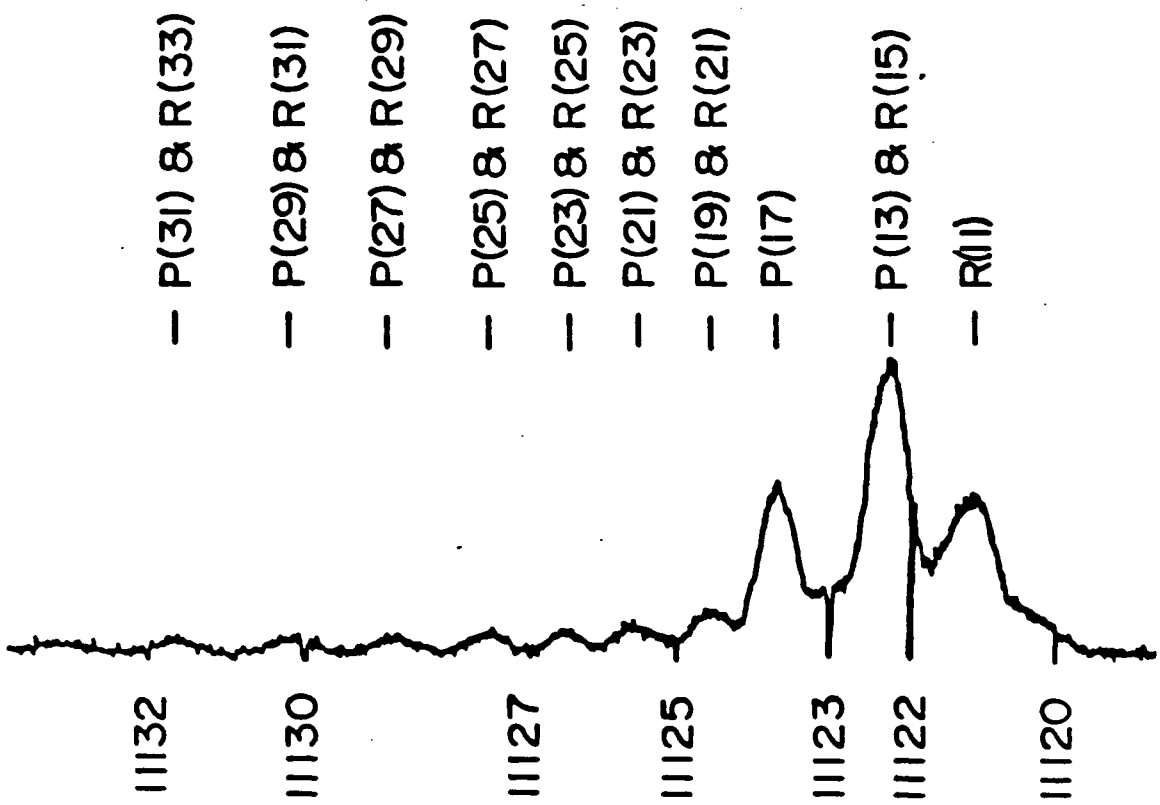

Figure 4.4. The fluorescence spectrum of an iodine cell (about 150-200 mtorr) excited by a Coherent CR-15SG argon ion laser tuned to the 5145 Å as recorded with a McPherson 0.75 m grating monochromator equipped with a 30,000 line per inch grating. The above trace displays the 43'-7" band observed in second order on the grating. The lower numbers displays the wavelength scale while above the peaks the line assignment is given. Notice that all the lines correspond to odd rotational transitions implying that primarily the ortho-iodine molecules are being excited.

molecules. As this cross-section is unknown let it be assumed to be about the size of the iodine molecule (about 2 $Å^2$) so that the mean free path becomes 24 cm.

Hence if the above assumption is true then any iodine atom produced will strike the wall before ever encountering an iodine molecule in either cell. However, if it is wrong and the mean free path is only of the order of 0.5 cm (or $\sigma \simeq 190 Å^2$) then it could be that the iodine atoms are extremely efficient at scrambling the ortho and para species resulting in no observed shift in the natural ratio.

It is also possible that the material used to construct the test cells plays a major role in these experiments. The cells used by this author were pyrex while those of Letokhov et al were made of molybdenum glass. Unfortunately, our glassblower was unable to obtain any information about this material and as a result the test cells had to be made of pyrex. It is conceivable that molybdenum glass is a much better scavenger than pyrex for iodine atoms and, hence, a net effect may not be possible with pyrex.

The power densities of the beam used in each case were slightly different also. Letokhov et al employed a 2.5 mm, 2.2 watt laser beam while this author used an 8 mm, 4 watt beam. This corresponds to the power density of Letokhov's laser being about six times greater than that used in the experiments previously reported here. This may have changed the characteristic time of the reaction from 150 to 900 minutes. Thus, after 120 minutes of irradiation with the

lower power density one might expect to see the results obtained by Letokhov after about 20 minutes. From reference (3), one has an enrichment factor of about 1.32 after 20 minutes of irradiation or roughly a 25% shift in the ortho-iodine to para-iodine ratio. To within a 5% uncertainty, no such shift was observed.

Finally, the pressure to which the test cell was evacuated before use was about 2×10^{-5} torr here versus about 10^{-4} torr for Letokhov. It would seem logical to assume that the lower this value the better the results should be as this reduces the possibility of contamination of the cell by paramagnetic species. At worst, Letokhov et al could have had about 2% contamination in their cells when the initial iodine pressure was 5 mtorr while the contamination in this investigation would have been about 0.7%. (This, of course, assumes that no other degasing of the cell takes place during an experiment)

To summarize, the main differences between Letokhov's work and this first series of experiments were (1) cell material and dimensions, (2) the argon ion laser power density in the cell, (3) the background pressure in the test cells before filling, and (4) the method of monitoring the ortho- and para-iodine concentrations.

2. DUAL BEAM IRRADIATION TECHNIQUE

Another set of experiments with iodine vapour test cells was prepared with as many of the aforementioned

parameters adjusted to agree more closely with Letokhov's. A new cell was constructed of pyrex in a T shape having dimensions of about 6 mm diameter, 15 cm length, and, a 6.0 cm^3 volume. This was outfitted with a teflon stopcock so as to avoid any contamination of the cell due to heating up the pyrex to remove it from the gas manifold after preparation. The reason for the T shape was to allow the experiment to be performed with two laser beams going through the cell perpendicular to one another simultaneously.

The new cells were placed in the apparatus shown in figure 4.5. In these experiments prism P1 was replaced with a beam splitter which sent part of the argon ion radiation to the test cell and the rest to power the dye laser. This arrangement allowed roughly 2 watts of argon ion laser beam and about 80 milliwatts of dye laser power to enter the test cell simultaneously. Notice, too, that in this arrangement no water bath was used to control the cell temperature. Again, both signals were recorded by either an EMI 9558B or 9558QB photomultiplier whose signals were sent to a PHILLIPS PM8252A strip chart recorder. A typical experiment and the interesting results are described below.

The pyrex test cell was prepared for use by baking the cell (to about 200°C) while evacuating it for a period of roughly twenty four hours. A residual pressure of 8×10^{-6} torr was obtained this way.

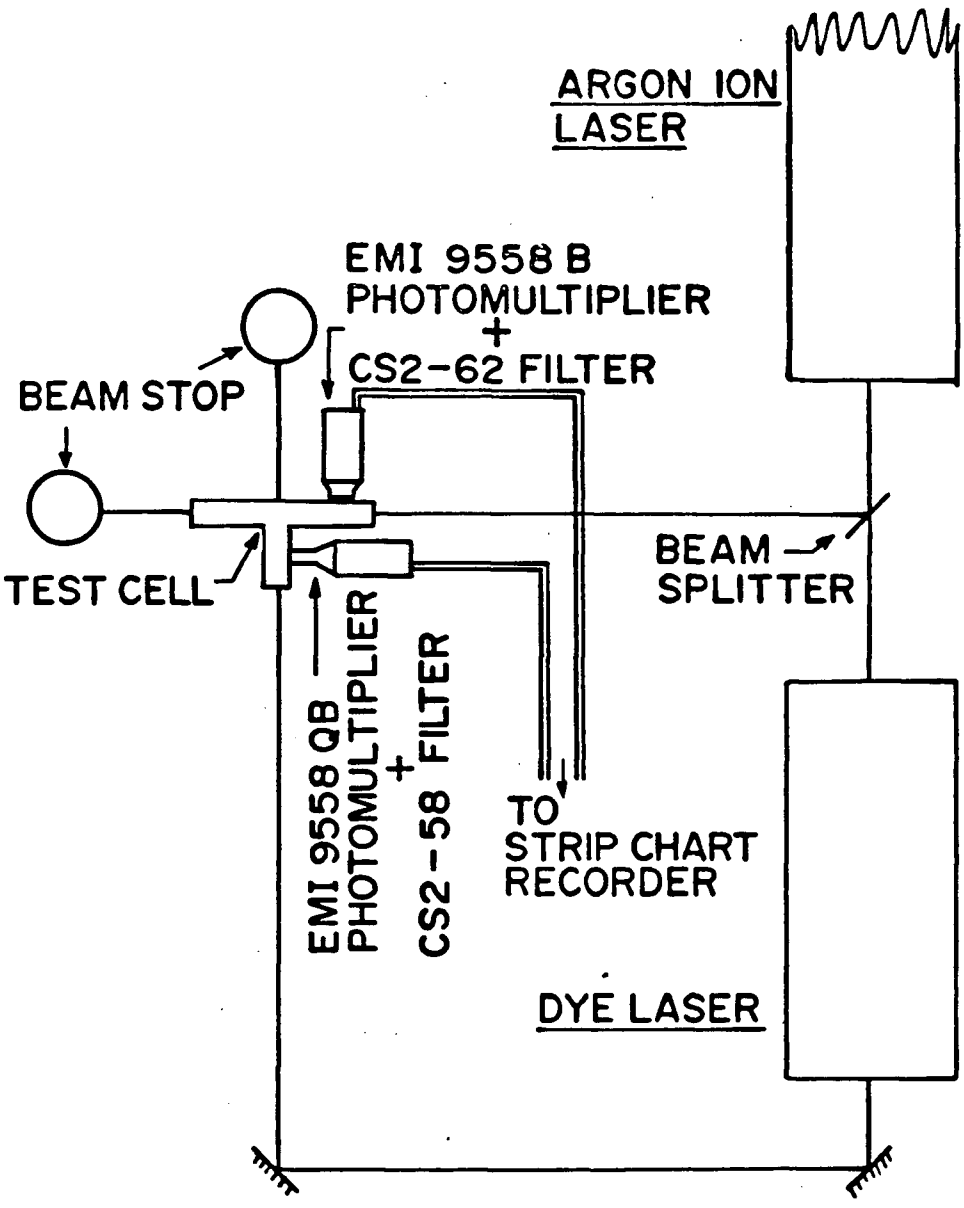

Figure 4.5. Dual laser beam experimental arrangement is shown above. Prism P1 was replaced with a beam splitter which sent part of the argon ion beam to the test cell with the remainder powering the dye laser. This set up allowed both laser beams to enter the T shaped test cell (6 mm diameter, 15 cm length) simultaneously. The fluorescence induced by each beam was recorded by EMI photomultipliers shielded by Corning red pass filters as before.

The cell was then allowed to cool to room temperature and filled, as previously described, via temperature controlled vapour pressure to (3.00±0.15) mtorr. This cell was then placed in the experimental apparatus.

The region over which the dye laser scanned was changed from the 14'-1" P(77) and R(82) lines ($\nu \simeq 17034\ cm^{-1}$ to the 15'-0" R(30) and P(25) spectral lines ($\nu \simeq 17408\ cm^{-1}$). This region, shown in figure 4.6, produced slightly more laser power and had a comparable relative predissociation rate to the previous range.[1]

TABLE 4.4 Experimental Conditions

BACKGROUND PRESSURE	$8x10^{-6}$torr
INITIAL IODINE PRESSURE	(3.00±0.15)mtorr
ARGON ION LASER POWER	(1.8±0.1)W
DYE LASER POWER	(80±10)mW
DURATION OF EXPERIMENT	160 minutes
DYE LASER MONITOR LINES	B X (15'- 0") P(25),R(30) $\nu \simeq 17034\ cm^{-1}$
SCAN LENGTH	10 GHz
SCAN TIME	25s

---

[1]From the doctoral thesis of J. Vigué[9] the predissociation quantum yield of the 15'-0" P(25) and 14'-1" P(69) lines may be deduced as (0.0576±0.0462) and (0.0526±0.0504) respectively.

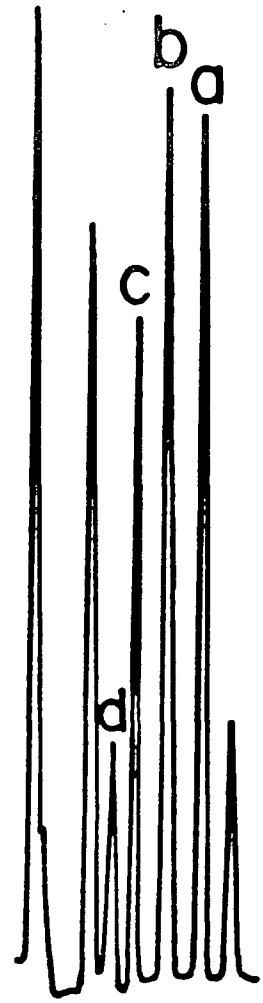

Figure 4.6. The above figure shows the 17408 cm^{-1} region of the molecular iodine spectrum excited by the dye laser. The transitions labelled a, b, c, and d are the 15'-0" R(30), 15'-0" P(25), 18'-1" P(84), and 19'-1" P(121) peaks respectively.

The argon ion laser was periodically sent through the test cell while the dye laser continuously scanned across the selected region for a period of about 40 minutes. After this time the lasers were cut off and the system left in the dark for 120 minutes. The lasers were turned on again and the results shown in figures 4.7 to 4.9.

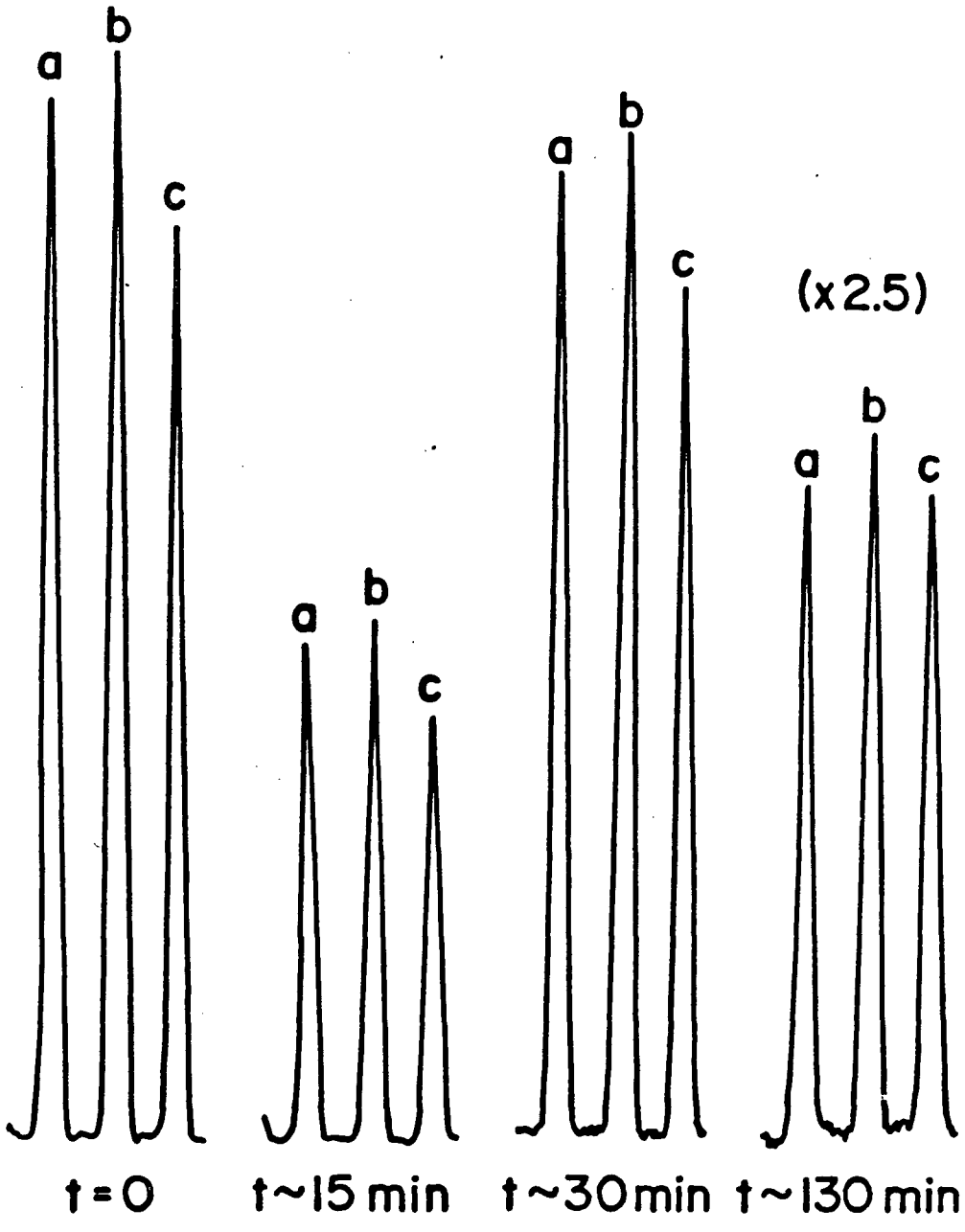

Figure 4.7. The 15'-0" P(25) [peak a], 15'-0" R(30) [peak b], and the 18'-1" P(84) [peak c] transitions observed in a (3.00±0.15)mtorr iodine vapour test cell after different amounts of exposure to the argon ion laser [traces (1) to (3)] and after being left in the dark for about 100 minutes.[trace (4)] Notice how the relative strength of the 18'-1" P(84) peak increases over time with respect to the 15'-0" P(25) and R(30) transitions.

TABLE 4.5 15'-0" P(25), 15'-0" R(30), and 18'-1" P(84) Peak Height Ratios versus Time.

Time (min.±1 min.)	15'-0" P(25) / 15'-0" R(30)	15'-0" P(25) / 18'-1" P(84)
0	1.043±0.036	1.258±0.048
3.0	1.051±0.043	1.270±0.057
5.6	1.043±0.045	1.227±0.058
10.3	1.038±0.049	1.263±0.066
15.0	1.054±0.060	1.230±0.076
18.5	1.034±0.056	1.216±0.072
22.8	1.037±0.023	1.206±0.029
25.1	1.044±0.026	1.200±0.032
32.8	1.028±0.031	1.194±0.039
37.9	1.035±0.029	1.163±0.035
160	1.077±0.059	1.113±0.058

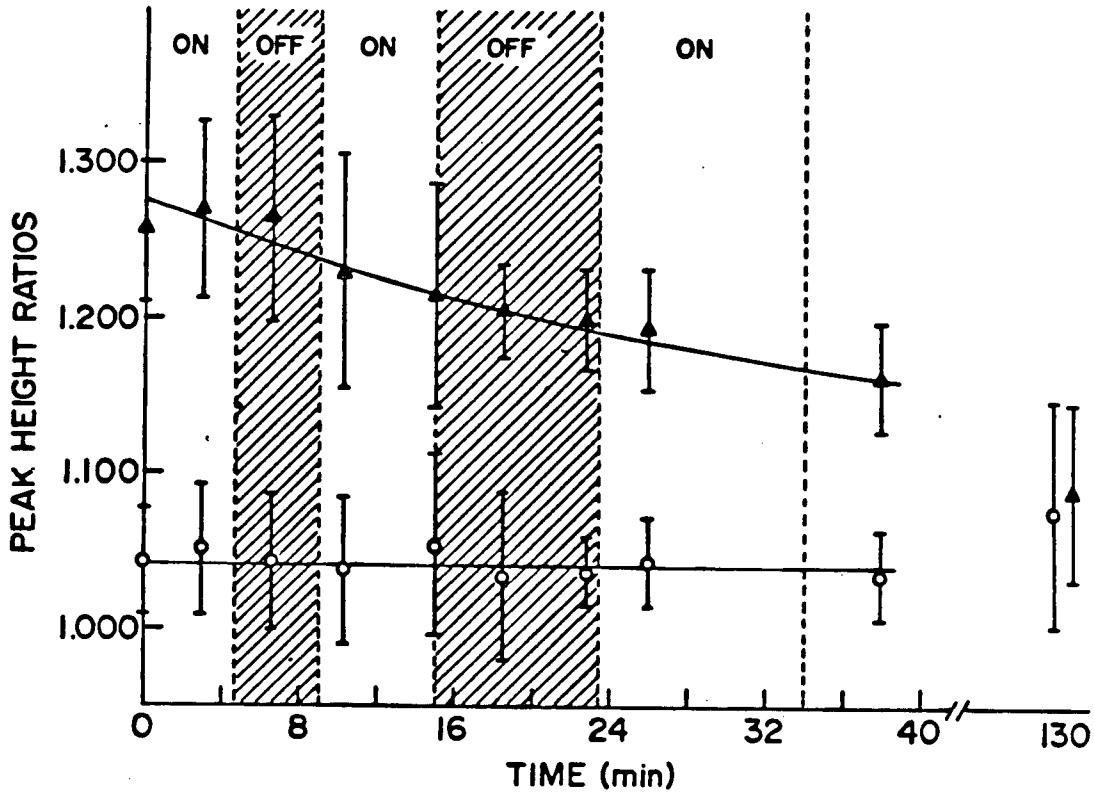

Figure 4.8 A plot of the 15'-0" P(25) : R(30) (O), and, 15'-0" P(25) : 18'-1" P(121) (▲), peak heights over produced in a (3.00±0.15)mtorr iodine vapour cell over the course of the experiment is shown above. From this graph the variation of the 15'-0" P(25) : 18'-1" P(84) peak heights is more clearly seen. A laser induced enhancement of the para-iodine cannot be concluded from this as the ratio continues to decrease even in the absence of the 5145 Å irradiation and because the 15'-0" P(25) : 15'-0" R(30) ratio remains constant throughout. (As before, the periods when the argon ion laser is prevented from entering the test cell are marked by the shaded regions on the graph with the exception of the region displayed after the 34 minute mark which, although not shaded, did not have the 5145 Å beam entering the cell.)

TABLE 4.6 Argon Ion Induced Fluorescence versus Time

TIME (min.±1.0 min.)	FLUORESCENCE (arb.)
0	1.000
3.0	0.847±0.026
4.6	0.807±0.025
off	...
9.1	0.829±0.026
10.3	0.742±0.024
15.0	0.644±0.023
15.2	0.641±0.023
off	...
23.4	0.671±0.023
25.0	0.604±0.022
32.8	0.491±0.021
33.0	0.480±0.021
off	...

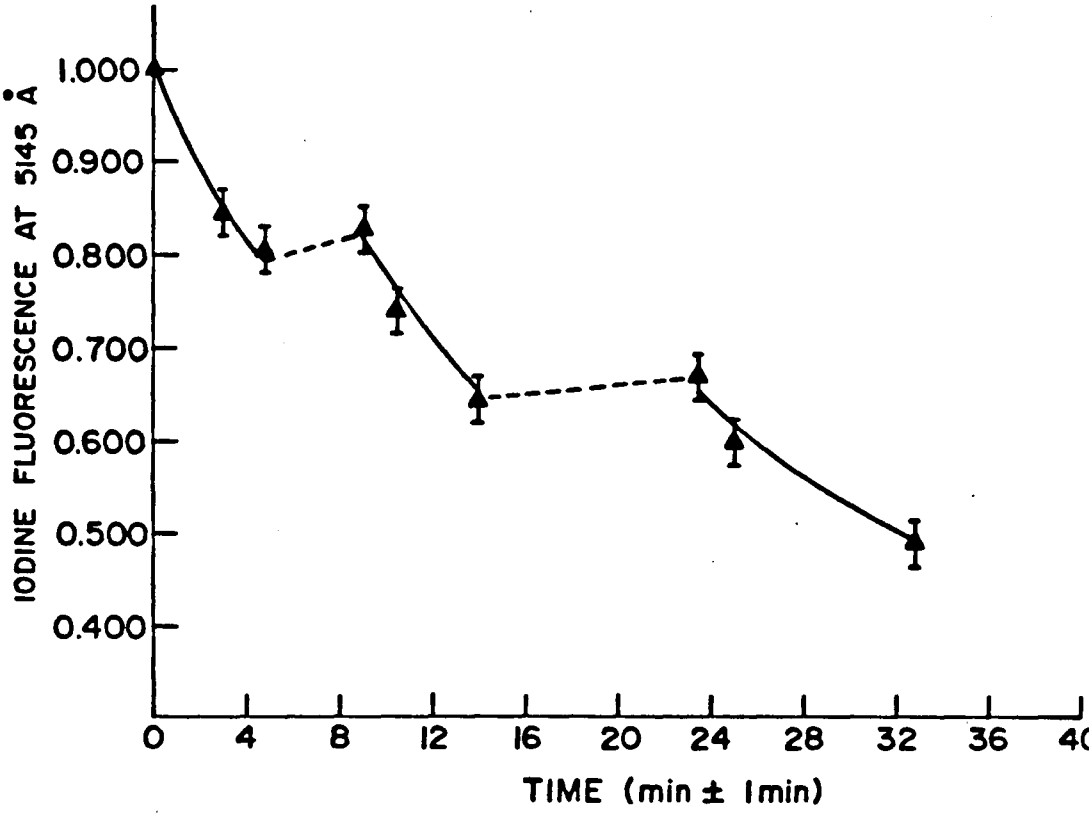

Figure 4.9 The decay of the argon ion induced fluorescence over the course of the experiment is shown above. The periods when the 5145 Å radiation was turned off are indicated by the dashed lines between the experimental points.

Again, based upon the ratio of the 15'-0" P(25) to R(30) spectral lines ther is no ortho to para shift to within 5% uncertainty. However, an extremely interesting result is obtained with the ratio of the 15'-0" P(25) to 18'-1" P(84) lines. This ratio seems to decrease over time and would appear to indicate that an ortho- to para-iodine shift has indeed been obtained, with an enrichment factor of,

$$E \sim \frac{(1.268 \pm 0.048)}{(1.163 \pm 0.055)} = 1.08 \pm 0.07$$

over a period of thirty minutes.(Letokhov reports an enrichment of 1.3 after thirty minutes of irradiation in a 5 mtorr iodine cell.) This enhancement is not close to the value reported by the Russian authors but it does show that the ratio of two spectral lines belonging to different vibrational transitions and with very different rotational quantum numbers tend to indicate a variation in the ortho- to para-iodine ratio over time. Indeed a most fascinating result occurs after having left the test cell in the dark for about two hours and re-irradiating the system – the 15'-0" P(25) to 18'-1" P(84) ratio has dropped even further while the 15'-0" P(25) to R(30) ratio remained constant.

A first clue as to what may be happening may be obtained by comparing this region of spectrum ($\nu \simeq 17408$ cm^{-1}) in a low pressure iodine cell to a high pressure iodine cell as shown in figure 4.10. One remarks immediately

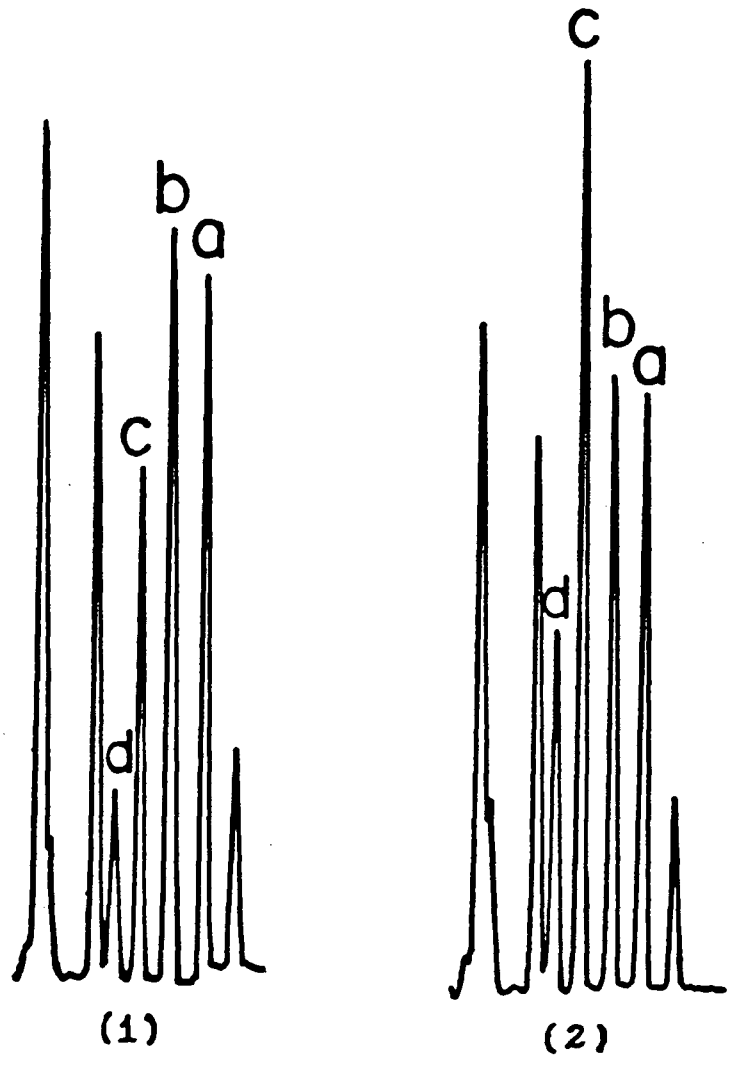

Figure 4.10. Typical iodine spectra produced in the 17408 cm^{-1} region via dye laser induced fluorescence in a low pressure iodine cell (about 3 mtorr) in [1] and a high pressure iodine cell (about 30 mtorr) in [2]. The peaks, a, b, c, and, d, are identified as the 15'-0" R(30), 15'-0" P(25), 18'-1" P(84), and the 19'-1" P(121) transitions respectively. In the the high pressure case, [2], the 18'-1" P(84) and 19'-1" P(121) peaks are more predominant than the corresponding peaks in the low pressure spectrum owing probably to greater self-quenching in the high pressure case.

that the 18'-1" P(84) and the 19'-1" P(121) lines (labelled "c" and "d" in the figure respectively) are much more predominant at high pressures than at low pressures. This may be attributed to the fact that the lifetime of a given state may be written as,

$$\tau = \frac{\tau_o}{A + B_{pred} + Q} \qquad (4.1)$$

where B_{pred} is a factor depending upon the predissociation rate of a given state, and Q is a factor depending upon the collisional quenching of a given state by either a foreign gas or by self-quenching.

For a state that is highly predissociated, the lifetime is not expected to be strongly modified by the addition of some foreign gas. A state that is not strongly predissociated, on the other hand, may be greatly affected depending upon the relative size of the parameters A, B, and Q. In the case of the 15'-0" P(25) state the predissociation quantum yield is roughly (0.0576±0.0462) while the 18'-1" P(84) and 19'-1" P(121) transitions have quantum yields roughly (0.287±0.191) and (0.539±0.394) respectively. (These values were extrapolated from reference (9)) Hence, if the cell is leaking, outgasing, or if the iodine atoms are driving some impurities off of the walls of the test cell, then, over time the internal pressure in the cell will

increase and could cause some differential quenching of the various transitions.

In these experiments, the most probable cause of an increase in internal pressure would be due to outgasing. Leakage by the teflon stopcocks may be ruled out as these produce a very good seal especially over a two to three hour period. Also, if iodine atoms are driving impurities off of the walls of the container to a large extent, then one would expect that the peak height ratios would remain more or less constant after the argon ion laser beam was stopped from entering the cell. However, this was not observed to be so.

To test this outgasing hypothesis one should prepare several test cells which vary in the degree to which they were evacuated. That is, when one evacuates a cell the pressure time dependence goes as,

$$\frac{dP}{dt} \sim -\gamma P + D \qquad (4.2)$$

where P is the pressure in system, γ is a factor proportional to the pumping rate of the system, and D is an outgasing rate. Clearly, as one reduces the ultimate pressure obtained then the degasing factor also decreases. i.e. at equilibrium, $D = \gamma P(\infty)$. The lower $P(\infty)$ is the slower the degasing rate of the cell when it is removed from the pump.

By preparing cells with different background pressures and filling them with roughly the same amounts of iodine

vapour, one may test the hypothesis.

A series of such experiments was performed with each of the cells being tested as previously described using the simultaneous irradiation technique. The results obtained are reported below.

(a) Run Number 1: $P(\infty) = 5 \times 10^{-6}$ torr

A cell was prepared by baking it (to about 200°C) while evacuating it for roughly 6 days prior to filling. The cell was next filled with (4.5±0.3)mtorr of iodine vapour and irradiated with both laser beams simultaneously.

TABLE 4.7 Experimental Conditions

BACKGROUND PRESSURE	5×10^{-6}torr
INITIAL IODINE PRESSURE	(4.5±0.3)mtorr
ARGON ION LASER POWER	(1.85±0.10)W
DYE LASER POWER	80mW
DURATION OF EXPERIMENT	110 minutes
DYE LASER MONITOR LINES	B X (15'- 0") P(25),R(30) $\nu \simeq 17408$ cm^{-1}
SCAN LENGTH	30 GHz
SCAN TIME	75 s

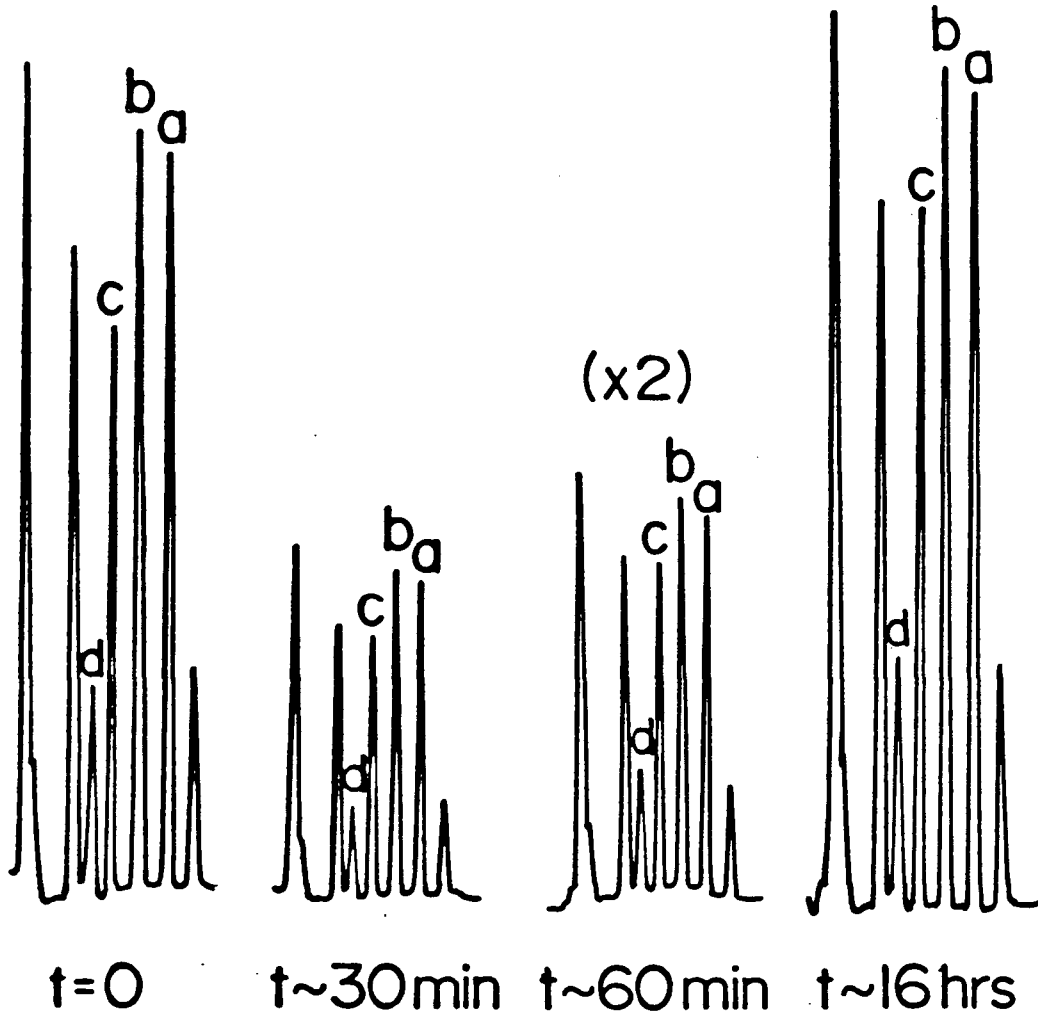

Figure 4.11. Typical iodine spectra in the 17408 cm^{-1} region induced in a (4.5±0.3)mtorr iodine cell prepared by evacuating the cell to a residual pressure of about $5x10^{-6}$torr prior to use, as a function of time during the experiment are given above. In this case the peaks, identified as a - 15'-0" R(30), b - 15'-0" P(25), c - 18'-1" P(84), and d - 19'-1" P(121), maintained constant relative heights over the duration of the excitation with the argon ion laser but varied after a 16 hour period of leaving the cell in the dark.

TABLE 4.8 Peak Height Ratios versus Time

Time (min.±1 min.)	$\frac{15'-0" P(25)}{15'-0" R(30)}$ (±0.055)	$\frac{15'-0" P(25)}{18'-1" P(84)}$ (±0.080)	$\frac{15'-0" P(25)}{19'-1" P(121)}$ (±0.125)
0	1.054	1.438	3.682
4.6	1.060	1.454	3.872
7.1	1.061	1.431	3.827
9.6	1.063	1.444	3.844
12.1	1.069	1.464	3.889
14.6	1.063	1.436	3.792
27.6	1.047	1.441	3.868
32.6	1.057	1.438	3.772
36.4	1.055	1.450	3.918
43.4	1.061	1.451	3.843
45.9	1.058	1.452	3.847
48.4	1.048	1.454	3.842
52.2	1.042	1.464	3.835
57.1	1.049	1.448	3.845
16 hrs	1.031	1.172	3.212

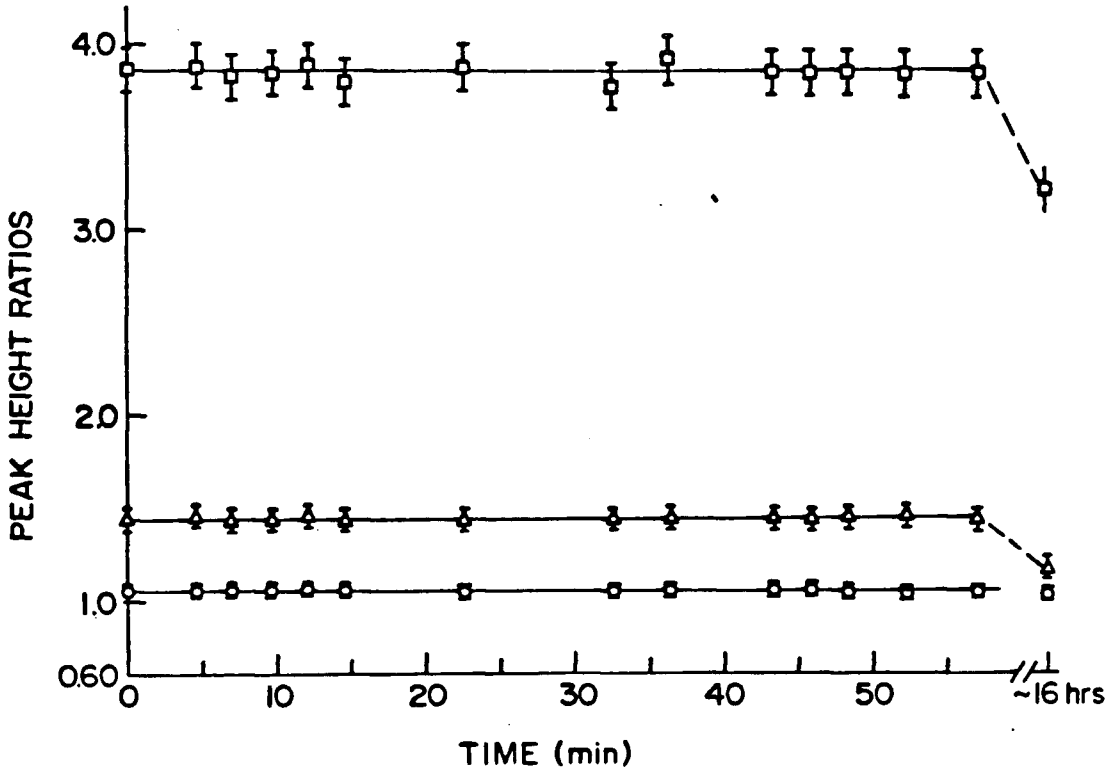

Figure 4.12. The 15'-0" P(25) : 15'-0" R(30) (O), 15'-0" P(25) : 18'-1" P(84) (Δ), and 15'-0" P(25) : 19'-1" P(121) (□), peak height ratios over the course of the experiment in a test cell evacuated to about 5×10^{-6}torr prior to use and filled with (4.5±0.3)mtorr of iodine vapour. All the ratios appear to remain constant during the irradiation of the cell with the argon ion laser but vary after having left the cell in the dark for a sixteen hour period.

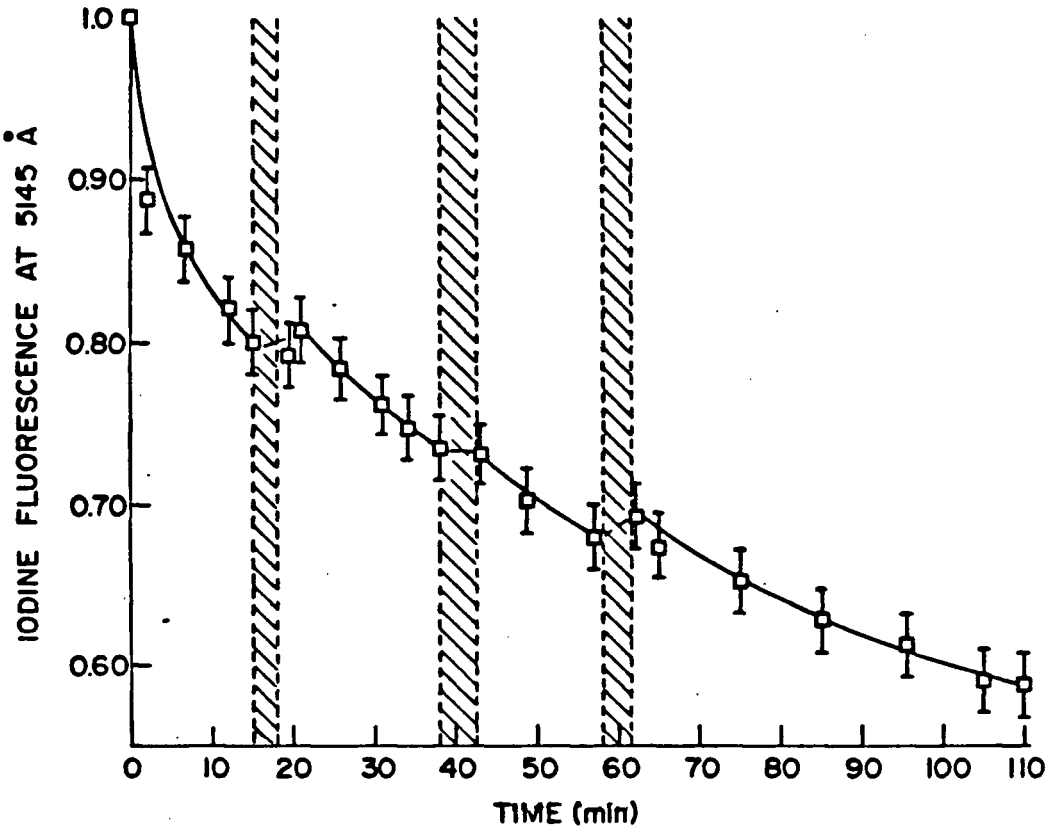

Figure 4.13 The decay of the argon ion induced fluorescence observed in a test cell filled with (4.5±0.3)mtorr of iodine vapour in a cell evacuated to about 5×10^{-6}torr before use. Again, the shaded regions indicate the periods during which the 5145 Å radiation was prevented from entering the test cell.

TABLE 4.9 Argon Ion Laser Induced Fluorescence versus Time

TIME (min.±1.0 min.)	FLUORESCENCE (arb.) (±0.020)
0	1.000
2.0	0.888
6.9	0.857
11.9	0.821
14.9	0.800
18.0	...
19.5	0.792
20.9	0.808
25.9	0.784
30.9	0.762
34.2	0.748
38.0	0.735
38.0	...
42.5	on
43.2	0.731
48.2	0.705
57.2	0.680
58.0	off
61.5	on
62.2	0.693
65.2	0.674

(...cont.)

75.2	0.653
85.2	0.628
95.5	0.613
105.2	0.591
110.2	0.588

Hence one observes that no ortho to para ratio shift has been obtained but that the variation in the relative peak heights was less than the previous trial. This would seem to support the degasing hypothesis, however still more data was required.

(b) Run Number 2: $P(\infty) = 1.6 \times 10^{-5}$ torr

This sample cell was prepared as before by baking it out over night while evacuating it but without using a liquid nitrogen cold trap on the gas manifold. The resulting residual pressure was 1.6×10^{-5} torr.

TABLE 4.10 Experimental Conditions

BACKGROUND PRESSURE	1.6×10^{-5}torr
INITIAL IODINE PRESSURE	(3.3±0.3)mtorr
ARGON ION LASER POWER	(1.9±0.1)W
DYE LASER POWER	50mW
DURATION OF EXPERIMENT	60 minutes
DYE LASER MONITOR LINES	B X (15'- 0") P(25),R(30) $\nu \simeq 17408$ cm^{-1}
SCAN LENGTH	30 GHz
SCAN TIME	75 s

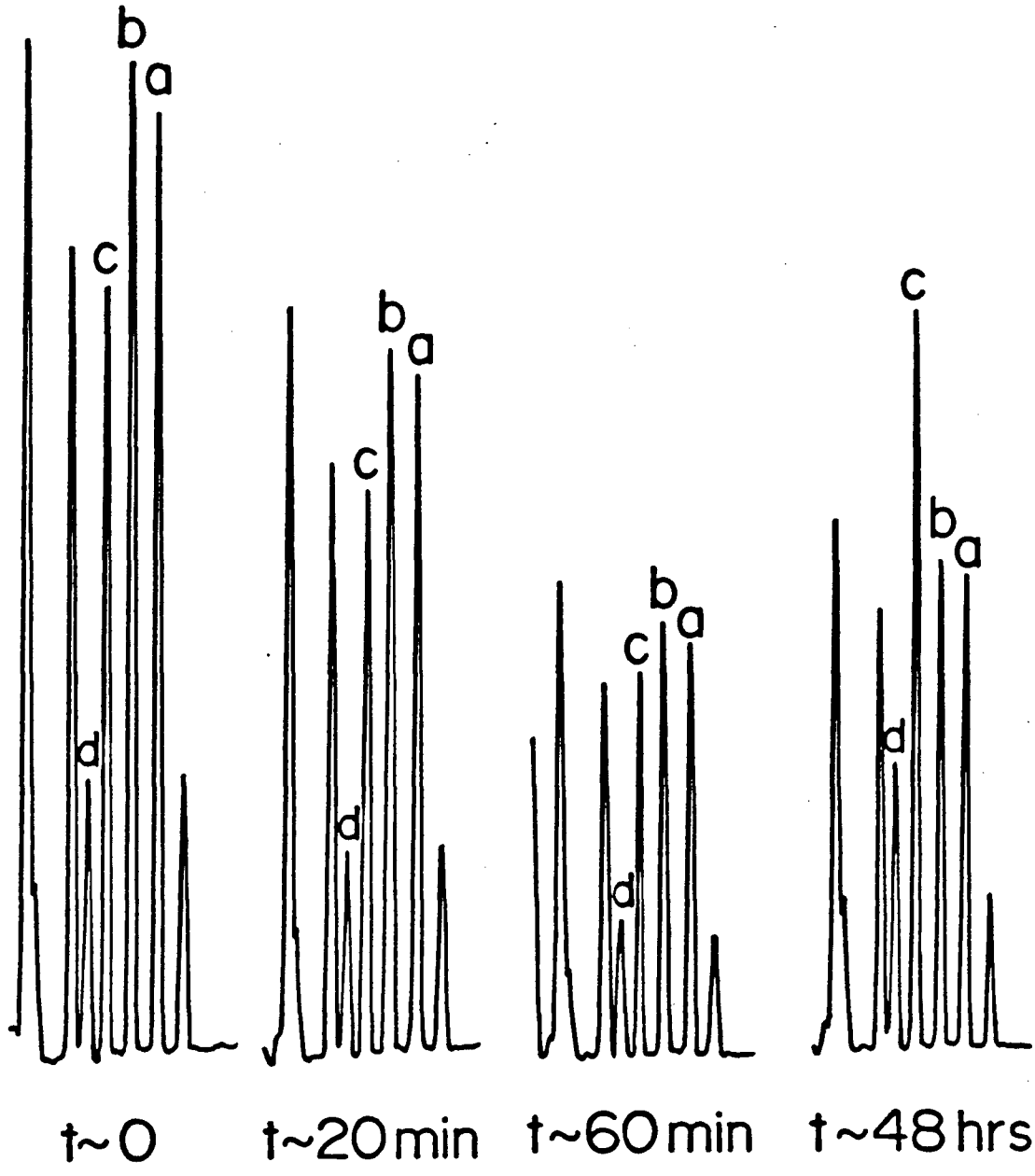

Figure 4.14. Typical iodine spectra in the 17408 cm^{-1} region induced in a (3.3±0.3)mtorr iodine cell prepared by evacuating the cell to a residual pressure of about 1.6×10^{-5}torr prior to use, as a function of time during the experiment are given above. In this case the peaks, identified as a - 15'-0" R(30), b - 15'-0" P(25), c - 18'-1" P(84), and d - 19'-1" P(121), varied in relative heights over the duration of the excitation with the argon ion laser and to a greater extent after leaving the cell in the dark for about 48 hours.

TABLE 4.11 Peak Height Ratios versus Time

Time (min.±1 min.)	15'-0" P(25) / 15'-0" R(30) (±0.055)	15'-0" P(25) / 18'-1" P(84) (±0.080)	15'-0" P(25) / 19'-1" P(121) (±0.125)
0.0	1.072±0.030	1.280±0.030	3.520±0.120
3.4	1.060±0.026	1.288±0.035	3.473±0.114
8.0	1.055±0.028	1.305±0.038	3.493±0.122
11.1	1.047±0.030	1.256±0.039	3.400±0.127
16.1	1.042±0.031	1.258±0.042	3.381±0.133
21.3	1.041±0.036	1.234±0.046	3.389±0.153
55.0	1.043±0.028	1.126±0.028	2.992±0.159
60.0	1.033±0.029	1.115±0.032	3.092±0.108
48hrs	1.042±0.027	0.672±0.014	1.678±0.040

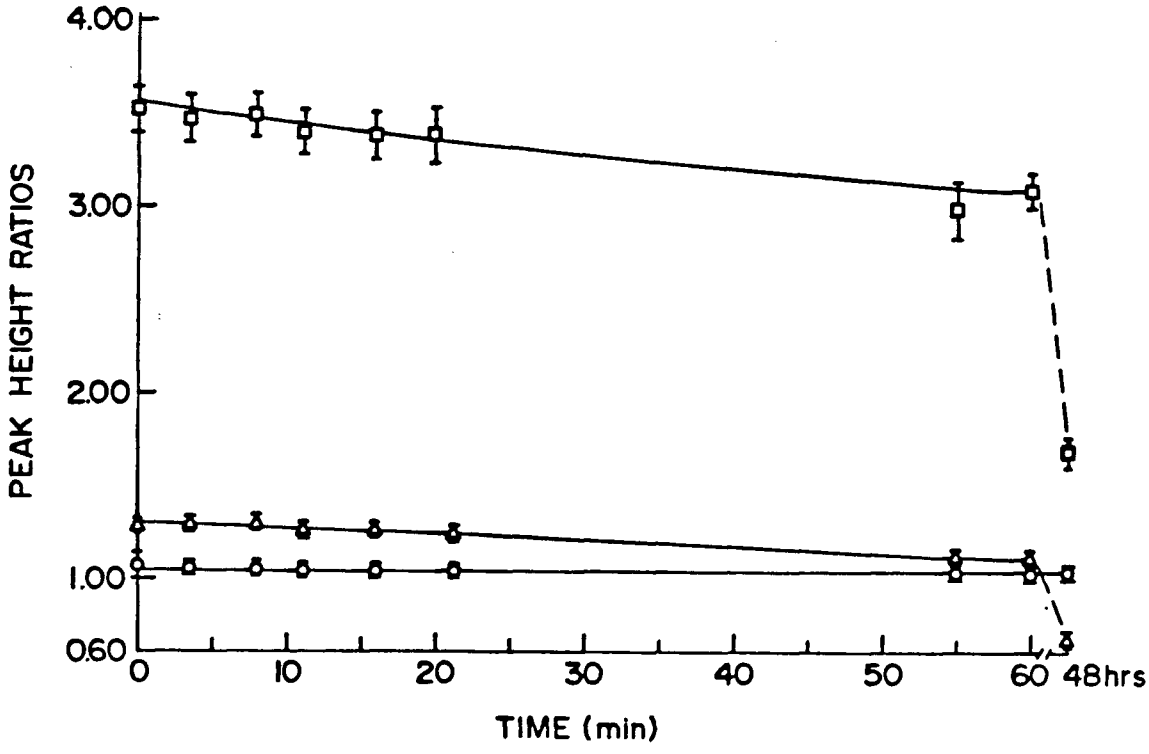

Figure 4.15. The 15'-0" P(25) : 15'-0" R(30) (O), 15'-0" P(25) : 18'-1" P(84) (Δ), and 15'-0" P(25) : 19'-1" P(121) (□), peak height ratios over the course of the experiment in a test cell evacuated to about 1.6×10^{-5}torr prior to use and filled with (3.3±0.3)mtorr of iodine vapour. As in the cases with the test cell evacuated to 8×10^{-6}torr originally, (see page), during the irradiation of the cell with the argon ion laser, the ratios of the 15'-0" P(25) : 18'-1" P(84) and the 15'-0" P(25) : 19'-1" P(121) ratios decreased and continued to do so even when the test cell was kept in the dark for about 48 hours.

TABLE 4.12 Argon Ion Laser Induced Fluorescence versus Time.

TIME (min.±1.0 min.)	FLUORESCENCE (arb.±0.030)
0	1.000
2.2	0.944
7.2	0.896
12.2	0.848
17.2	0.814
22.2	0.785
36.2	0.723
50.4	0.679
55.4	0.670
60.4	0.662
62.0	0.642

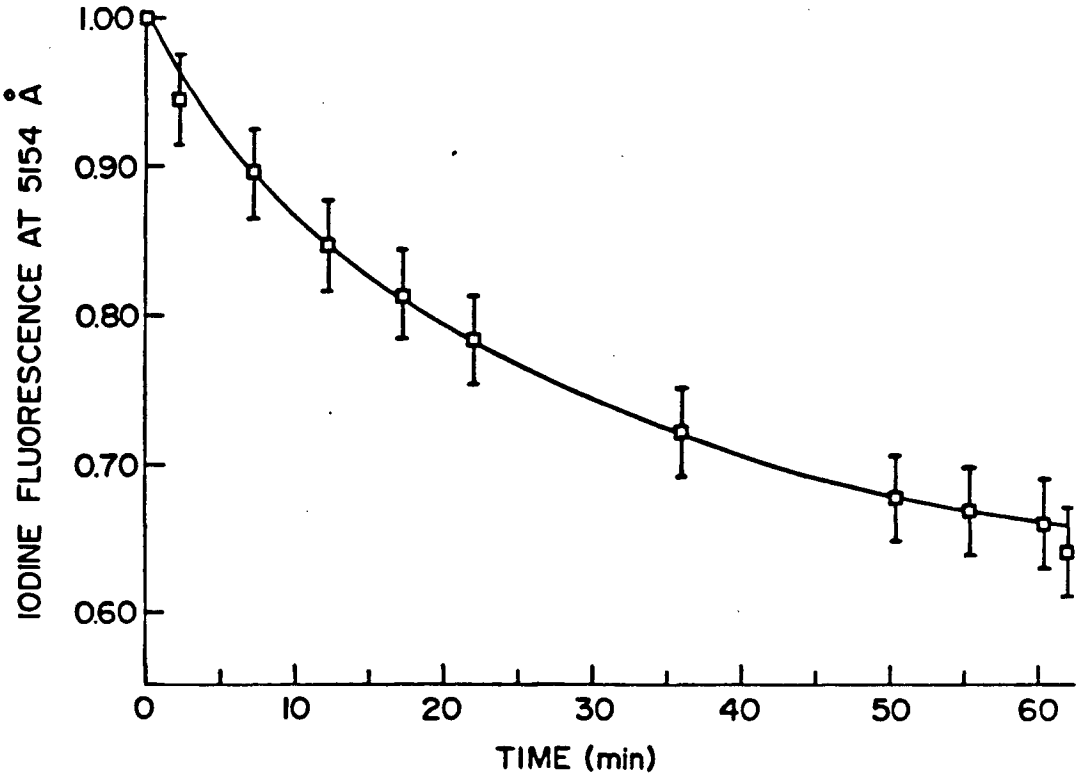

Figure 4.16 The decay of the argon ion induced fluorescence observed in a test cell filled with (3.3±0.3)mtorr of iodine vapour in a cell evacuated to about 1.6×10^{-5}torr before use. The behavior of the decay is similar to that prevously observed in run #1.

(c) Run Number 3: $P(\infty) = 9.5 \times 10^{-5}$

Again the test cell was baked out overnight and the liquid nitrogen cold trap removed from the system. In order to decrease the vacuum further from the readily obtainable 2×10^{-5} torr level, one manifold of the gas filling system which had been pumped down to only about 10^{-3} torr was opened to the manifold containing the cell alone briefly. This resulted in an increase in pressure to 9.5×10^{-5} torr. At this point the pumps were closed off from the main manifold and the cell filled with roughly (3.3±0.3) mtorr of iodine. Unfortunately, as this vacuum pressure was not easily obtainable it is expected that the results of this experiment would be the most questionable.

TABLE 4.13 Experimental Conditions

BACKGROUND PRESSURE	9.5×10^{-5}torr
INITIAL IODINE PRESSURE	(3.3±0.3)mtorr
ARGON ION LASER POWER	(1.7±0.1)W
DYE LASER POWER	100mW
DURATION OF EXPERIMENT	60 minutes
DYE LASER MONITOR LINES	B X (15'-0") P(25),R(30) $\nu \simeq 17408$ cm^{-1}
SCAN LENGTH	30 GHz
SCAN TIME	75 s

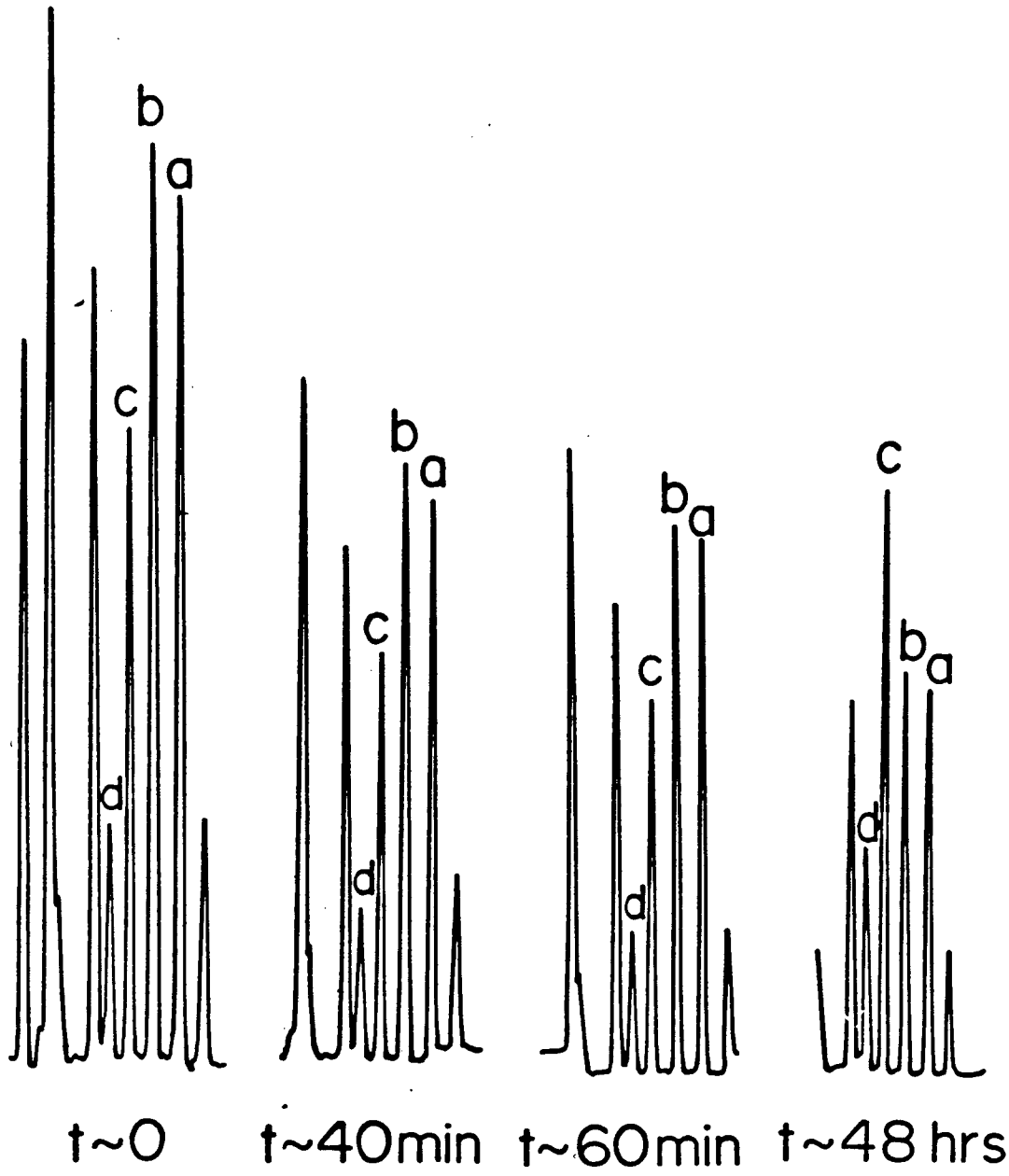

Figure 4.17. Typical iodine spectra in the 17408 cm^{-1} region induced in a (3.3±0.3)mtorr iodine cell prepared by evacuating the cell to a residual pressure of about 9.5×10^{-5}torr prior to use, as a function of time during the experiment are given above. In this case the peaks, identified as a - 15'-0" R(30), b - 15'-0" P(25), c - 18'-1" P(84), and d - 19'-1" P(121), varied in relative heights over the duration of the excitation with the argon ion laser and after leaving the cell in the dark for about 48 hours in a manner comparable to that of the previous cell.

TABLE 4.14 Peak Height Ratios versus Time

Time (min.±1 min.)	15'-0" P(25) / 15'-0" R(30)	15'-0" P(25) / 18'-1" P(84)	15'-0" P(25) / 19'-1" P(121)
0	1.031±0.035	1.310±0.051	3.487±0.160
2.9	1.037±0.039	1.323±0.057	3.593±0.187
4.8	1.033±0.022	1.334±0.032	3.644±0.174
8.5	1.034±0.025	1.328±0.036	3.526±0.188
11.0	1.032±0.027	1.300±0.038	3.531±0.204
13.4	1.034±0.029	1.294±0.040	3.607±0.227
15.6	1.039±0.030	1.310±0.044	3.521±0.229
17.9	1.028±0.032	1.285±0.045	3.476±0.146
20.2	1.026±0.034	1.293±0.048	3.454±0.152
24.7	1.034±0.037	1.292±0.052	3.486±0.170
29.2	1.030±0.020	1.235±0.027	3.333±0.140
54.7	1.044±0.032	1.191±0.039	3.232±0.203
57.0	1.041±0.016	1.177±0.020	3.180±0.102
61.4	1.024±0.017	1.197±0.021	3.258±0.112
48hrs	1.044±0.080	0.700±0.025	1.768±0.130

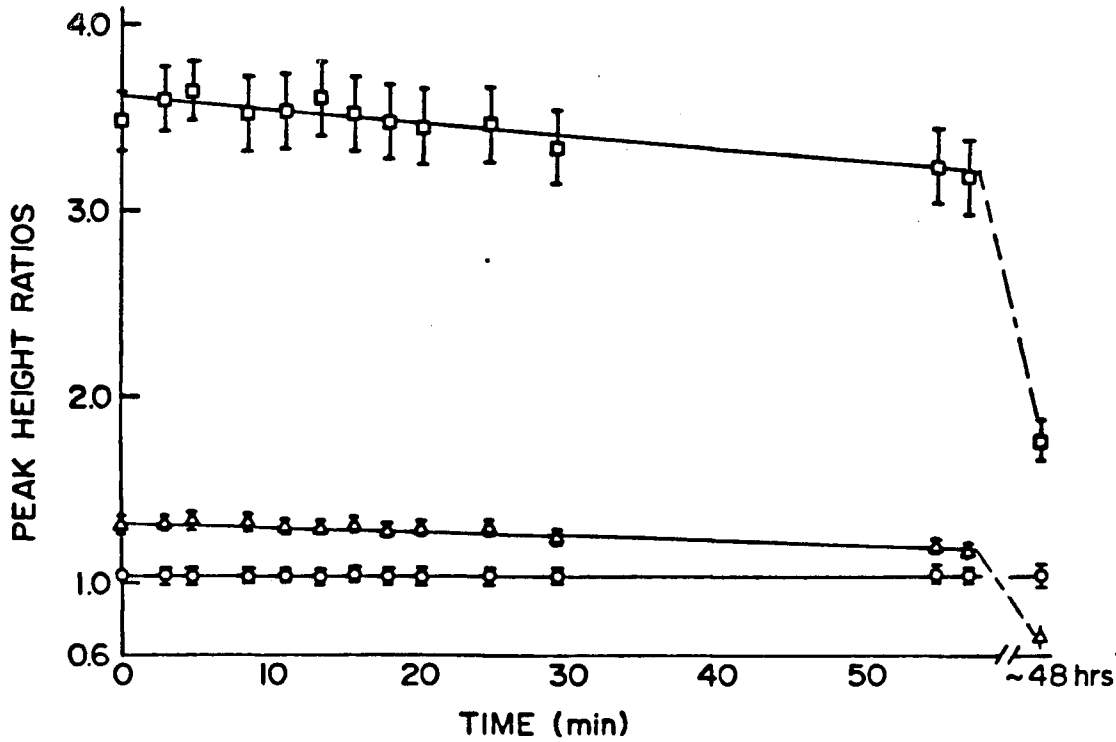

Figure 4.18. The 15'-0" P(25) : 15'-0" R(30) (O), 15'-0" P(25) : 18'-1" P(84) (Δ), and 15'-0" P(25) : 19'-1" P(121)(□)peak height ratios over the course of the experiment in a test cell evacuated to about 9.5×10^{-5}torr prior to use and filled with (3.3±0.3)mtorr of iodine vapour. As in run #2, during the irradiation of the cell with the argon ion laser, the ratios of the 15'-0" P(25) : 18'-1" P(84) and the 15'-0" P(25) : 19'-1" P(121) ratios decreased and continued to do so even when the test cell was kept in the dark for about 48 hours.

TABLE 4.15 Argon Ion Laser Induced Fluorescence versus Time.

TIME (min.±1.0 min.)	FLUORESCENCE (arb.±0.030)
5.2	0.872±0.037
10.2	0.802±0.042
15.2	0.742±0.040
20.2	0.694±0.039
25.2	0.669±0.030
30.2	0.640±0.038
35.1	0.610±0.037
40.1	0.592±0.027
45.1	0.574±0.028
50.1	0.559±0.025
53.0	0.551±0.026
54.4	0.543±0.025
57.7	0.548±0.048
61.7	0.545±0.025

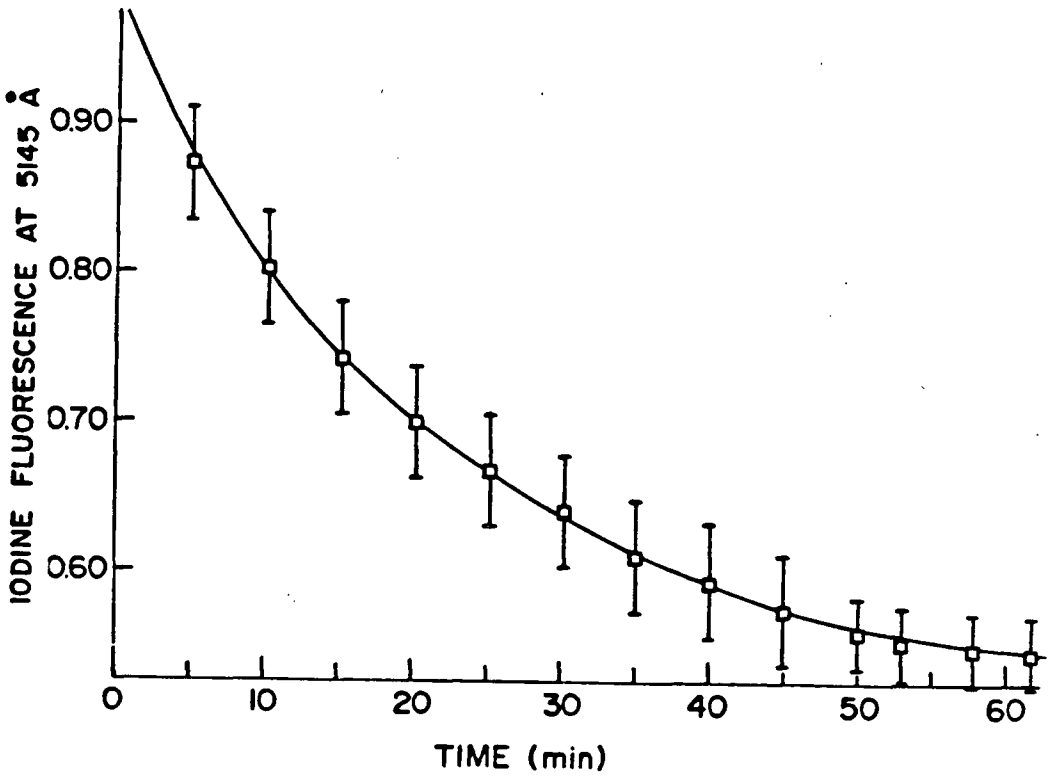

Figure 4.19 The decay of the argon ion induced fluorescence observed in a test cell filled with (3.3±0.3)mtorr of iodine vapour in a cell evacuated to about 1.6×10^{-5}torr before use. The behavior of the decay is similar to that prevously observed in run #1.

From these results one observes that indeed no ortho to para enhancement is produced during the selective irradiation of the iodine but that the ratios of the heights of spectral lines belonging to different vibrational and rotational states do vary over the course of the experiment. Further, this variation appears to depend heavily upon how clean the test cell was made prior to use supporting the hypothesis that the above variation is caused by differential quenching of the vibrational states by impurities outgased by the cell walls during the experiment. Hence, no ortho-iodine to para-iodine shift is possible by this method.

B. IODINE AND SCAVENGERS

The major problem, it would be fair to assume, was that iodine atoms can very efficiently scramble the ortho- and para-iodine molecules via,

$$I + o\text{-}I_2 \longleftrightarrow p\text{-}I_2 + I$$

to quickly return the ratios of these two species to the original value. The logical step, then, is to add a suitable scavenger to the system which will effectively mop up either the atoms or the excited iodine molecules immediately after they have been formed. To this end several different organic molecules and some inorganic ones were used and the results described below.

1. IODINE AND 2-HEXENE

The first choice for a scavenger was 2-hexene as this was reported to react readily with either the excited iodine molecules or iodine atoms by both Badger and Urmston[27] and Letokhov et al[23].

A mixture of cis- and trans-2-hexene was obtained from the Alderich Chemical Company (GOLD, 99+%). This was placed in a pyrex vessel and attached to the gas filling manifold on the vacuum line then distilled between two traps. The subsequent 2-hexene was stored in vacuo and covered by a dark cloth on the gas line and used as necessary.

The first experiment was performed based upon information supplied by Letokhov et al. As the enrichment factor increased with decreasing initial iodine pressure it was decided to use a very low pressure iodine cell to obtain the maximum effect. To this end a cell containing about 2 mtorr of iodine and 1.0 torr of 2-hexene was prepared and irradiated with the dye laser instead of the argon ion laser. The region used is shown in figure 4.20 and the monitor lines were the 18'-1" R(42) and P(37) transitions and the 19'-1" P(95) line was used to drive the reaction. The 19'-1" P(95) transition is more highly predissociated than the 43'-0" P(13) or R(15) lines excited by the argon ion laser. However, the argon ion laser produces more power and will excite two transitions from the v"=0 level which, at room temperature, is more highly populated than the v"=1. Thus, it is not clear whether or not the action of this

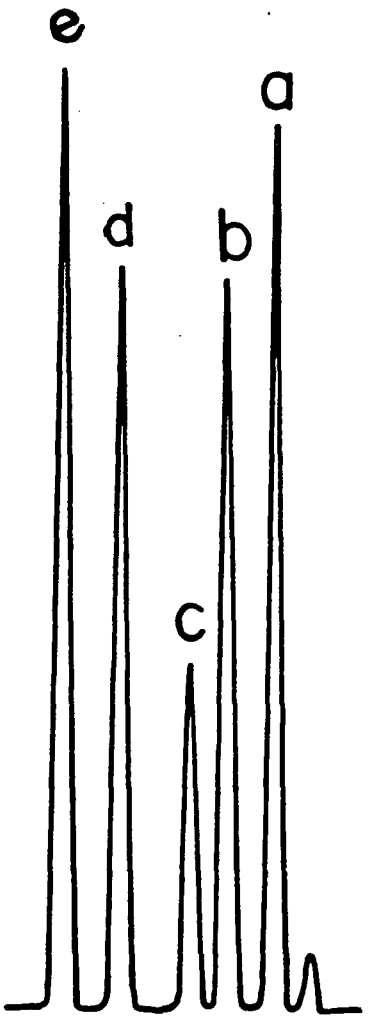

Figure 4.20. The 17476 cm^{-1} spectral region of molecular iodine is shown above. The peaks, a, b, c, d, and, e, are idenified as the 18'-1" P(37), 16'-0" R(61), 17'-0" R(111), 19'-1" P(95), and 18'-1" R(42) respectively.

transition will be similar to that of the argon ion laser or not. Indeed, if the dye laser produced more iodine atoms than the argon ion beam then this is bad from the point of view that Letokhov et al claimed that no reaction occurs between the 2-hexene and iodine atoms. The main reason for choosing this transition was the fact that using the dye laser alone made it very simple to monitor the ortho and para lines at specific time intervals and cut down on the noise in the signal. The only way to find out if this had been a bad choice was to perform the experiment.

To obtain a very low pressure of iodine vapour in the test cell a known volume volume, $V_B \simeq 6.0$ cm^3, equipped with a break seal was attached to the test cell (1.9 cm diameter, 30 cm length, and 79 cm^3 volume). This section, V_B, was evacuated to about 8×10^{-6} torr, filled with (30.0±0.3) mtorr of iodine vapour, and sealed. The test cell itself was then evacuated and filled with (1.0±0.3) torr of 2-hexene vapour. At this point the 2-hexene was condensed in a side arm of the test cell by immersing the arm in liquid nitrogen and the seal between the cell and volume V_B broken, allowing the iodine vapour into the test cell and subliming it in the side arm as well. After pinching off the volume, V_B, the pressure of the iodine could be calculated as (2.24±0.20) mtorr.

With both constituents still condensed, the test cell was reevacuated for ten minutes to remove any air that may have outgased during the filling procedure. Finally, the

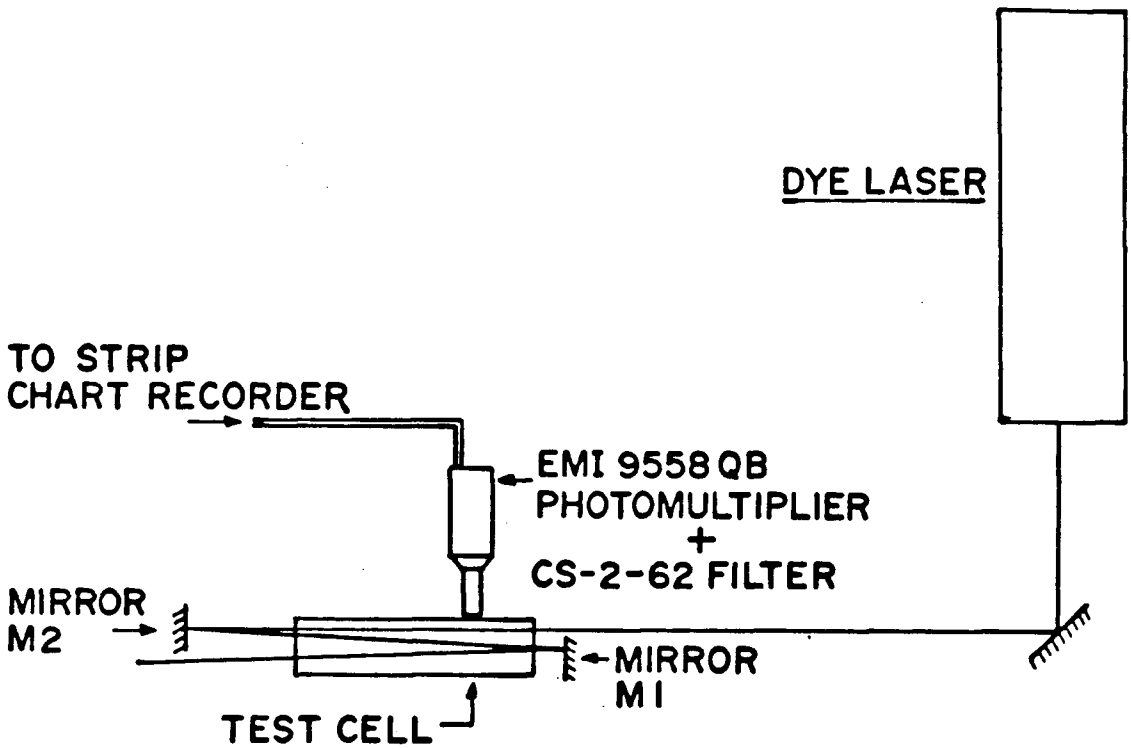

Figure 4.21 The experimental arrangement used for test cells (1.9 cm diameter, 30 cm length) containing about 2.24 mtorr of iodine vapour and 1 torr of 2-hexene gas. The dye laser was used both to drive the reaction using the 19'-1" P(95) spectral line and monitor the ortho- to para-iodine ratio with the 18'-1" P(37) and R(42) peaks. Note that the laser beam was sent through the test cell three times with mirrors M1 and M2.

cell was removed from the vacuum line and arranged as shown in figure 4.21.(Note that the dye laser beam transitted the cell volume three times with the aid of mirrors M1 and M2.)

The results of such an experiment are described below.

TABLE 4.16 Experimental Conditions

BACKGROUND PRESSURE	2×10^{-5} torr
INITIAL IODINE PRESSURE	(2.24±0.20)mtorr
INITIAL 2-HEXENE PRESSURE	(1.0±0.2)torr
DYE LASER POWER	(310±10)mW
EXCITATION LINE	B X (19'-1") P(95)
DYE LASER MONITOR LINES	B X (18'-1") P(37),R(42)
	$\nu \simeq 17476$ cm^{-1}
SCAN LENGTH	30 GHz
SCAN TIME	75 s

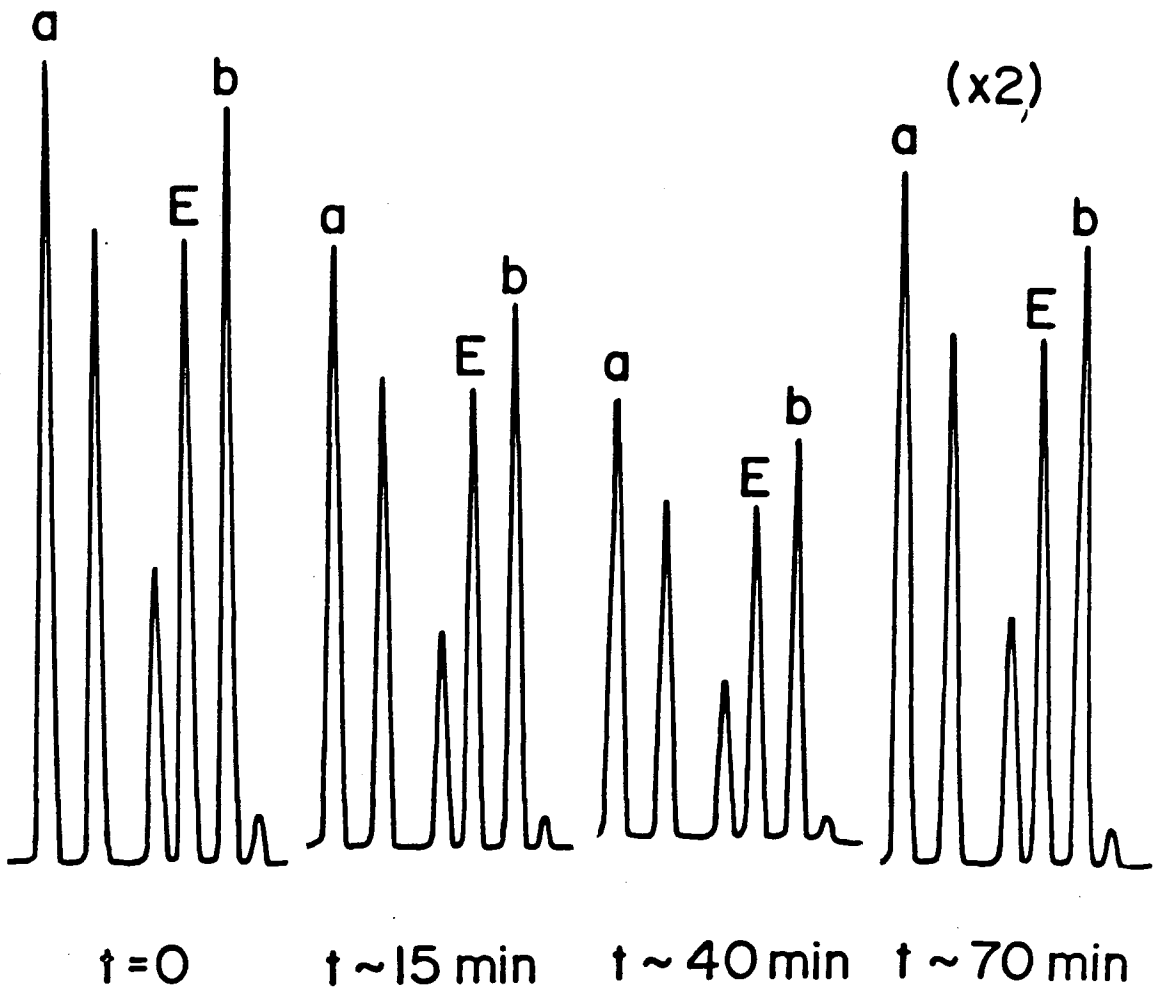

Figure 4.22 The time dependent behaviour of the 17476 cm^{-1} region of the iodine spectrum in a test cell containing about 2.24 mtorr of iodine and 1 torr of 2-hexene. The line being used to drive the reaction between the two species, the 19'-1" P(95) transition, is labelled above as E and the peaks used to monitor the ortho to para ratio of the sample are the 18'-1" P(37), [a], and the 18'-1" R(42), [b], lines. No ortho- to para-iodine ratio shift is apparent.

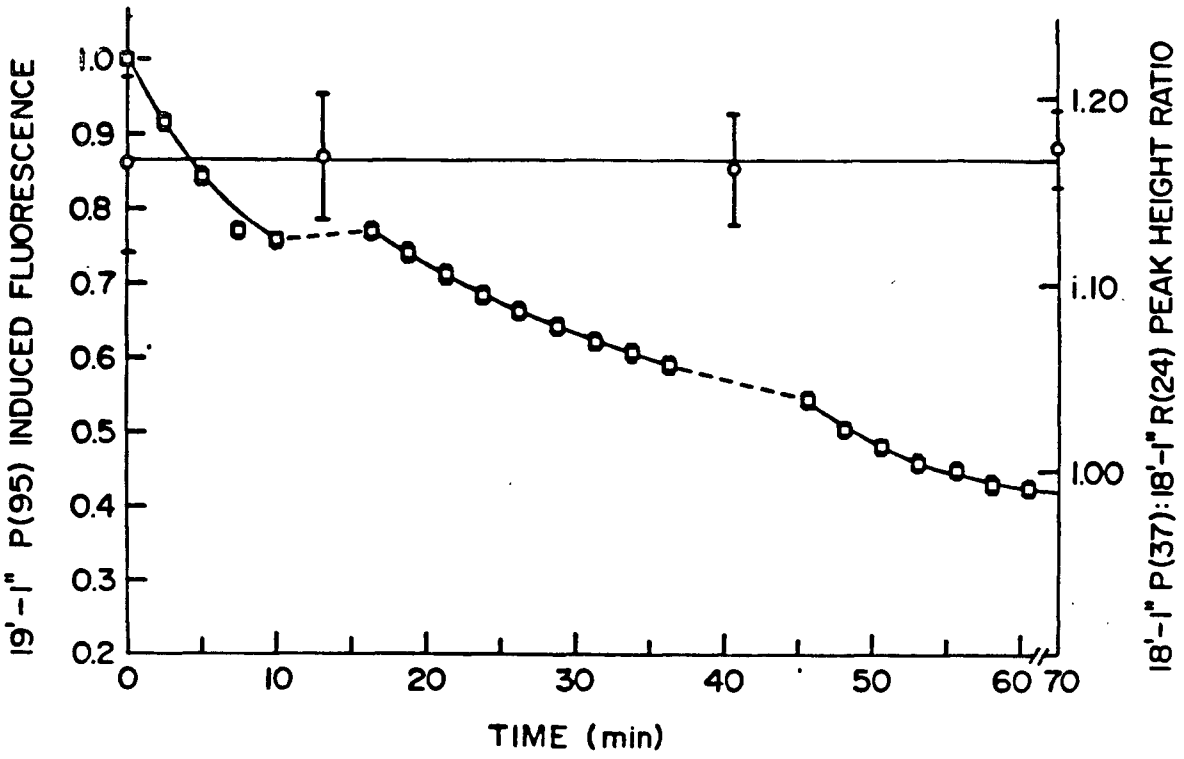

Figure 4.23. A plot of the decay of the 19'-1" P(95) induced fluorescence (□), and the 18'-1" P(37) : R(42) peak height ratio, (O), in a cell containing about 2.24 mtorr of iodine vapour and 1 torr of 2-hexene gas over the course of the experiment is shown above. As before, the dashed lines indicate the period for which the reaction was not being driven with the 19'-1" P(95) transition.

TABLE 4.17 19'-1" P(95) Fluorescence Signal versus Time

TIME (min.±1.0 min.)	FLUORESCENCE (arb.±0.010)
0	1.000
2.5	0.915
5.0	0.843
7.5	0.770
10.0	0.759
16.3	0.769
18.8	0.740
21.3	0.714
23.8	0.682
26.3	0.664
28.8	0.642
31.3	0.623
33.8	0.602
36.3	0.589
45.6	0.544
48.1	0.503
50.6	0.483
53.1	0.462
55.6	0.448
58.1	0.432
60.6	0.423
63.1	0.412

(...cont.)	
65.6	0.397
67.1	0.391

TABLE 4.18 18'-1" P(37):R(42) Peak Height Ratios versus Time

TIME (min.±1.0 min.)	$\frac{18'\text{-}1''\ P(37)}{18'\text{-}1''\ R(42)}$
0.0	1.164±0.049
13.0	1.168±0.020
41.0	1.174±0.025
70.0	1.192±0.026

No ortho to para ratio shift was observed. The reason for this is ambiguous, however, as it may simply be caused by the fact that too many iodine atoms were produced and were not scavenged by the 2-hexene.

To settle this matter an experiment was performed closely reproducing the conditions reported by Letokhov et al. A mixture of roughly 30 mtorr of iodine and 2 torr of 2-hexene vapour contained in a T-shaped test cell (6 mm diameter, 15 cm length and about 18.0 cm^3 volume) was irradiated with the 5145 Å argon ion line and the dye laser tuned to the 17408 cm^{-1} region simultaneously. The resulting fluorescence was recorded on a strip chart recorder.

The test cell was prepared for use by baking it out under a vacuum for 24 hours prior to use. Iodine vapour was added to the cell by diffusion as previously described to give (30±3) mtorr of pressure.

The 2-hexene was added to the cell by placing a (-20.0±0.5)°C bath around the 2-hexene vessel. The vessel was opened to part of the manifold (volume $V_1 \simeq 135.05 cm^3$) and the pressure in this section allowed to reach the equilibrium value for this temperature, 16.5 torr. The 2-hexene container was sealed off and the gas in volume V_1 allowed to expand into a second part of the manifold (volume $V_2 \simeq 821.39\ cm^3$) and the test cell in the dark so as to avoid initiating a reaction between the iodine and 2-hexene prematurely. The net result of this was to produce a test sample containing (2.3±0.5) torr of 2-hexene in addition to the iodine. This cell, kept in the dark, was placed in the expeimental setup shown in figure 4.5 and the experiment initiated.

TABLE 4.19 Experimental Conditions

BACKGROUND PRESSURE	6×10^{-6} torr
INITIAL IODINE PRESSURE	(30±3)mtorr
INITIAL 2-HEXENE PRESSURE	(2.3±0.5)torr
ARGON ION LASER POWER	(1.60±0.10)W
DYE LASER POWER	80mW
DURATION OF EXPERIMENT	20 minutes
DYE LASER MONITOR LINES	B X (15'-0") P(25),R(30)
	$\nu \simeq 17408\ cm^{-1}$
SCAN LENGTH	30 GHz
SCAN TIME	75 s

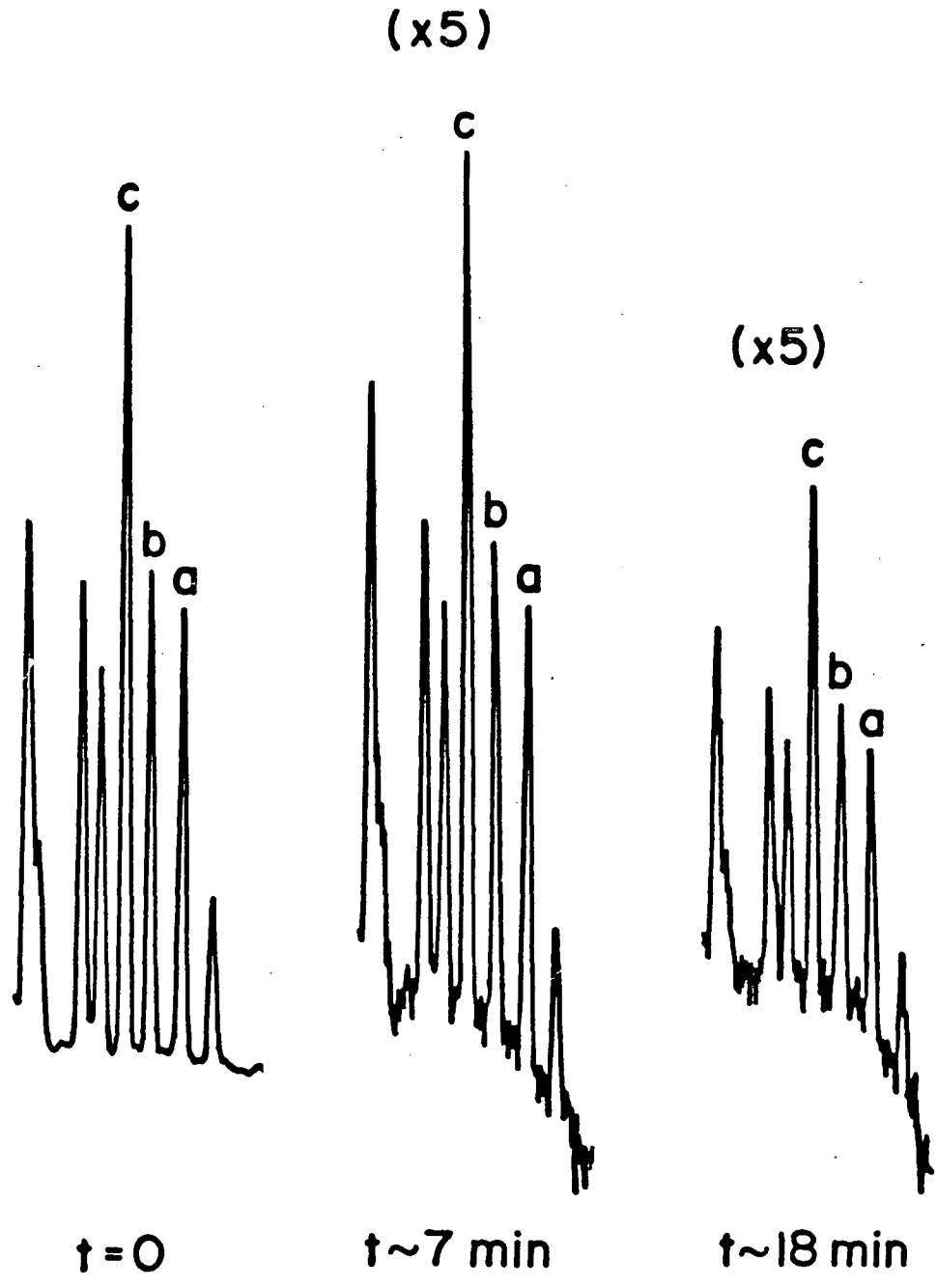

Figure 4.24. Typical fluorescence spectra of the 17408 cm^{-1} region excited in a test cell (6 mm diameter, 15 cm length) containing (30±3)mtorr of iodine vapour and (2.3±0.5)torr of 2-hexene. In this case, the dual beam irradiation technique was used once again so that the reaction was initiated with the 5145 Å argon ion laser line and the ortho- and para-iodine ratios were monitored with the 15'-0" P(25) and R(30) transitions. (The peaks labelled a, b, and c are the 15'-0" R(30), 15'-0" P(25), and the 18'-1" P(84) lines respectively.)

TABLE 4.20 15'-0" P(25):R(30) Peak Height Ratio versus Time

TIME (min.±1.0 min.)	15'-0" P(25) / 15'-0" R(30)
0	1.063±0.033
3.4	1.044±0.051
4.6	1.074±0.061
6.2	1.072±0.065
7.4	1.078±0.066
12.4	1.028±0.175
17.6	1.076±0.104
20.0	1.076±0.105

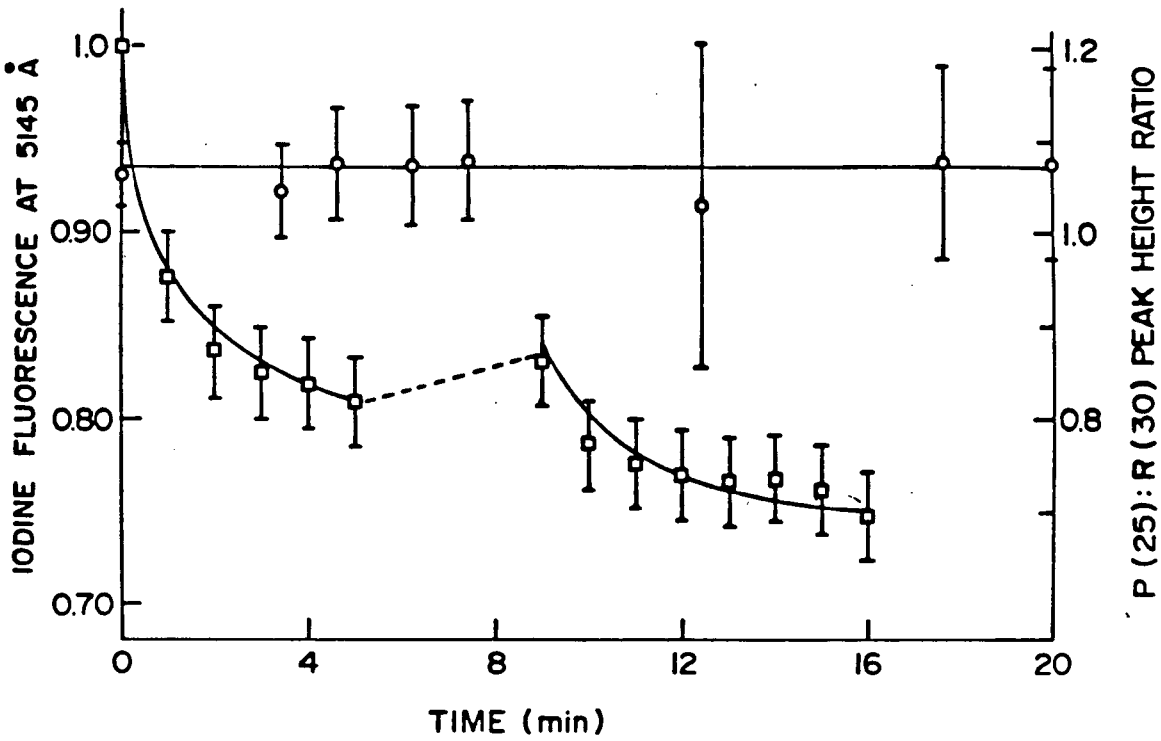

Figure 4.25. A plot of the decay of the 5145 Å induced fluorescence (□), and the 15'-0" P(25) : R(30) peak height ratio, (O), in a cell containing about 30 mtorr of iodine vapour and 2.3 torr of 2-hexene gas over the course of the experiment is shown above.

TABLE 4.21 Argon Ion Induced Fluorescence versus Time

TIME (min.±1.0 min.)	FLUORESCENCE (arb.)
0	1.000
1.0	0.876±0.024
2.0	0.837±0.024
3.0	0.825±0.023
4.0	0.819±0.023
5.0	0.809±0.023
8.0	0.831±0.024
9.0	0.787±0.023
10.0	0.776±0.023
11.0	0.776±0.023
12.0	0.770±0.023
13.0	0.766±0.022
14.0	0.768±0.022
15.0	0.762±0.022
16.0	0.756±0.022

Based upon these results, after roughly 12 minutes of irradiation with the argon ion laser beam, no ortho to para enrichment has occurred to within a 10 percent uncertainty. Again this contradicts the findings of Letokhov et al who claimed that with these initial pressures an enrichment factor in excess of 4 was to be expected – a 75% decrease in the ortho- to para-iodine ratio – over this time period.

Possible causes for this could be that either the 2-hexene is not reacting with the iodine molecules or atoms or that the reaction does proceed via a radical chain. i.e. let X represent a 2-hexene molecule,

$$o\text{-}I_2 \longrightarrow 2I$$

$$I + X \longrightarrow XI$$

$$XI + I_2 \longrightarrow I + XI_2$$

$$XI + I \longrightarrow XI_2$$

As the concentration of iodine molecules is larger than that of the atoms, at least initially, then if such a mechanism is operating the most probable result of it would be that the XI radicals formed would attack the molecular iodine and liberate iodine atoms. Both the XI and I species could conceivably scramble any enhancement produced. However, Letokhov et al ruled out this possibility based on the argument that the reaction rate of the iodine molecules with 2-hexene does not follow the expected form for such a mechanism (see chapter 3) and that when a mixture of 2-hexene and iodine was irradiated at 4880 Å,which lies above the dissociation limit of the $B^3\Pi_{0^+u}$ state of molecular iodine, no change in the molecular concentration was observed. Unfortunately, no data was provided to support the latter claim.

As it was not the purpose of this investigation to study the kinetics and reaction mechanism of the above

species, this area of research was abandonned in search of a more favorable scavenger.

2. IODINE AND ACETYLENE

A series of three papers were produced by V. S. Kushawaha[29,30,31] in which laser induced photochemical reactions between molecular iodine and acetylene, C_2H_2, were performed. The paper of the most relevance to this work[30] described a laser induced isotope separation of I_2^{129} from I_2^{127} using acetylene as a scavenger. The details of the experiment are listed in table 4.21.

TABLE 4.22 Experimental Conditions for I_2^{129} Isotope separation.

BACKGROUND PRESSURE	10^{-5}torr
INITIAL AMOUNT OF IODINE 127	1.0×10^{-4}g
INITIAL AMOUNT OF IODINE 129	1.0×10^{-4}g (?)
INITIAL AMOUNT OF ACETYLENE	30 torr
TEST CELL DIMENSIONS	(PYREX) 2.5 cm diameter
	5.0 cm length
DYE LASER IRRADIATION REGION	(6040±2)Å
DYE LASER POWER	(i) 100mW before reaction
	(ii) 15mW during reaction

To effect an isotope separation, Kushawaha prepared two cells, one containing iodine-127 alone – the intracavity cell – and one containing an equal mixture of of the two isotopes and some acetylene – the test cell. The test cell was irradiated with a dye laser beam, (6040±2)Å, at 100 mW of power for roughly 10 minutes and the products sent through a mass spectrometer for analysis. A second similarly prepared cell was irradiated with th dye laser beam but with the iodine-127 spectral lines removed by placing the intracavity cell inside the laser cavity. In this case about 15 mW of power exitted the dye laser and the cell irradiated for 60 minutes after which time the products were again analyzed by a mass spectrometer. Kushawaha's results are shown in figure 4.26 (taken from reference 30)

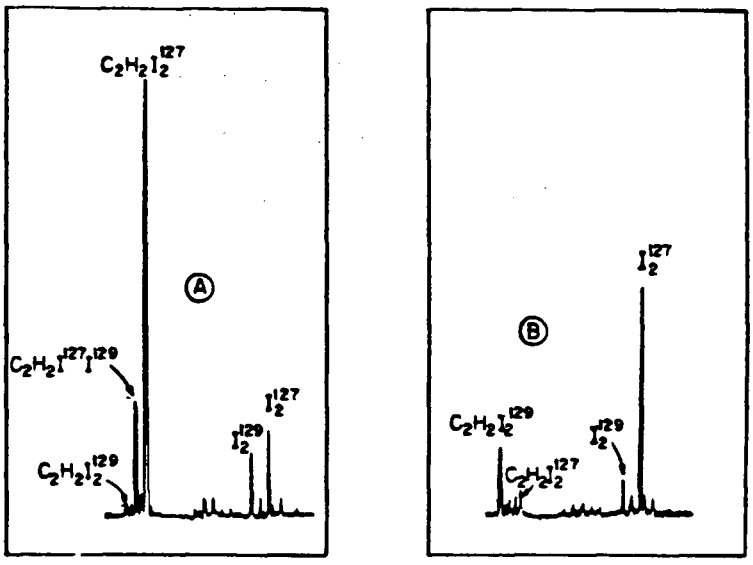

Figure 4.26. Results obtained by V. S. Kushawaha[30] using acetylene in an isotopic separation of iodine-129. The above two mass spectographs show the I_2^n and the $C_2H_2I_2^n$ peaks after non-selective irradiation of a test cell containing iodine-127, iodine-129, and acetylene, A, and after selective irradiation of the I_2^{129}, B.

From the above spectographs it appears that, indeed, an isotope separation has been produced. However, several unaddressed problems need to be pointed out. First, iodine-129 is a radioactive substance and, as such, hard to handle. As a result of this Kushawaha placed a crystal of the substance in each test cell without weighing it and judged the weight by comparing its size to the size of an iodine-127 crystal weighing about 1.0×10^{-4} gram also placed in the cell. The actual amount of the iodine-129 originally in any given test cell was unknown and very likely varied considerably from preparation to preparation. Thus one can not rigorously compare results obtained from different test cells.

A curious feature of the result obtained when the sample was irradiated on all the spectral lines is the fairly large $C_2H_2I^{127}I^{129}$ peak. This would seem to indicate the existence of some scrambling mechanism taking place during the reaction as there was very little of this mixed species originally present in the test cells. That is, if the reaction proceeded solely via the reaction,

$$I^{2n\,*} + C_2H_2 \longrightarrow C_2H_2I_2{}^{n}$$

then one would expect the final products to reflect the original ratios of the $I_2{}^{127}$: $I_2{}^{129}$: $I^{127}I^{129}$ species. This dilemma is further compounded by the fact that no mixed species peak was observed after the selective irradiation of

the iodine-129.

With these concerns aside, the data provided appears quite promising. Indeed if acetylene gas does react preferentially with excited iodine molecules then it would proove to be an excellent scavenger with which to perform an ortho-para enhancement.

Acetylene gas, 99.6% pure, was obtained from Matheson Co. and introduced to storage bulb attached to the vacuum line. The gas was distilled from trap to trap several times to ensure its purity and remove any air that could have contaminated the sample while filling the bulb.

Obviously one wishes to avoid the formation of a radical chain during these experiments as these will lead to the formation of species that may be able to scramble the ortho- and para-iodine. To avoid this difficulty the 15'-0" P(25) line, which has low predissociation, was chosen to drive the reaction and, along with the 15'-0" R(30), used to monitor the ortho to para ratio.

The first experiments performed with acetylene and iodine was carried out in a pyrex cell with a 1.9 cm diameter and 30 cm length evacuated and filled with the desired amounts of iodine and acetylene. The cell was then removed from the vacuum line and arranged in an apparatus shown in figure 4.27. The dye laser beam was expanded to roughly a 1.5 cm diameter before entering the cell and the fluorescence recorded, as before, on a strip chart recorder. Note that when the dye laser was

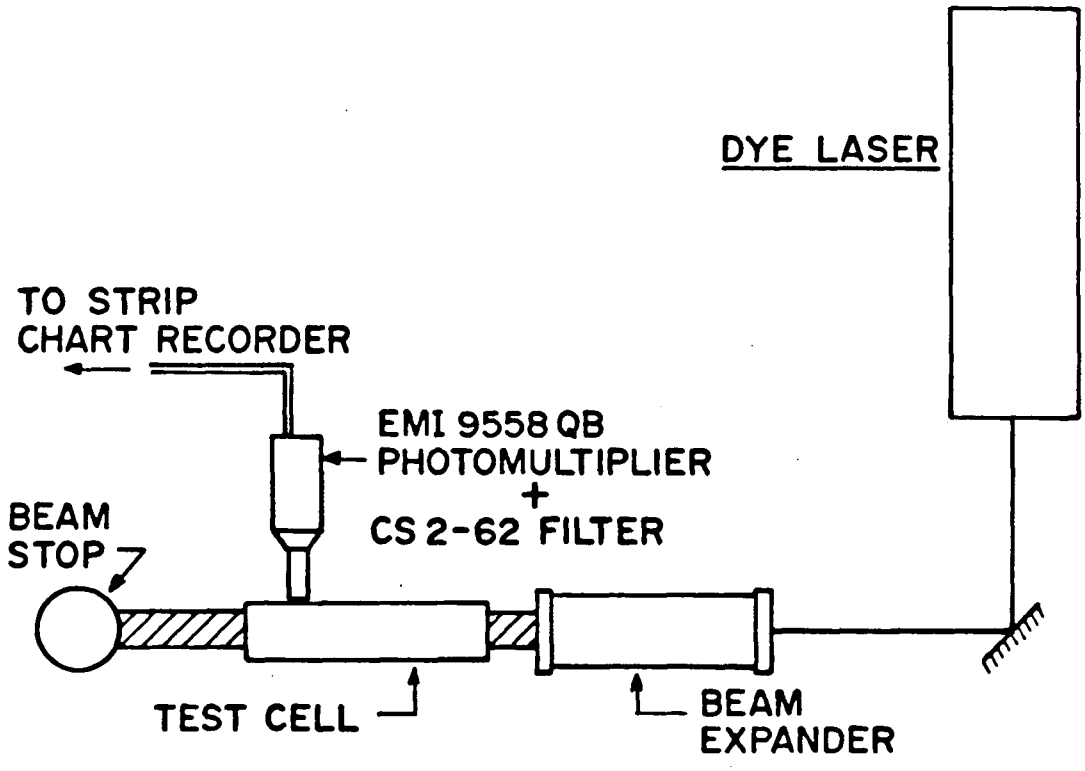

Figure 4.27 The experimental arrangement used for the selective irradiation of ortho-iodine in the presence of acetylene. A test cell, (1.9 cm diameter, 30 cm length), containing about (27±3)mtorr of iodine vapour and (30±2) torr of acetylene gas was irradiated with the dye laser both to drive the reaction using the 15'-0" P(25) spectral line and monitor the ortho- to para-iodine ratio with the 15'-0" P(25) and R(30) peaks. Note that the laser beam was expanded befor entering the cell.

set to scan across the spectral region of interest to monitor the ortho- and para-iodine peaks the intensity of the beam was decreased by a factor of 100 with the use of a 2.0 neutral density filter.

TABLE 4.23 Experimental Conditions

BACKGROUND PRESSURE	3×10^{-5}torr
INITIAL IODINE PRESSURE	(27±3)mtorr
INITIAL ACETYLENE PRESSURE	(30±2)torr
TEST CELL DIMENSIONS	(PYREX) 1.9 cm diameter 30 cm length
DYE LASER POWER	(150±10)mW
EXCITATION LINE	15'-0" P(25)
DYE LASER MONITOR LINES	B X (15'-0") P(25),R(30) $\nu\simeq17408$ cm^{-1}
SCAN LENGTH	30 GHz
SCAN TIME	75 s

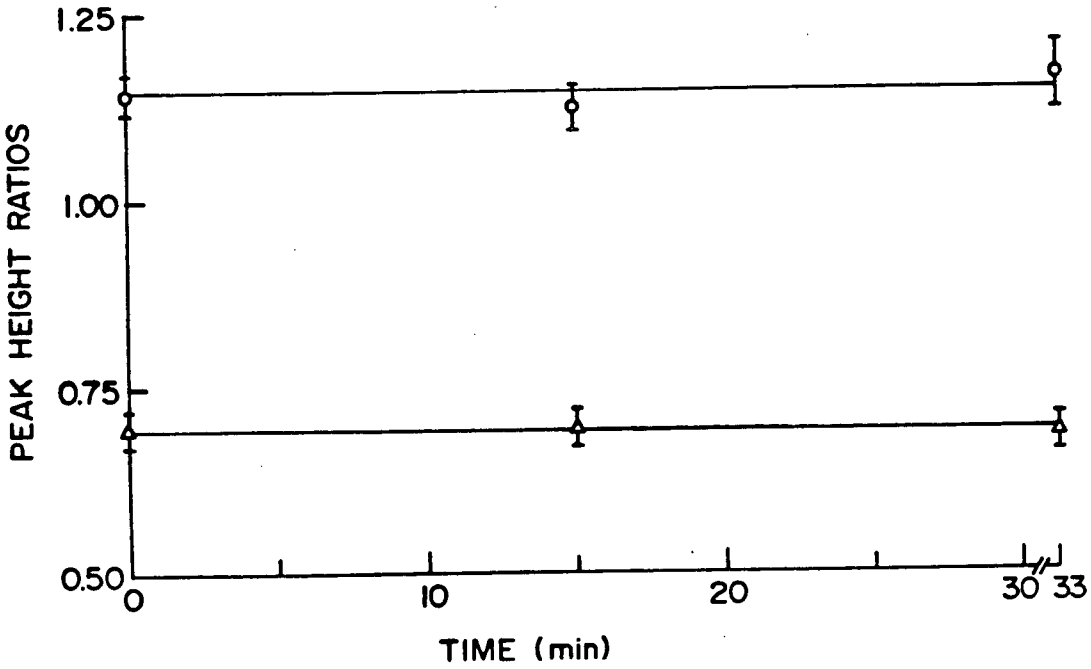

Figure 4.28 The 15'-0" P(25) : R(30) (O), and 15'-0" P(25) : 18'-1" P(84) (Δ), peak height ratios as a function of time over the course of the experiment observed in a cell containing about 27 mtorr of iodine and 30 torr of acetylene.

TABLE 4.24 Peak Height Ratios versus Time

Time (min.±1 min.)	15'-0" P(25) / 15'-0" R(30)	15'-0" P(25) / 18'-1" P(84)
0	1.143±0.032	0.645±0.024
15	1.126±0.031	0.643±0.020
33	1.165±0.045	0.636±0.019
82	1.158±0.048	0.638±0.024

In this experiment the dye laser scanned across the 30 GHz section of spectrum several times and then tuned to the 15'-0" P(25) line. At this frequency the cell was irradiated for about fifteen minutes and then the spectrum rescanned several times. This procedure was repeated twice more irradiating the cell with the P(25) peak for 13 and 45 minutes respectively. As is readily observed from the results shown on figure 4.28 and table 4.24, no evidence for any shift in the ratio of the ortho-iodine to para-iodine was observed to within 5%.

A final attempt to produce an enhancement using acetylene as a scavenger was made. This time the laser power was decreased to about 150 mW without expanding the beam, the initial pressures of iodine and acetylene were decreased, and the size of the cell used was decreased.

As before the test cell was prepared by baking it out while evacuating it for roughly 21 hours prior to use.

Iodine vapour and acetylene gas were allowed to diffuse into the cell controlled by constant temperature baths.

TABLE 4.25 Experimental Conditions

BACKGROUND PRESSURE	3.6×10^{-6} torr
INITIAL IODINE PRESSURE	(17±1)mtorr
INITIAL ACETYLENE PRESSURE	(7.0±0.4)torr
TEST CELL DIMENSIONS	(PYREX) 0.6 cm diameter 15 cm length
DYE LASER POWER	(170±10)mW
EXCITATION LINE	15'-0" P(25)
DYE LASER MONITOR LINES	B X (15'-0") P(25),R(30) $\nu \simeq 17408$ cm^{-1}
SCAN LENGTH	30 GHz
SCAN TIME	75 s

TABLE 4.26 Peak Height Ratios versus Time

Time (min.±1 min.)	$\frac{\text{15'-0" P(25)}}{\text{15'-0" R(30)}}$	$\frac{\text{15'-0" P(25)}}{\text{18'-1" P(84)}}$
0	1.083±0.028	0.634±0.013
31	1.111±0.032	0.639±0.014
44	1.083±0.033	0.631±0.015

Again, no ortho to para ratio shift was observed.

3. IODINE AND NITRIC OXIDE

After these setbacks an attempt to find a simpler scavenger was initiated. A paper written by N. Basco and J. E. Hunt[56] reported on the recombination of iodine atoms in the presence of nitric oxide and argon. The proposed mechanism was,

$$I + NO + Ar \longrightarrow INO + Ar$$

$$I + INO \longrightarrow I_2 + NO$$

$$2INO \longrightarrow I_2 + NO$$

where $k_1 \simeq 3.5 \times 10^9 l^2/mole^2 s$, $k_2 \simeq 1 \times 10^{11} l/mole\ s$, and $k_3 \simeq 2.1 \times 10^7 l/mole\ s$.

Nitric oxide may make a good scavenger for the iodine molecules or perhaps simply help them to recombine. Unfortunately, nitric oxide is a paramagnetic species and, as such, capable of converting ortho-iodine to para-iodine and vice-versa. If the rate at which this conversion occurs is large compared to k_1 and k_3 then no shift will be observed. On the other hand, for the case where the rate constant is of the same order of magnitude as that for the conversion in hydrogen then the half-life for the conversion will be about 17 minutes for a cell containing 50 torr of nitric oxide and 330 minutes for one with 3 torr.

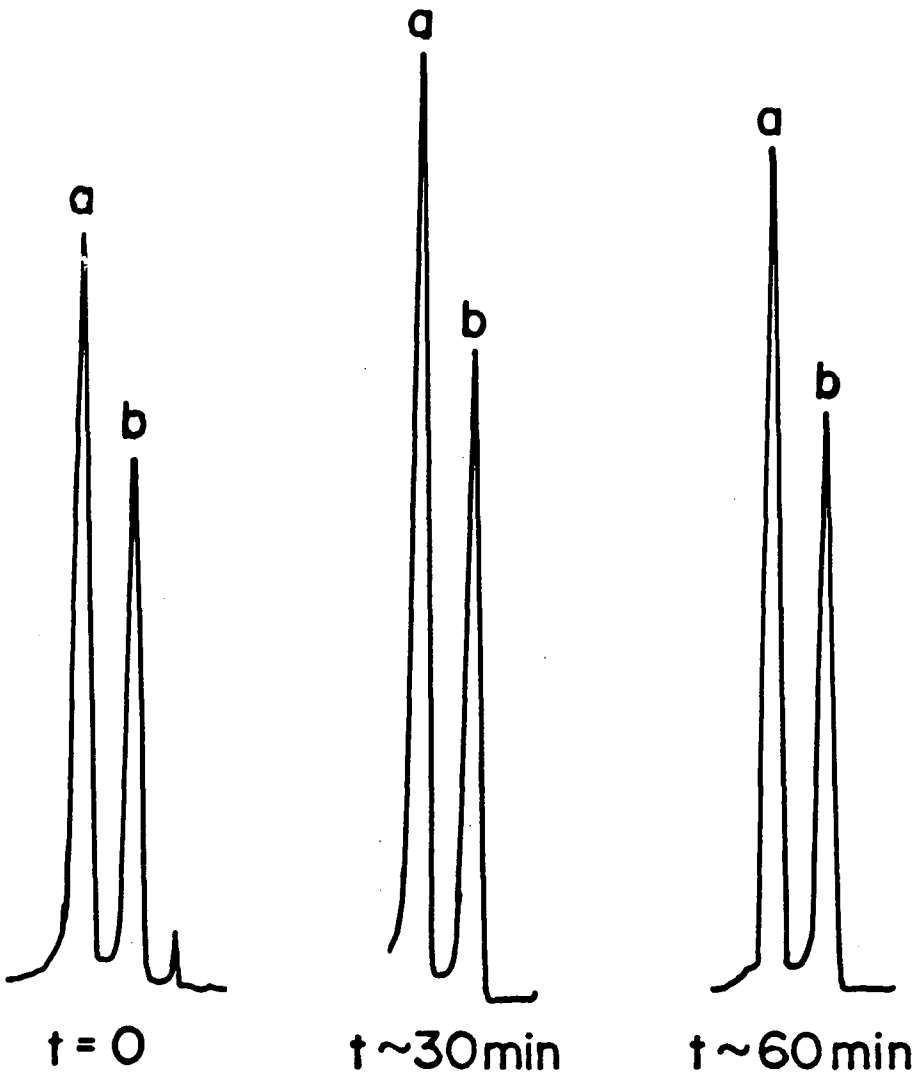

Figure 4.29. The above are typical spectra of the 14'-1" P(77) [a] and 14'-1" R(82) [b] peaks observed in a cell containing about 3 mtorr of iodine and 3 torr of nitric oxide after different amounts of argon ion laser irradiation. Notice that the spectra do not vary appreciably, not even in height.

To find out if this would work as a scavenger, several experiments were performed using the method discribed on page on cells containing roughly 3 mtorr of iodine, 20 torr of helium,(helium was used instead of argon because it quenches the fluorescence of iodine to a lesser extent) and between 3 and 58 torr of nitric oxide. As summarized by figure 4.29 which displays a typical spectrum, no evidence for any enhancement was observed. This was the case when the excitation line was the argon ion beam or the dye laser beam tuned to the 16'-1" P(83), a more highly predissociating transition. Thus one must conclude that the nitric oxide readily scrambled the two species.

4. IODINE AND NITROSYL CHLORIDE

To try and avoid the problems encountered with having a free radical present, the nitric oxide was replaced with nitrosyl chloride, NOCl. It was hoped that this compound would provide efficient scavenging of the excited iodine molecules via ,

$$I_2^* + NOCl \longrightarrow INO + ICl$$

The same procedure as previously described using the dye laser both to drive the reaction and monitor the ortho- and para-iodine concentrations was employed on test cells filled with roughly 3 torr of nitrosyl chloride and 150

mtorr of iodine vapour. Typical experimental conditions are listed in table 4.27.

TABLE 4.27 Experimental Conditions

BACKGROUND PRESSURE	3×10^{-5}torr
INITIAL IODINE PRESSURE	(150±10)mtorr
INITIAL NOCl PRESSURE	(3±1)torr
TEST CELL DIMENSIONS	(PYREX) 1.9 cm diameter
	30 cm length
DYE LASER POWER	(300±10)mW
EXCITATION LINE	19'-1" P(95)
DYE LASER MONITOR LINES	B X (18'-1") P(37),R(42)
	$\nu\simeq17408\ cm^{-1}$
SCAN LENGTH	30 GHz
SCAN TIME	75 s

The results of these experiments were quite unexpected. Upon first irradiating the test cell while scanning the 30 GHz region of interest no molecular iodine spectrum was evident. With the aid of a cell containing iodine vapour by itself, the dye laser was tuned to the 19'-1" P(95) peak and the test cell was irradiated at this wavelength for about fifteen minutes. During this time the fluorescence caused by the dye laser beam at this frequency increased by a factor of two. Upon rescanning the dye laser, molecular iodine peaks were clearly visible. This procedure was

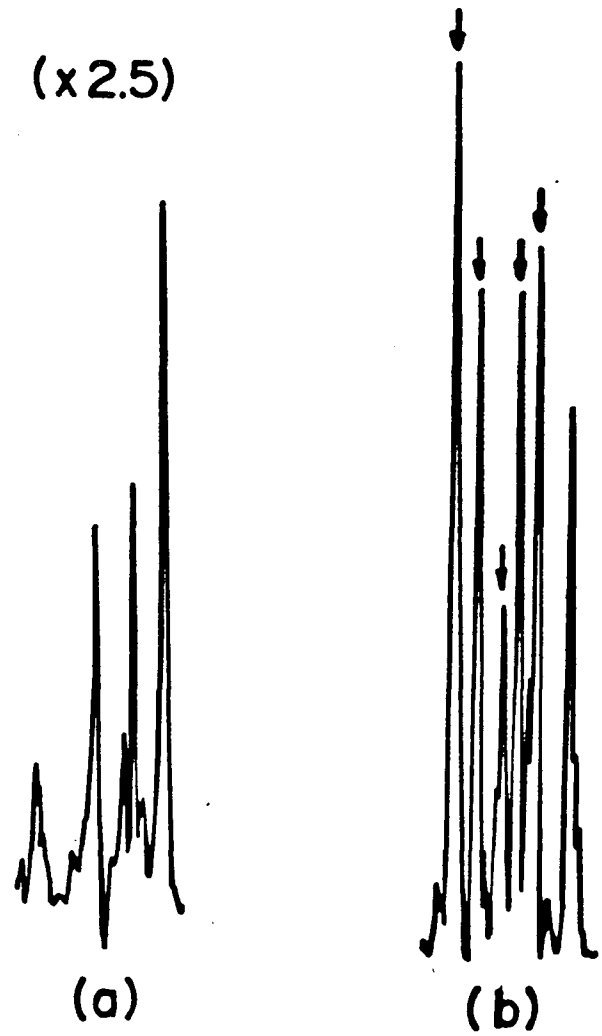

Figure 4.30. The above two spectra were recorded with the dye laser scanning across the 17408 cm^{-1} region irradiating a test cell containing about 150 mtorr of iodine and 3 torr of nitrosyl chloride. The first trace, (a), was taken before any strong irradiation of the cell had taken place. The second trace, (b), was recorded after irradiating the mixture for about 15 minutes with the the 19'-1" P(95) transition. The iodine spectrum is clearly visible after the irradiation of the test cell (as indicated by the arrows above) but not discernable originally.

repeated once more and the iodine lines became more pronounced.

From these results it would appear that nitrosyl chloride reacted with the ground state molecules to form perhaps ICl. Upon irradiation, the ICl dissociated to produce I_2 and Cl_2. i.e.

$$I_2 + NOCl \longrightarrow I + ICl + NO$$

$$I + NOCl \longrightarrow ICl + NO$$

$$2ICl + h\nu \longrightarrow I_2 + Cl_2$$

This is not necessarily what happens, but is a plausible explanation. In any case, nitrosyl chloride is obviously a poor choice for a scavenger of excited iodine molecules alone.

5. IODINE AND ETHYL IODIDE

All of the previous results indicate that the iodine molecules are very susceptible to any free radical contamination, such as free iodine atoms, nitric oxide, or a complex radical formed by the addition of an iodine atom to an organic compound.

A final idea that was tried was to exchange an iodine atom from the selectively excited iodine molecule with one attached to an iodinated organic compound. This is similar to what R. N. Zare et al[33] did to produce a photochemical

isotopic separation of $^{35}Cl_2$ and $^{37}Cl_2$. It involved taking a nonradical compound containing at least one iodine atom attached to it, XI. Theoretically, as the excited iodine molecule came into contact with XI it would exchange one of its iodine atoms with one already attached to the scavenger. In the best possible scenario the species, XI, would react solely with the excited iodine molecules and be inert as regards the ground state molecules. After each exchange the resulting iodine molecule would have a 7/12 chance of being an ortho-iodine and a 5/12 chance of being a para-iodine. Hence, if one were selectively exciting the ortho species, one would obtain a net decrease in the number of ortho molecules in the system. Ethyl-iodide, C_2H_5I, (abbreviated EI here) was chosen as a trial exchange partner mainly due to time constraints, the fact that it was readily available, and because some data on methyl-iodide, CH_3I[34], a similar molecule, suggested that methyl-iodide exchanges atoms with molecular iodine in the gas phase.

Fischer certified ethyl-iodide was placed on the vacuum line and prepared for use by trap to trap distillation and then stored in a pyrex container attached to the manifold.

A test cell was prepared by evacuating it for about 24 hours and then filling it with the desired pressures of each substance. The cell was then pinched off of the system.

To drive the reaction the 15'-0" P(25) spectral line was chosen to have as few iodine atoms present as possible during the experiment. As usual, the dye laser was scanned

across a preselected region of iodine spectrum several times before initiating the experiment and the fluorescence recorded to ascertain the time zero peak height ratio. This accomplished, the dye laser was tuned to the P(25) transition and the cell irradiated for a specific amount of time and then the dye laser scanned again. The results of this procedure are given below.

TABLE 4.28 Experimental Conditions

BACKGROUND PRESSURE	3×10^{-5} torr
INITIAL IODINE PRESSURE	(30±2)mtorr
INITIAL ETHYL IODIDE PRESSURE	(13±2)torr
TEST CELL DIMENSIONS	(PYREX) 1.9 cm diameter 30 cm length
DYE LASER POWER	(190±10)mW
EXCITATION LINE	15'-0" P(25)
DYE LASER MONITOR LINES	B X (15'-0") P(25),R(30) $\nu \simeq 17408$ cm^{-1}
SCAN LENGTH	30 GHz
SCAN TIME	75 s

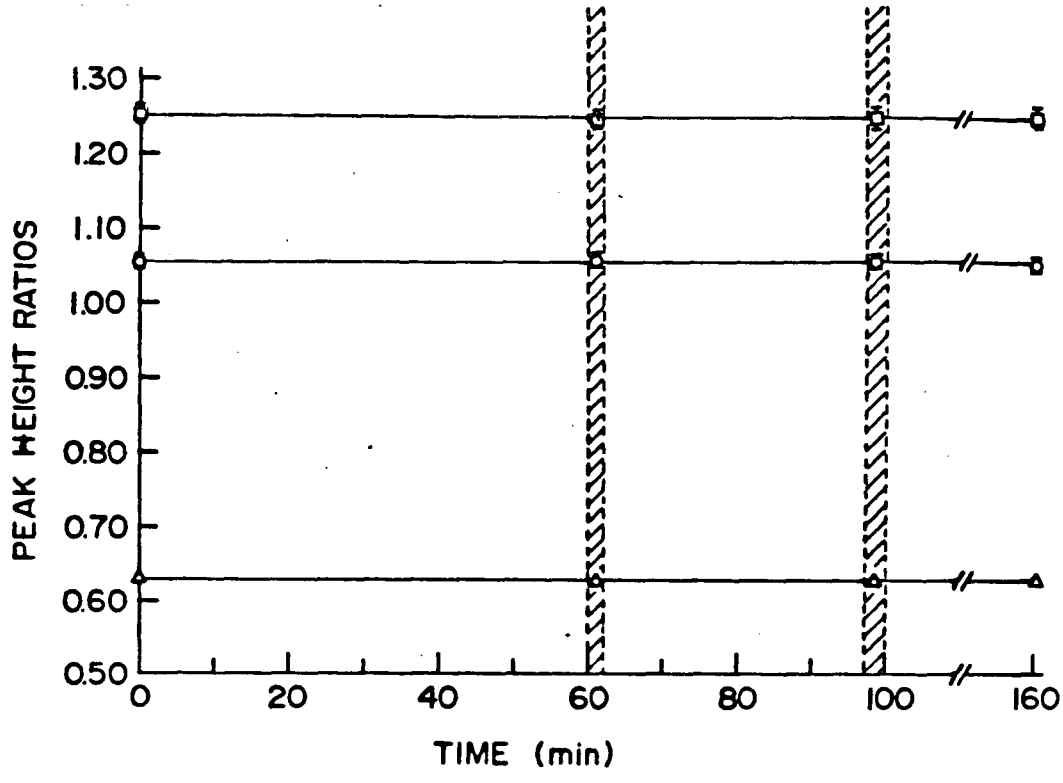

Figure 4.31. A plot of 15'-0" P(25) : 15'-0" R(30), (O), 15'-0" P(25) : 18'-1" P(84), (Δ), and 15'-0" P(25) : 19'-1" P(121), (□), peak height ratios versus time in a cell containing about 30 mtorr of iodine and 13 torr of ethylene iodide. No evidence for an ortho- to para-iodine ratio shift was observed.

TABLE 4.29 Peak Height Ratios versus Time

Time (min.±1 min.)	15'-0" P(25) / 15'-0" R(30)	15'-0" P(25) / 18'-1" P(84)	15'-0" P(25) / 19'-1" P(121)
0	1.056±0.011	0.631±0.005	1.253±0.010
62.3	1.060±0.013	0.633±0.006	1.248±0.017
97.0	1.062±0.013	0.629±0.012	1.251±0.017
161.0	1.055±0.014	0.629±0.008	1.253±0.018

As in all of the previous experiments, an indication that an ortho to para ratio shift could have occurred would have been a decrease in the 15'-0" P(25) induced fluorescence during the irradiation period. In this case almost no change was observed at all and, indeed, the ratios of the ortho-iodine peak height to the para-iodine peak heights displayed no trace of a shift.

V. CONCLUSIONS AND DISCUSSION

A. COMMENTS ON THIS RESEARCH

The main impetus for this research, as has been stated previously, began with the promising results reported by Letokhov et al and, indeed, this author attempted to reproduce their experimental conditions as closely as possible. Unfortunately, the findings of this work show no evidence to support the claim that selective predissociation of the ortho-iodine molecules with the 5145 Å line of an argon ion laser leads to any relative enhancement of the para-iodine population either in a system of pure iodine vapour or in a mixture of iodine and any of the scavengers 2-hexene, acetylene, nitric oxide, nitrosyl chloride, or ethyl-iodide. The question immediately arises as how to reconcile the two claims. To address this question the experiments involving iodine vapour alone and those with a mixture of iodine plus some other constituent will be examined separately.

In the former case, the system is much simpler than the latter as it involves primarily only iodine molecules, atoms, and, perhaps, some wall effects. In both the investigations of Letokhov et al and this author fluorescence measurements were used to determine the relative amounts of ortho- and para-iodine. However, the technique employed here, namely using a dye laser to scan across a specific region of the molecular iodine spectrum

containing at least one ortho and one para peak belonging to the same vibrational transition and having similar rotational quantum numbers, was superior to that of Letokhov et al especially when the dye laser and the argon ion laser were used simultaneously. First of all this technique reduced the possibility of relative peak height changes in ortho and para species due to heating of the test cell by the laser and to differences of collisional quenching of different vibrational transitions. The former may not be very important but the latter, as was indicated by the series of experiments in which the residual pressure to which the test cells were evacuated, may play a large role. It seems that the vibrational states are differentially quenched by foreign gas. Thus if the cell degases over the course of the experiment (1 to 2 hours) then as the pressure inside the cell increases relative line strengths vary. This variation would be the most apparant at low initial vapour pressures of iodine as in these cases there is little self quenching. Secondly, this technique allows the experimenter to more readily observe any change occurring in the concentrations of each iodine modification without having to stop the primary irradiation process and preventing any extra reverse reaction from occurring.

The wild card in this whole affair was the material used for constructing the test cells. Letokhov et al made their cells of molybdenum glass while the ones used for this research were pyrex. As previously stated, our glassblower

was unable to obtain any information on this type of glass and, hence, the cell material was not modified during the experiments described in chapter 4. In a recent personal communication with Dr. W. Majewski, who visited the University of British Columbia to give a seminar, informed me that molybdenum glass is a type of glass made to have the same coefficient of expansion as molybdenum so that molybdenum electrodes may be placed inside glass cells. Generally it is slightly more porous than pyrex. It may be that the iodine atoms are more readily adsorbed and held by this glass than by pyrex and that this surface is a better one to use to obtain the desired effect.

In the cases where scavenger for the iodine atoms and/or molecules were added to the system the interpretation of the results is more complicated and more speculative. For example, in the case of 2-hexene, the results once again contradicted the finding of Letokhov et al. As mentioned before, Letokhov claimed an enrichment factor of up to 4 with mixtures of 40 mtorr of iodine vapour and about 2 torr of 2-hexene, with the lowest value of 2 at somewhat higher pressures of iodine vapour. The experiments reported here showed no enrichment whatsoever when similar mixtures were studied. From the results given in chapter 4 it would be postulated that the reaction mechanism of the two molecules involved a radical chain in which the 2-hexene picked up an iodine atom from the excited molecule and producing a free atom plus the radical XI. Both of these species may be able

to attack the ground state molecules by either breaking them up thereby perpetuating the chain or causing ortho- to para-iodine conversions and vice-versa. Letokhov, however, states that the initial rate of change in the ortho-iodine concentration goes as the square root of the 2-hexene concentration which does not support such a radical chain mechanism nor does it follow from the direct addition of an excited iodine molecule to the 2-hexene. Again, it could be that the direct addition of the excited iodine molecules to the 2-hexene is catalysed somehow by the molybdenum glass but not by pyrex.

Acetylene, too, I believe, reacts with the excited iodine via a radical chain as described above. This is contrary to the view of Kushawaha. However, the basis for his claim is questionable. As previously pointed out, problems with Kushawaha's interpretation of the data stem from inherent uncertainty in the method of filling each test cell with the iodine-129 which makes reproducibility and comparison of results dubious. Another difficulty lay in the fact that the two mass spectographs published in reference (30) concerning the isotopic separation of iodine do not follow one's intuition as to what should happen for a direct addition reaction(see p.127) but points to a radical chain, at least in the first case of the nonselective irradiation of the sample. Indeed if a selective irradiation of ths iodine-129 resulted in an isotopic separation then an ortho- to para-iodine shift should also have been observed.

Unfortunately, the results of the investigations reported here show no evidence for such a shift.

Ultimately nitric oxide, nitrosyl chloride, and ethyl iodide prooved ineffective also in the efforts to shift the ratio. The explanations for each of these is somewhat simpler. Nitric oxide itself is paramagnetic and, hence, undoubtedly causes ortho-para conversion fairly rapidly in molecular iodine. As discussed in chapter 2, the rate of conversion of ortho-iodine to para-iodine may be from 25 to 10^5 times larger than the corresponding rate in molecular hydrogen. Hence at 3 torr of nitric oxide a 330 minute half-life for the shift is expected for hydrogen which may drop down to only a matter of seconds in the case of iodine.

Nitrosyl chloride is not useful as a scavenger simply because it appears to react with the ground state iodine molecules spontaneously. It is interesting, though, that upon irradiation with a laser beam the molecular iodine species reappears and does not seem to disappear again, at least over the course of about half an hour. (By comparison the nitrosyl chloride originally reacted with the iodine within a period of ten minutes while the test cell was kept in the dark.) As previously postulated, this may be due to the spontaneous formation of ICl and its decomposition into I_2 and Cl_2 under irradiation.

Ethyl iodide, which had appeared to be the most promising method to obtain an enhancement, did not exchange iodine atoms to any observable extent over the course of the

irradiation period. It is possible that much more energy is required to obtain such an exchange than was provided by the frequency to which the dye laser was tuned.

Based upon these findings, no ortho- to para-iodine ratio shift has been detected to within an uncertainty of five percent via the selective predissociation of ortho-iodine molecules using laser irradiation or a laser induced photochemical reaction of ortho-iodine molecules with the scavengers 2-hexene, acetylene, nitric oxide, nitrosyl chloride, or ethyl iodide. The observations and results obtained seem to indicate the formation of free radicals during the aforementioned processes and it appears that molecular iodine is quite susceptible to ortho-para conversion catalysed by these radicals.

B. SUGGESTIONS FOR FUTURE WORK

This research left the question as to how important the material used for the construction of the test cell is to the outcome of the experiment. Specifically, do molybdenum glass cells behave very differently from pyrex ones? If one were to continue this work, then, it would be desirable to repeat the iodine vapour and iodine plus 2-hexene experiments using the two laser simultaneous irradiation technique with the samples contained in molybdenum glass cells. (Indeed, Dr.W. Majewski believes that Corning produces a type of glass similar to the type used by

Letokhov et al)

Another promising tactic would be to search more carefully for a species like ethyl iodide to produce an enhancement. Ideally this technique has the major advantage of catalysing a shift in the ortho to para ratio without producing any iodine atoms. Conceivably this would eliminate every possibility of paramagnetic conversion of the para-iodine molecules (assuming that one is selectively exciting the ortho modification) and one may be able to obtain substantial enhancement. For an exchange partner I would suggest a stable organic molecule having a good vapour pressure at room temperature, and containing several iodine atoms attached to it. This would help provide more exchange sites on each molecule and reduce the bond energy between the iodine atoms and the main core of the compound making atomic iodine exchange simpler.

If one were to begin this research anew, it would be advisable to attempt an ortho to para enhancement in bromine or chlorine first rather than iodine. The reason for this is that both of these species occur naturally in two isotopes, ^{35}Cl, ^{37}Cl, and ^{79}Br, ^{81}Br and the mixed species $^{35}Cl^{37}Cl$ and $^{79}Br^{81}Br$. By selectively exciting an ortho or para modification of one of the isotopes in the presence of a scavenger one could have observed whether any isotopic and/or ortho-para separation had occurred. If the isotopic separation occurred but no ortho-para enhancement then one would have some information about the relaxation of the

ortho and para species. If neither occurs but rather a completely nonselective reaction takes place then one has more evidence that radical chains are involved. Hence the presence of two isotopes, albeit more complicated from a spectroscopic viewpoint, provide a much better diagnostic tool.

Indeed this project has proved to be a very challenging one combining selective photochemistry, spectroscopy, and many hours of thought. I am certain that this subject is not yet closed but that some new research into this topic will inevitably be undertaken.

BIBLIOGRAPHY

1. Bazhutin,S. A., Letokhov,V. S., Makarov,A. A., and Semchishen,V. A., Sov. Phys. JETP Letters, **18**, 303 (1973).

2. Letokhov, V.S. and Semchishen, V.A., Sov. Phys. Dokl., **20**, 423 (1974).

3. Balykin, V. I., Letokhov, V. S., Mishen, V. I., and, Semchishen, V. A., Chem. Phys.(Neths.), **17**, 111 (1976).

4. Herzberg, G., Molecular Spectra and Molecular Structure I. Spectra of Diatomic Molecules, 2nd Ed.(D.Van Nostrand Company, Inc., New York, 1965)

5. Pauling, L. and Wilson, E. B., Introduction to Quantum Mechanics, (McGraw-Hill, New York,1935)

6. Goldstein, H., Classical Mechanics,(Addison-Wesley, New York, 1964)p.107 ff.

7. Kronig, R.de L. and Rabi, I. I., Phys. Rev., **20**, 262, (1927)

8. Broyer, M., Thèse de Doctorat d'État, Université Pierre et Marie Curie, Paris VI, 1977.

9. Vigué, J., Thèse de Doctorat d'État, Université Pierre et Marie Curie, 1978.

10. Broyer, M., Vigué, J., and Lehmann,J. C., Journal de Physique, **39**, 591 (1978).

11. Ramsey, N. F., Nuclear Moments, (John Wiley and Sons, New York, 1953)

12. Pique, J. P., Hartmann, F., Bacis, R., Churassy, S., and Koffend, J. B., Phys. Rev. Lett., **57**, 267 (1984).

13. Raich, J. C. and Good, R. H., Jr., Astrophys. J. (U.S.A.), **139**, 1004 (1964)

14. Farkas, A., Orthohydrogen, Parahydrogen, and Heavy Hydrogen, (Cambridge University Press, London, 1935)

15. Wigner, E., Z. f. physikal Chemie, **B4**, 126 (1929)

16. Kalkar, F. and Teller, E., Proc. Roy. Soc. (London), **A150**, 528 (1935)

17. Edmonds, A. R., Angular Momentum in Quantum Mechanics, (Princeton 528 (1935) University Press, New Jersey, 1974)

18. Heisenberg, W., Z. f. Physik, **38**, 411 (1926)

19. Hund, F., Z. f. Physik, **42**, 93 (1927)

20. Bonhoeffer, K. F. and Harteck, P., Naturwiss.,**17**, 182 (1929)

21. Bonhoeffer, K. F. and Harteck, P., Sitzber. Preuss. Akad. Wiss.,**1929**, 103

22. Bonhoeffer, K. F. and Harteck, P., Z. f. physikal Chemie, **B4**, 113 (1929)

23. Bonhoeffer, K. F. and Harteck, P., Z. f. Electrochemie., **35**, 621 (1929)

24. Farkas, A.and Bonhoeffer, K. F., Z. f. physikal Chemie, B, Bondensteinband, 638 (1931)

25. Geib, K. H., and Harteck, P., Z. f. physikal Chemie, **B10**, 419 (1930)

26. Farkas, L. and Sachsse, H., Sitz. Preuss. Akad. Wiss., **1933**, 268

27. Badger, R. M. and Urmston, J. W., Proc. Nat. Acad. Sci.,**16**, 808 (1930)

28. Gerstenkorn, S. and Luc, P., Atlas du Spectre d'Absorption de la Molecule d'Iode, Laboratiore Aime-Cotton, C.N.R.S. II, 91405, Orsay, France (1977)

29. Kushawaha, V. S., J. Amer. Chem Soc., **102**, 256 (1980)

30. Kushawaha, V. S., Opt. and Quant. Electr., **12**, 269 (1980)

31. Kushawaha, V. S., Chem. Phys. Lett., **72**, 451 (1980)

32. Basco, N. and Hunt, J. E., Int. J. Chem. Kinet., **10**, 733 (1978)

33. Brenner, D. M., Datta, S. and Zare, R. N., J. Amer. Chem. Soc., **97**, 2557 (1975)

34. Schmied, H. and Fink, R. W., J. Chem. Phys., **27**, 1034 (1957)

35. Vanderlinde, J., Levy, C. D. P., Bicchi, P. and Dalby, F. W., Phys. Rev., A, **30**, 1325 (1984)

APPENDIX A : ORDER OF MAGNITUDE ESTIMATE OF THE HYPERFINE ORTHO-PARA COUPLING

As has been stated, the hyperfine effects in molecular iodine may couple ortho and para levels from u and g electronic states thereby destroying this symmetry. The purpose of this appendix is to estimate the order of magnitude of this mixing.

The magnetic dipole and electric quadrupole terms, being the dominant interactions, alone will be considered.

(a) Magnetic Dipole Terms

The magnetic dipole interactions,

$$H_{MD} = H_{MD}(1) + H_{MD}(2) + H_{MD}(1,2) \qquad (A.1)$$

where each term has been defined previously on page is capable of coupling ortho and para states through $H_{MD}(1)$ and $H_{MD}(2)$.

$$H_{MD}(i) = H_{LI}(i) + H_{SI}(i) + H_{FI}(i) \qquad (A.2)$$
$$i = 1, 2$$

Explicitly,

$$H_{LI}(i) = -\sum_e 2\mu_B\mu_N g_{I_i} \frac{\vec{I}_i\cdot\vec{l}_e}{r_{ie}^3} \quad (a)$$

$$H_{SI}(i) = -\sum_e g_s g_{I_i}\mu_B\mu_N \left\{ \frac{3(\vec{S}_e\cdot\vec{r}_{ie})(\vec{I}_i\cdot\vec{r}_{ie}) - (\vec{I}_i\cdot\vec{S}_e)(\vec{r}_{ie}\cdot\vec{r}_{ie})}{r_{ie}^5} \right\} \quad (b) \quad (A.3)$$

$$H_{FI}(i) = -\sum_e g_s g_{I_i}\mu_B\mu_N \left(\frac{8\pi}{3}\right) \vec{I}_i\cdot\vec{S}_e\,\delta(\vec{r}_{ie}) \quad (c)$$

Consider first the H_{LI} terms and expand the quantities r_{ie}^{-3} according to figure A.1.

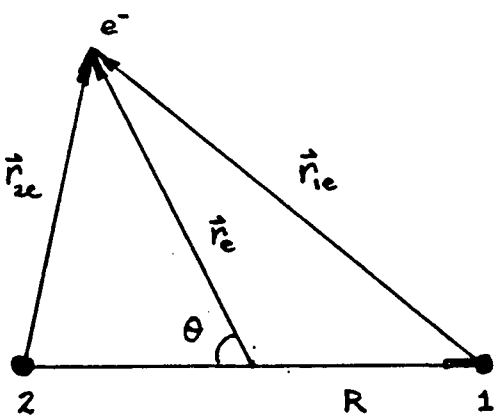

Figure A.1 The coordinate system used to describe the positions of the electrons and nuclei in a diatomic molecule in this appendix is shown above.

$$\frac{1}{r_{1e}^3} = \frac{1}{[r_e^2 + R^2 + 2Rr_e\cos\theta]^{\frac{3}{2}}} \simeq \frac{1}{r_e^3}\left\{1 - \frac{3R}{r_e}\cos\theta + \cdots\right\} \quad (A4a)$$

$$\frac{1}{r_{2e}^3} = \frac{1}{[r_e^2 + R^2 - 2Rr_e\cos\theta]^{\frac{3}{2}}} \simeq \frac{1}{r_e^3}\left\{1 + \frac{3R}{r_e}\cos\theta + \cdots\right\} \quad (A4b)$$

For the purposes of this estimation it will suffice to truncate the series after the R/r_e terms so that equations (A3a) and (A3b) become simply,

$$\frac{1}{r_{1e}^3} \simeq \frac{1}{r_e^3}\left\{1 - \frac{3R\cos\theta}{r_e}\right\} \qquad (A.4c)$$

$$\frac{1}{r_{2e}^3} \simeq \frac{1}{r_e^3}\left\{1 + \frac{3R\cos\theta}{r_e}\right\} \qquad (A.4d)$$

Thus using (A4c) and (A4d),

$$H_{LI}(1) + H_{LI}(2) = -\sum_e 2\mu_B\mu_N g_{I_1}\left\{\frac{\vec{I}_1\cdot\vec{l}_e}{r_{1e}^3} + \frac{\vec{I}_2\cdot\vec{l}_e}{r_{2e}^3}\right\} \qquad (A5)$$

becomes,

$$H_{LI}(1) + H_{LI}(2) \simeq -\sum_e 2\mu_B\mu_N g_{I_1}\left\{\left(1 + \frac{3R}{r_e}\cos\theta\right)(\vec{I}\cdot\vec{l}_e) - \frac{2R}{r_e}\cos\theta\,(\vec{I}_1\cdot\vec{l}_e)\right\} \qquad (A6)$$

To couple ortho and para states one must mix u and g electronic states by the symmetry arguments mentioned in chapter 2. This is only possible by having terms like $\cos\theta$, $\cos^3\theta$, etc. in the operator H_{hf}. Further, the mixing Hamiltonian must operate on either I_1 or I_2 alone and not on I as in the former case states with $\Delta I=1$ is possible while in the latter $\Delta I=0$ holds[17]. Consequently only the final term in equation(A6) satifies these criteria.

$$H_{LI}^{o\text{-}p} \simeq 4\sum_e \frac{\mu_B\mu_N}{r_e^3} g_{I_1}\left(\frac{Rze}{r_e^2}\right)(\vec{I}_1\cdot\vec{l}_e) \qquad (A.7)$$

where $z_e = r_e \cos\theta$.

The matrix element shown in eqation (A8) will yield the strength of the coupling.

$$M_{LI} = \langle S', \Sigma', \Lambda', \Omega', v', J', I', F', M_F' | H_{LI}^{e\text{-}p} | S, \Sigma, J, M_I \rangle \tag{A.8}$$

which using Hund's coupling scheme (a) becomes,

$$M_{LI} \simeq 4\mu_N \mu_B g_I \sum_e \langle J' v' \Omega' | \frac{R z_e}{r_e^3} | J v \Omega \rangle \times \langle J' I' F' M_F' | \vec{I} \cdot \vec{l}_e | J I F M_F \rangle \tag{A.9}$$

To estimate this quantity consider each term separately beginning with the second, T_2

$$T_2 = \langle J' I' F' M_F' | \vec{I} \cdot \vec{l}_e | J I F M_F \rangle \tag{A.10}$$

But,

$$\vec{I} \cdot \vec{l}_e = \frac{I_+ l_- + I_- l_+}{2} + I_z l_z \simeq I_+ l_- + I_z l_z \tag{A.11}$$

Consider the first term,

$$T_2^a = \langle J' I' F' M_F' | I_+ l_- | J I F M_F \rangle \tag{A.12}$$

which may be evaluated with the help of Clebsche-Gordon coefficients. For an angular momentum $\bar{j}_3 = \bar{j}_2 + \bar{j}_3$, a given state $|j_3 m_3\rangle$ may be decomposed as,

$$|j_3 m_3\rangle = \sum_{m_1, m_2} \langle j_1 m_1 j_2 m_2 | j_1 j_2 j_3 m_3 \rangle |j_1 m_1 j_2 m_2\rangle \qquad \text{A.13}$$

where $m_3 = m_1 + m_2$ and $\langle j_1 m_1 j_2 m_2 | j_1 j_2 j_3 m_3 \rangle$ is the Clebshe-Gordan coupling coefficient.

In equation (A12) $\bar{F} = \bar{I} + \bar{J}$ and $\bar{I} = \bar{I}_1 + \bar{I}_2$ so that,

$$|I J F M_F\rangle = \sum_{\substack{m_1, m_2 \\ M_I, M_J}} |I_1 m_1 I_2 m_2\rangle \langle I_1 m_1 I_2 m_2 | I_1 I_2 I M_I\rangle \times \langle I M_I J M_J | I J F M_F\rangle \qquad \text{A.14}$$

Hence equation (A12) becomes,

$$\begin{aligned} T_2^a = \sum_{m_1, M_I} & \sqrt{(I_1 - m_1)(I_1 + m_1 + 1)}\ \sqrt{(L + \Lambda)(L - \Lambda + 1)} \\ & \times \langle J' I' F' M_F' | I' M_I + 1\ J' M_F - M_I\rangle \\ & \times \langle I_1 I_2 I' M_I + 1 | I_1 m_1 + 1\ I_2 m_2\rangle \\ & \times \langle I_1 m_1 + 1\ I_2 M_I - m_2 | I M_I J M_F - M_I\rangle \\ & \times \langle I M_I J M_F - M_I | I J F M_F\rangle \end{aligned} \qquad \text{A.15}$$

Using the relations,

$$\langle I_{1+}\rangle = \delta(m_1', m_1 + 1)\ \delta(m_2', m_2)\sqrt{(I_1 - m_1)(I_1 + m_1 + 1)} \qquad \text{A.16}$$

$$\langle le-\rangle = \delta(M_J', M_J - 1)\sqrt{(L + \Lambda)(L - \Lambda + 1)} \qquad \text{A.17}$$

and simplifying the sums relying upon the delta functions above and $M_F = M_J + M_I$, $M_I = m_1 + m_2$, T_2^a reduces to,

$$\begin{aligned} T_2^a = \sum_{\substack{m_1, m_2 \\ m_1', m_2' \\ M_I, M_J \\ M_I', M_J'}} & \langle J' I' F' M_F' | I' M_I' J' M_J'\rangle \langle I_1 I_2 I' M_I' | I_1 m_1' I_2 m_2'\rangle \\ & \times \langle I_1 m_1' I_2 m_2' | I_{1+} | I_1 m_1 I_2 m_2\rangle \\ & \times \langle J' M_J' | le- | J M_J\rangle \\ & \times \langle I_1 m_1 I_2 m_2 | I_1 I_2 I M_I\rangle \langle I M_I J M_J | I J F M_F\rangle \end{aligned} \qquad (A.18)$$

To evaluate (A18) consider the maximum possible values of each of the quantities in the square roots. For the nuclear spin term,

$$\frac{\partial}{\partial m_1}\left[(I_1-m_1)(I_1+m_1+1)\right] = -(I_1+m_1+1)+I_1-m_1 = 0 \qquad (A.19)$$

the maximum occurs for $m_1=0.5$ or,

$$\left(\sqrt{(I_1-m_1)(I_1+m_1+1)}\right)_{MAX} = 3 \qquad (A.20)$$

The electronic angular momentum obeys a similar relationship, however Λ is a whole number so that,

$$\sqrt{(L+\Lambda)(L-\Lambda+1)} \leq \sqrt{L(L+1)} \qquad (A.21)$$

For states coupled as $\bar{J}=\bar{R}+(\bar{L}+\bar{S})$ with $\Omega=0$, and $S=1$, $L_{max}= 2J+1$ so that

$$\sqrt{(L+\Lambda)(L-\Lambda+1)} \leq (2J+1) \qquad (A.22)$$

Using these relations T_2^a becomes

$$T_2^a \lesssim \sum_{M_I, m_1} \begin{aligned} & 3(2J+1)\langle J' I' F' M_F' \mid I' M_I+1\ J\ M_P-M_I\rangle \\ & \times \langle I_1 I_2\ I' M_I+1 \mid I_1\ m_1+1\ I_2\ m_2\rangle \\ & \times \langle I_1\ m_1+1\ I_2\ m_2 \mid I\ M_I\ J\ M_P-M_I\rangle \\ & \times \langle I\ M_I\ J\ M_P-M_I \mid I\ J\ F\ M_F\rangle \end{aligned} \qquad (A.23)$$

To evaluate the Clebsche-Gordan coefficients cnsider their properties; for an angular momentum state $|\, j_3 m_3\rangle$ composed of $\vec{j}_1+\vec{j}_2$ with $|\vec{j}_1| \leq |\vec{j}_2|$ there will be, at most, $2j_1+1$ terms $|j_1 m_1 j_2 m_2\rangle$ making up this state. That is,

$$|j_3 m_3\rangle = a_1 |j_1 j_1 \,;\, j_2, m_3 - j_1\rangle + a_2 |j_1 j_1-1 \,;\, j_2\, m_3-j_1+1\rangle + \cdots + a_{2j_1+1} |j_1 -j_1 \,;\, j_2\, m_3+j_1\rangle \tag{A.24}$$

The sum of these Clebsche-Gordan coefficients, a_i, has the property that,

$$S = \sum_i a_i \leq \sqrt{2j_1+1} \tag{A.25}$$

This may be shown as follows; consider that using the normalization condition,

$$\sum_i |a_i|^2 = 1 \tag{A.26}$$

the sum, S, may be written as (letting $n=2j_1+1$)

$$S = a_1 + a_2 + a_3 + \cdots + a_n$$

$$S = \sqrt{1 - a_2^2 - a_3^2 - \cdots - a_n^2} + a_2 + \cdots + a_n \tag{A.27}$$

To find local minima or maxima one needs to take the partial derivatives of S with respect to each of the a_i and set them equal to zero. To begin,

$$\frac{\partial S}{\partial a_2} = \frac{-a_2}{\sqrt{1 - a_2^2 - \cdots - a_n^2}} + 1 = 0 \qquad (A.28a)$$

or,

$$a_2 = \sqrt{\frac{1 - a_3^2 - a_4^2 - \cdots - a_n^2}{2}} \qquad (A.28b)$$

which, when replaced in equation (A25) gives,

$$S_{max} = 1 + 2\sqrt{\frac{1 - a_3^2 - a_4^2 - \cdots - a_n^2}{2}} + a_3^2 + \cdots + a_n^2 \qquad (A29)$$

By continuing this process for each coefficient one eventually obtains,

$$S_{max} = a_n + (n-1)\sqrt{\frac{1 - a_n^2}{(n-1)}}$$

and

$$\frac{\partial S}{\partial a_n} = \frac{-a_n}{\sqrt{\frac{1 - a_n^2}{(n-1)}}} + 1 = 0$$

or,

$$a_n = \frac{1}{\sqrt{n}} \qquad (A.30)$$

and

$$a_{n-1} = \frac{\sqrt{1-a_n^2}}{\sqrt{(n-1)}} = \frac{\sqrt{n-1}}{\sqrt{n(n-1)}} = \frac{1}{\sqrt{n}}$$

$$a_{n-2} = \sqrt{\frac{1-a_{n-1}^2-a_n^2}{(n-2)}} = \sqrt{\frac{(n-2)}{n(n-2)}} = \frac{1}{\sqrt{n}}$$

etc.

Ultimately one obtains $a_1=a_2=\ldots=a_n=1/\sqrt{n}$ so that,

$$S_{max} = \sum_{i=1}^{2j_1+1} a_i = \sqrt{2j_1+1} \qquad (A.31)$$

To show that the above is indeed a maximum consider

$$\frac{\partial^2 S}{\partial a_i \partial a_j} < 0 \qquad (A.32)$$

for a maximum.

Case (1) $i \neq j$

Let S be expressed as,

$$S = \sqrt{1-a_2^2-a_3^2-\cdots-a_n^2} + a_2 + \cdots + a_n$$

so that,

$$\frac{\partial^2 S}{\partial a_i \partial a_j} = \frac{-a_i a_j}{(1-a_2^2-\cdots-a_n^2)^{\frac{3}{2}}} \qquad (A.33)$$

This quantity is less than zero for the choice of the $a_i = 1/\sqrt{n}$.

Case (2) i=j

Again,

$$\frac{\partial^2 S}{\partial a_i^2} = \frac{-a_1^2 - a_i^2}{(1 \; a_2^2 - \cdots - a_n^2)^{\frac{3}{2}}} \qquad (A.34)$$

this is less than zero for the above choice of the coefficients. Thus the claim that these values lead to a maximum in S is correct.

Using relation (A30) in equation (A23) one obtains,

$$T_2^a \leq \sum_{m_i M_I} 3(2J+1) \cdot \frac{1}{\sqrt{2M_I+1}} \cdot \frac{1}{\sqrt{2m_i+1}} \cdot \frac{1}{\sqrt{2m_i+1}} \cdot \frac{1}{\sqrt{2M_I+1}}$$

$$T_2^a \lesssim 3(2J+1) \qquad (A.35)$$

The next quantity to estimate is T_2^b.

$$T_2^b = \langle J'I'F'M_F' | I_{iz} l_{ez} | JIFM_F \rangle \qquad (A.36)$$

This term will behave exactly as the previous one as regards Clebsche-Gordan coefficients and the only difference will be that instead of taking the maximum values of I_{1+} and l_{e-}, one need only consider m_1^{max} and Σl_{ez}^{max} i.e.

$$T_2^b \lesssim I_1 \cdot \Lambda \qquad (A.37)$$

Finally one must estimate,

$$T_1 = \langle J' v' \Omega' \left| \sum_e \frac{R z_e}{r_e^5} \right| J v \Omega \rangle \qquad (A.38)$$

In the $B^3\Pi_{0^+u}$ and $X^1\Sigma_g^+$ states of I_2 the internuclear distance, 2R, is between one and two angstroms. Consequently, one would expect that

$$\left\langle \frac{R z_e}{r_e^5} \right\rangle \lesssim \left\langle \frac{1}{r_e^3} \right\rangle \lesssim \left\langle \frac{1}{R^3} \right\rangle \approx 10^{24}\,cm^{-3} \qquad (A.39)$$

Hence,

$$T_1 \lesssim 10^{24}\,cm^{-3} \langle v'|v \rangle \qquad (A.40)$$

Combining these results,

$$M \lesssim 4 \mu_B \mu_N g_{I_1} (10^{24} cm^{-3}) \langle v'|v \rangle \left[3(2J+1) + \tfrac{5}{2}\Lambda\right] \qquad (A.41)$$

For a state with $\Lambda=0$,

$$M \sim (0.012) \langle v'|v \rangle (2J+1) \quad cm^{-1} \qquad (A.42)$$

Assuming similar contributions from the H_{SI} and H_{FI} terms,

$$M \sim (0.036) \langle v'|v \rangle (2J+1) \ cm^{-1} \qquad (A.43)$$

for a $\Lambda=0$ state, and

$$M \sim (0.036) \langle v'|v \rangle (2J+\tfrac{4}{6}) \ cm^{-1} \qquad (A.44)$$

for a $\Lambda=1$ state.

To obtain an order of magnitude estimate assume that $\langle v'|v \rangle \simeq N_v^{-1}$ where N_v is the number of vibrational states in a given electronic level. Here $N_v \simeq 80$, and, for J=10 one obtains,

$$\langle \nu', I \pm 1 \mid H_{MD}^{o-p} \mid \nu, I \rangle \sim 0.0098 \ cm^{-1} \qquad (A.45)$$

(b) ELectric Quadrupole Terms

$$H_{EQ}(i) = - \frac{eQ}{2I_i(2I_i-1)(2J+3)(2J-1)} \left(\frac{\partial^2 V^e}{\partial z^2}\right)_{av} \left\{ 3(\vec{I}_i \cdot \vec{J})^2 + \tfrac{3}{2}(\vec{I}_i \cdot \vec{J}) - I_i^2 J^2 \right\} \qquad (A.46)$$

or

$$H_{EQ}(i) = + \frac{eqQ}{2I_i(2I_i-1)J(2J-1)} \left\{ 3(\vec{I}_i \cdot \vec{J})^2 + \tfrac{3}{2}(\vec{I}_i \cdot \vec{J}) - I_i^2 J^2 \right\} \qquad (A.47)$$

Expanding the second derivatives of the potential, V, for $H_{EQ}(1)$ and $H_{EQ}(2)$ and adding the two together, keeping only those terms which are able to couple u and g electronic states and ortho and para states in analogy with the magnetic dipole terms one obtains,

$$H_{EQ}^{o-p} \simeq \frac{3eQq}{2I_1(2I_1-1)(2J+1)(2J+3)} \left\{(\hat{I}\cdot\hat{J})(\hat{I}_1\cdot\hat{J}) + (\hat{I}_1\cdot\hat{J})(\hat{I}\cdot\hat{J}) + (\hat{I}_1\cdot\hat{J})\right\} \quad (A.48)$$

Let K_2 be

$$K_2 = \langle I'J'F'M_F' \left| \left\{(\hat{I}\cdot\hat{J})(\hat{I}_1\cdot\hat{J}) + (\hat{I}_1\cdot\hat{J})(\hat{I}\cdot\hat{J}) + (\hat{I}_1\cdot\hat{J})\right\} \right| IJFM_F\rangle \quad (A.49)$$

so that

$$K_2 = \left\{\frac{F'(F'+1) - J'(J'+1) - I'(I'+1)}{2} + \frac{F(F+1) - J(J+1) - I(I+1)}{2} + 1\right\} \quad (A.50)$$
$$\times \langle I'J'F'M_F' \left| \hat{I}_1\cdot\hat{J} \right| IJFM_F\rangle$$

where $F' \leq F+1$, $J' = J\pm1$, and $I' = I\pm1$,

Thus,

$$K_2 \leq 2(I+1)(J+1) \langle I'J'F'M_F' \left| \hat{I}_1\cdot\hat{J} \right| IJFM_F\rangle \quad (A.51)$$

The above expression has already been evaluated in the first section of this appendix and as the value of (eQq) is known for both the $X^1\Sigma_g^+$ and the $B^3\Pi_{0^+u}$ electronic states of iodine and may be taken from reference (35), one may readily estimate the quadrupole mixing as,

$$\langle v', I\pm1 | H_{EQ}^{o\text{-}p} | v I\rangle \sim \frac{3(eQq)}{2I_1(2I_1-1)J(2J-1)} \frac{2(I+1)(J+1)(3(2J+1)+\frac{5}{2}\Lambda)}{} \langle v'|v\rangle \qquad (A.52)$$

Further, as $I_1=5/2$ and $I\leq5$,

$$\langle v', I\pm1 | H_{EQ}^{o\text{-}p} | v I\rangle \sim \frac{9(eQq)\langle v'|v\rangle (J+1)(3(2J+1)+\frac{5}{2}\Lambda)}{5J(2J-1)} \qquad (A.53)$$

which becomes

$$\langle v', I\pm1 | H_{EQ}^{o\text{-}p} | v I\rangle \sim 0.007 \text{ cm}^{-1} \qquad (A.54)$$

in the $X^1\Sigma_g^+$ and

$$\langle v' I\pm1 | H_{EQ}^{o\text{-}p} | v I\rangle \sim 0.001 \text{ cm}^{-1} \qquad (A.55)$$

in the $B^3\Pi_{0^+u}$ state.

Thus the net contribution of the hyperfine magnetic and quadrupole coupling of the ortho and para levels between a u and g electronic state is

$$\langle v' I \pm 1 | H_{EQ}^{o\text{-}p} + H_{MD}^{o\text{-}p} | v I \rangle \sim 0.01\ cm^{-1} \quad (A.60)$$